Study on the arsenic load of the food chain in an agricultural affected area of the Inner Mongolia, Hetao-Plain, China

Diplomarbeit

an der Universität Karlsruhe (TH)

vorgelegt von

cand.-geoökol. Harald Neidhardt

März 2008

Referentin: Prof. Dr. Doris Stüben

Koreferent: Prof. Dr. Harald Krug

Erklärung:

Hiermit versichere ich, dass ich die hier vorliegende Arbeit selbst verfasst und keine nicht angegebenen Hilfsmittel verwendet habe.

Ort, Datum

Unterschrift

Acknowledgment

I would like to thank hereby everybody being involved in this diploma thesis.

Special thanks go to:

-Mrs. Prof. Dr. D. Stüben for making this diploma thesis possible and supervising my work

-Mr. Professor Dr. H. Krug for acting as secondary corrector

-PD S. Norra for supervising and helping with words and deeds at any time

-Ph.D. Associate Professor H. Guo from the China University of Geosciences for the great support and friendship I received during the field trip

-PD Dr. T. Neumann and Dr. Z. Berner for the possibility of problem discussion

-Dr. U. Kramar for the measuring time at the ANKA and help by carrying out ED-RFA measurements and interpretation

-Mrs. C. Mößner for the countless measurements at the HR-ICP-MS, aid with microwave digestions and providing assistance with all occurring analytical problems

-Mrs C. Haug for carrying out the filter digestions and help in lab

- Mrs. B. Oetzel for her patience in explaining me converting XRD data and use of the CSA

-Mr. Nikoloski for making the thin sections and using his equipment

-Mrs. G. Preuss for support in all lab belongings

-Mr. H.-P. Schaupp and G. Ott for technical support

-my new Chinese friends Jam Bua, Apple, Li Yuen, Phoebe, Jerry and Michael for making me feel so welcome in Beijing and taking care of me during my entire sojourn in the People's Republic of China

-my girlfriend Stephanie and my friends Shahjahan, Jens and Oli for proofreading

-and of course my parents for giving me encouragement during my studies

Table of contents

Table of figures

APPENDIX:

Index of table

APPENDIX:

Zusammenfassung:

Thema dieser Fallstudie sind die Konsequenzen der Bewässerung von mit Arsen (im Folgenden mit As abgekürzt) belastetem Grundwasser in der Hetao Ebene, Teil der zu China gehörigen Autonomen Region Innere Mongolei. Um die Belastung der Nahrungskette mit As zu bestimmen, wurde in einem repräsentativen, land-wirtschaftlichen Dorf im Nordwesten der Hetao Ebene die Verteilung von As innerhalb des Wasser-Boden-Pflanzen-Systems untersucht. Von besonderem Interesse waren hierbei die horizontale bzw. vertikale Verteilung von As im Ackerboden sowie die Belastung darauf angebauter Feldfrüchte.

Zwei Äcker (ein Sonnenblumen- und ein Maisfeld) wurden daher im Juli 2007 beprobt, welche jeweils innerhalb der letzten 3 Jahre zwei mal monatlich mit alkalischem und salzhaltigem Grundwasser bewässert wurden. Auf beiden Untersuchungsflächen wurden Bodengruben von $1m^3$ Größe ausgehoben und ein Raster für die Beprobung des Oberbodens eingerichtet. Zusätzlich wurden auf den Feldern sowie im näheren Umfeld Wasser- und Pflanzenproben entnommen.

Um die Probenzusammensetzung zu analysieren, wurde eine Vielzahl an Methoden eingesetzt, wie beispielsweise energie-dispersive Röntgenfluoreszenzanalyse (ED-XRF), Mikro-Synchrotonstrahlung basierte Röntgenfluoreszenzanalyse (µ-SyXRF)), Röntgen-diffraktometrie (XRD), Fließinjektions-Atomadsorptionsspektroskopie (FIAS) sowie hochauflösende Massenspektrometrie mit induktiv gekoppeltem Plasma (HR-ICP-MS).
Die Messungen ergaben As Konzentrationen im Grundwasser von rund 150 µg/l im Fall von Feld 1 und 240 µg/l bei Feld 2, was eine deutliche Überschreitung des Chinesischen Grenzwerts von 10µg/l für As im Trinkwasser darstellt. Die vertikale Verteilung von As im Bodenprofil deutet auf eine leichte Anreicherung im Oberboden hin und einen möglichen Zusammenhang mit der Korngrößenverteilung. Im Gegensatz dazu variiert die horizontale Verteilung des As in den ersten beiden Zentimetern des Oberbodens mit Konzentrationen zwischen 11 und 22 mg/kg recht stark und scheint dabei den Verlauf des Mikroreliefs nachzuzeichnen. Obwohl die As-Gehalte im Boden als nicht sonderlich hoch erscheinen, konnten in einigen der beprobten Pflanzen zum Teil deutliche Belastungen von bis zu 3210µg As/kg nachgewiesen werden.

Die Ergebnisse führen zu der Erkenntnis, dass die Bewässerung mit As belastetem Grundwasser innerhalb der Inneren Mongolei dringend weitergehender Beobachtung und Untersuchungen bedarf.

Abstract:

Subject of this case study were the consequences of irrigation by As contaminated water in the Hetao-Plain, part of the Inner Mongolia Autonomous Region in China. Therefore, the arsenic (As) distribution within the water-soil-plant-system was examined in a representative farming village in the North-West of the plain in order to assess As within the food chain. Especially the horizontal and vertical distribution of As in field soil was a matter of particular interest as well as the abundance of As in crops.

Two fields (a sunflower and a corn field) were sampled in July 2007, each irrigated twice a month since three years by groundwater, which is characterized by high salinity and alkaline pH. On both study sites, two soil pits of 1 m^3 were excavated and a grid for topsoil sampling installed. Additionally, water and plants were sampled at both fields and in the surroundings.

Various analysis were carried out by means of ED-XRF, µ-SyXRF, XRD, FIAS and HR-ICP-MS to determine the elemental and mineralogical compositions. Total As concentration in the groundwater used for irrigation of the corn was about 150 µg/l and 240 µg/l. Both concentrations clearly exceeded the Chinese drinking water standard of 10µg As/l. Vertical distribution of As in soil indicated a slight enrichment in topsoil and a possible relation to grain size. In contrast, the spatial distribution in topsoil (11.0 to 22.0 mg As/kg) varies strongly and seems to be reflecting the surface micro-relieve. Although the concentration in soil is not that serious, As could have also been detected in plant parts, ranging up to 3210µg/kg. The results allude to the necessity of further monitoring of the use of As contaminated groundwater for irrigation purposes in Inner Mongolia.

1. Introduction

1.1 Preamble and working hypotheses

This diploma thesis is supervised by Professor Dr. Doris Stüben and PD Dr. Stefan Norra from the Institute of Mineralogy and Geochemistry (IMG) from the University of Karlsruhe (TH). It emerged from a participation of the IMG within a Chinese cooperative project aided by the National Natural Science Foundation of China (NSFC) to assess the As situation in the Inner Mongolia Autonomous Region. Planning and realisation of the one week field survey into the investigation area was done in close collaboration with Ph.D. Associate Professor Huaming Guo from the Department of Water and Environment of the China University of Geosciences, Bejing, who established together with his team the basis for this work. Main results of this work are published in GUO et al.(2008).

Subject of this diploma thesis were the consequences of irrigation with high arsenic (As) burdened groundwater in a representative farming village in the Hetao-Plain, China. Main intention was to qualify the local As distribution and flow within the water-soil-plant-system in order to assess risk on human health and to educe recommendations for action in the entire region. The horizontal and vertical distribution of As in field soil is a matter of particular interest within this study. The results shall further be transferable to other As infected areas worldwide and make a contribution to understand the geochemical behaviour of As in the environment. Working hypothesis forming the basic of this diploma thesis is that irrigation with high As burdened groundwater causes enrichment in soil, food chain and human being.

1.2 Geochemistry of As

The geochemistry of As involves adsorption, mobilization and interaction processes with other soil or sedimentary components. In case of this study, it is important to understand

a) how, why and in which species As becomes mobilized and enriched within the aquifers;

b) the fate of As in the environment when brought up onto field by irrigation;

c) the consequences of using As enriched groundwater as drinking water.

As is a chemical element with the atomic number 33 and a molecular weight of 74.92 g/mol, belonging to the nitrogen group within the periodic table. It is a metalloid with 5 valence electrons and possible oxidation states -III (arsenide), ±0 (elemental As), +III (arsenite) and +V (arsenate). As a trace element, it is widely distributed in environment and occurs naturally in about 200 minerals, 60% belonging to arsenates, 20% to sulphides and sulfosalts and the remaining being distributed among arsenides, oxides, silicates and the solid form (BHATTACHARYA et al. 2007, KABATA-PENDIAS et al. 1984, ALLOWAY 1999). Most important minerals are arsenopyrite (FeAsS), realgar (As_4S_4) and orpigment (As_2S_3). Further, but less common As holding minerals are arsenolite (As_2O_3), loellingite ($FeAs_2$), safforlite (CoAs), niccolite (NiAs), rammelsbergite ($NiAs_2$), enargite (Cu_3AsS_4) and cobaltite (CoAsS). As is ubiquitous in rocks with concentrations ranging between 0.5 to 2.5 ppm and an average content within the continental crust of 2-3ppm. Elevated contents appear in ores, metals, coal (bituminous 8.2-9.8, peat 16-340ppm), sandstones (0.6-120 ppm) and shale and clay (0.3-490 ppm) (BHATTACHARYA et al. 2007, KABATA-PENDIAS et al. 1984).

As can be released into environment either by natural processes or anthropogenic activities. Natural processes are mainly chemical and biological weathering of rocks and sediments, hydrothermal depositions, volcanic eruptions, forest fires and sea salt spray. About 80% of As used by human is released diffusely into environment as constituent of herbicides, insecticides, desiccants, defoliants (agent blue), feed additives, wood preservation agents (CCA, copper-chrome-arsenic), pigments, drugs and alloying elements (BHATTACHARYA et al. 2007). Industrial activities, especially mining, smelting and coal combustion, are further important sources of As, released through refuse dumps, waste water and exhausted air. Application of sludge, showing strongly varying contents of up to 190mg As/kg on fields holds also risk of As input (ALLOWAY 1999). Figure 1 presents the fate of As in the environment, including important sources and transformation processes.

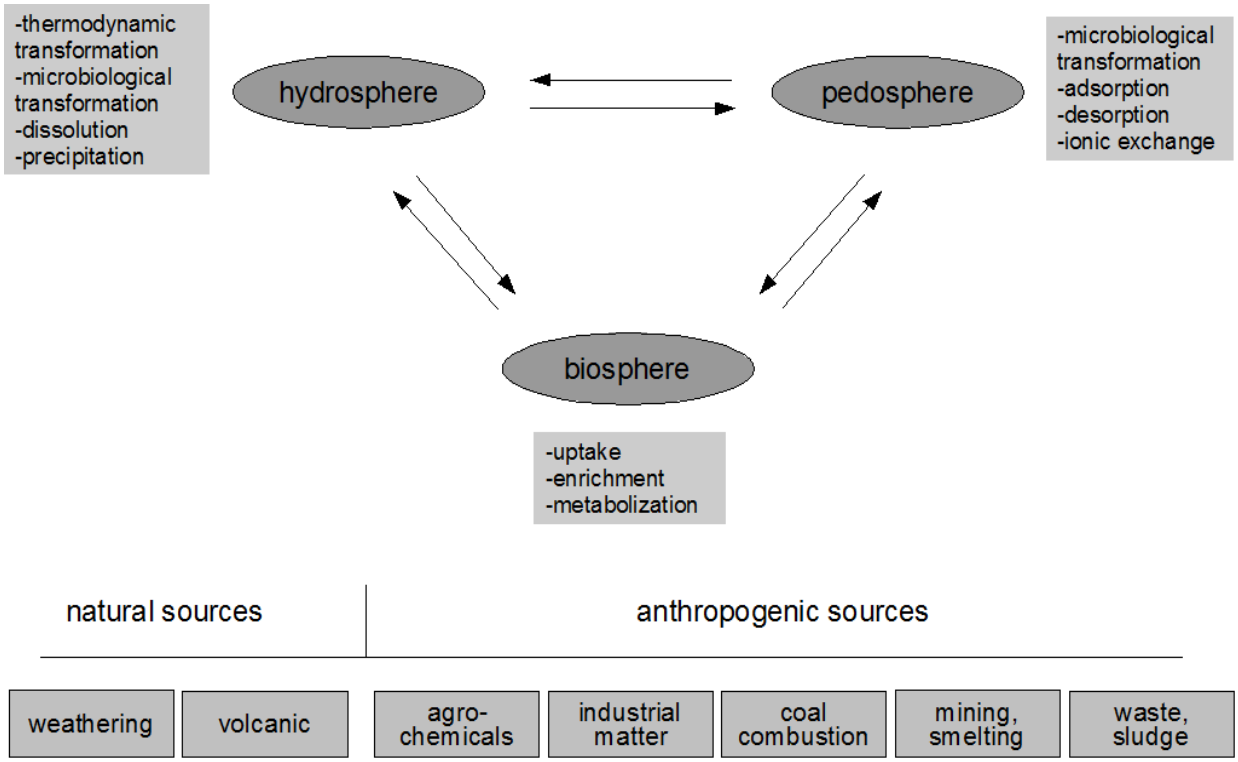

Figure 1: Sources and fate of As in environment (illustrated by author)

As in soils and sediments:

Soil and sediments can act both as source and sink of As, addicted to the prevailing geochemistry. Accumulation in soil can be a consequence of irrigation with As burdened groundwater, pesticide and fertilizer application, dry and wet deposition and weathering of As containing minerals. The worldwide As content in uncontaminated surface soils varies within a range of <1 and 95 ppm, with an average of between 6.7 and 8.7 ppm (KABATA-PENDIAS et al. 1984). The USEPA (United States Environmental Protection Agency) set in 2001 a limit of 10mg As/kg soil (NAIDU et al. 2006). Lowest values usually appear in sandy soils, highest in organic and clay rich fluvisols. Paddy soils with permanent reducing conditions are notably endangered when irrigated with As contaminated water. About 20% of the total As in soil are plant available (=easily mobile), the remaining 80% are strongly bound (KABATA-PENDIAS 2001 in NAIDU et al. 2006).

Speciation and mobility of As compounds in soils are primary related to interdependent soil characteristics, mainly redox potential, microbiological activity, mineralogical composition, pH conditions, grain size distribution and ionic strength in soil solution.

-*Redox potential:* The most common mobile forms of As in soil and water belong to the inorganic species of the oxy-acids arsenate (H_3AsO_4; pK_1=2.2, pK_2=6.98), dominating under oxidic conditions (positive Eh) and arsenite (H_3AsO_3; pK1= 9.2), occurring under reducing conditions (negative Eh) (OBERACKER et al. 2002, NAIDU et al. 2006).

-*Microbiological activity:* Organic As compounds exist as well as a result of microbiological transformations. Some organisms methylize As in detoxification processes, other are able to use it as an energy source (arsenate reduction under reducing conditions/ arsenite oxidation under oxidic conditions). Methylated As is volatile and gases out into atmosphere. Most important organic As compounds are DMAA (di-methylarsinic acid) , MMAA (mono-methylarsonous acid) and arsine (AsH_3).

-*Mineralogy:* Negatively charged As anions are electro-statical bound to positive charged solid surfaces, mainly Fe-oxyhydroxides like ferrihydride, goethite and hematite, which often surround other minerals as coatings. Other, less important As adsorbing soil constituents are Mn-and Al-oxyhydroxides, clay minerals, sulphates, calcium carbonates and organic acids (s. table 1 below).

Table 1: Sorption capacity (g As/kg) of soil constituents; conditions:12 hours; water/soil constituent ratio=700 (NAIDU et al. 2006, modified)

Soil/soil constituent	As^{III}	As^{V}
Synthetic		
Fe-oxyhydroxides	68.2 ± 0.2	43.1 ± 0.0
Al-oxyhydroxides	68.4 ± 0.2	63.9 ± 0.8
Mn-oxyhydroxides	25.1 ± 0.2	28.1 ± 0.1
Ca carbonate	21.0 ± 0.1	24.3 ± 0.2
Natural		
Kaolonit	15.2 ± 0.1	20.9 ± 0.2
Montmorillonite	16.9 ± 0.1	22.7 ± 0.2
Vermiculite	9.3 ± 0.1	10.4 ± 0.1

-*pH:* Adsorption to metal oxides is pH depending, because the point of zero charge appears at a certain pH (around pH 8). In range of normal soil pH (between 2.2 and around 8), arsenate is less mobile than arsenite, because arsenite is present as non-ionic form H_3AsO_3 (pK_1=9.2) and arsenate as de-protonated forms $H_2AsO_4^-$ and $HAsO_4^{2-}$. Increasing pH causes therefore decreasing arsenate adsorption, while maximum arsenite adsorption appears at high pH near its first dissociation constant (pK_1=9.22) (NAIDU et al. 2006).

-*Grain size:* Influence of grain size becomes apparent in a comparison of clayey soils to sandy soils. Clay minerals effectuate a surface extension and offer a multiple of possible As binding sites than simple organized quartz grains.

-*Ionic composition:* Competitive adsorption can emerge in soil solution between As and other negative charged anions like phosphate, sulphate, chloride, molybdate and dissolved organic acids, like fulvic and humic acids. Due to chemical similarity, phosphate is a strong antagonist to As. In general, anion exchange capacity of fine soil fraction decreases with increasing pH (GOH and LIM 2004). Fertilizing with P decreases As availability in heavy, clay rich soils, but in sandy soils, the opposite happens because phosphate displaces As from the few available binding sites. Artificial fertilizers exhibit at the same time potential As sources with up to 1200mg As/kg (ALLOWAY 1999). Hydroxyl anions (OH-), appearing above pH 7, are also strong competitors to As for binding sites. High anion concentration can further cause specific ligand exchange, leading to As^{V} desorption from binding sites. On the other hand, cations are able to decrease As release (NAIDU et al. 2006)

Once brought into the soil system, it is important to predict the behaviour of As to exclude any hazards to human being. Therefore, soil column experiments can be used to describe As leaching with physic-chemical models, using different adsorption equation theories like the Freundlich and Langmuir isotherms. Another, more practically orientated approach is the use of sequential extraction procedures to get information about the different As bounding fractions in the respective soil. As can be differed into ionically bound, strongly adsorbed, coprecipitated (with carbonates, amorphous and crystalline metal oxides and silicates) and incorporated residual phases (ZEIEN and BRÜMMER 1989, WENZEL et al. 2001, KEON et al. 2001). Studies on old orchards soils, treated for decades with As bearing pesticides, show that vertical As movement due to leaching is possible (NAIDU et al. 2006).

Further geomorphological factors like rainfall, evaporation, erosion, parental rock and groundwater infiltration have an important influence on distribution and mobility of As in soils and cause a strongly varying (horizontal and vertical) distribution of As in soils.

Release of As:

It is important to understand the mechanism of As release from sediments into groundwater within aquifers. There are different possibilities of natural As release in environment:

A widely held belief is As being released by microbiological oxidation of organic matter under reducing conditions, using Fe and Mn atoms as electron acceptors. This results in dissolution of Fe- and Mn-oxyhydroxides and release of dissolved As^{V}, Fe^{II}, Mn^{II} and CO_2. Other micro-organisms are further able to reduce released As^{V} to As^{III} (BHATTACHARYA et al. 2007, NAIDU et al. 2006).

Another possibility is the weathering of As minerals under oxidic conditions. A change from reductive to oxidic environment can be induced due to excessive withdrawal followed by groundwater table decrease.

Oxidation of arsenopyrite is, for example, a main source of As in ore areas:

$$FeAsS\ (s) + 13Fe^{3+} + 8H_2O <-> 14\ Fe^{2+} + SO_4^{2-} + 13\ H^{+} + H_3AsO_4\ (aq) \qquad (1)$$

A third aspect is As release by ligand-exchange reactions as mentioned above.

Concerning mobilization of As, there are still many open questions left to be answered. Most studies were carried out in Bangladesh, in a moist tropical climate, but less is known about processes in other As affected parts in the world, especially in dry arid climates (BHATTACHARYA 2006). The influence of groundwater table on microbiological induced As release in aquifers requires also further investigations.

As in water:

As can be transported in water (surface or groundwater) both in dissolved form and as suspended matter. Typical concentrations in fresh water range from 0.1 to 80 µg As/l (NAIDU et al. 2006). The ratio of As^{V} to As^{III} in water ranges between 0.1:1and 10:1, depending on geochemical conditions within the aquifer. Like in soil solution, As^{III} predominates under reducing conditions and is more mobile than As^{V} (BHATTACHARYA et al. 2007). As^{V} is the thermodynamically most stable form under oxidic conditions, but high concentrations of As^{III} can still appear due to kinetic inhibition (OBERACKER et al. 2002):

$$H_2AsO_4^{-} + 3H^{+} + 2e^{-} <-> H_3AsO_3 + H_2O \qquad E0=0{,}66\ V \qquad (2)$$

$$2\ H_3AsO_3 + O_2 <-> 2\ H_2AsO_4^{-} + H_2 \qquad (3)$$

As in plants:

Foodstuff as As source has not received that much attention so far in research. There is a lack of information on As in vegetables and especially animals and animal products used for human nutrition (BHATTACHARYA et al. 2007). Plants receive As in different forms from contaminated soils, irrigation water and agrochemicals. Most studies dealing with As accumulation in plants are focused on 1) dietary uptake, mainly rice and typical vegetables grown in South-east Asia (e.g. NORRA et al.2005, KICZKA 2005, BARNES et al. 2005); or 2) the possibility of phytoremediation (FAYIGA et al. 2007).

There is to this day no evidence that As is essential for plants. In contrast, inorganic As is toxic to plants and causes symptoms like growth reduction, leaf wilting, violet colouration (due to elevated anthocyanin production), root discolouration and cell plasmolysis. A tolerance for most cultivated plants is established as 2 mg As/kg DW (dry weight related), exceeding causes loss of yield (KABATA-PENDIAS et al. 1984). Typical concentrations in terrestrial plants grown on uncontaminated soils are 0.02 to 7 mg As/kg DW, in edible plants 0.01-1.5 mg/kg DW (NAIDU et al. 2006). Highest values are commonly observed in roots and old leaves, while fruits and seeds are nearly uncharged. There is normally a linear relationship between soil and plant As content, except so called (hyper-) accumulators. These plants show an above-average As enrichment within their tissues due to active As soil to plant transfer mechanisms. Most promising hyper accumulator is the Chinese brake fern (*Pteris vittata*), with an enrichment potential of up to 23000mg As/kg DW on contaminated soil (BHATTACHARYA et al. 2007). Other plants belong to the so called excluder type, which maintain only low amounts of As in all plant parts over a wide range of As concentration in soil until threshold is reached and phytotoxicity appears (NAIDU et al. 2006). It is not possible to predict yield loss based on total As content in soil, because of extremely variable soil characteristics and different plant species behaviour, but there is a small margin between soil background values and phytotoxic As concentrations.

Table 2: Average As [mg/kg] contents of vegetables (NAIDU et al. 2006)

Vegetables	grown on uncontaminated soil	grown on contaminated soil
Egg plant (*Solanum melongena*)	0.23	2.3
Potato (*Solanum tuberosum*)	0.62	0.71-2.43
Hot pepper (*Capsicum ssp.*)	0.41	1.52

The sorption-desorption equilibrium in soils determines the bioavailibilty of As to plants. As verified in plants is mainly inorganic, but methylated forms also occur. As^{V} is transported into cell plasma by the phosphate transfer system, causing competition between As and P anions. As^{III} is taken up via aquaporines in non-ionic form (pH<9.2), s. figure 2 below.

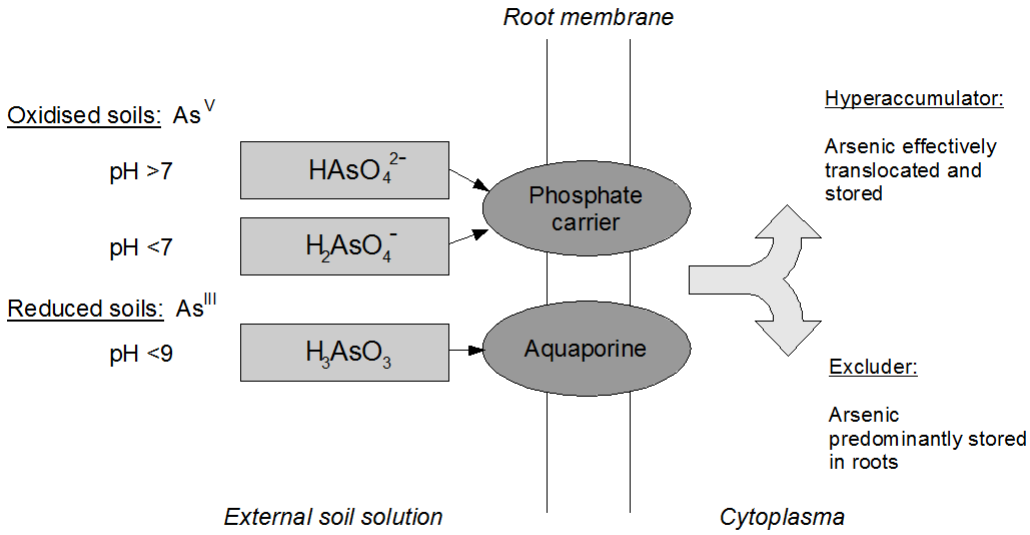

Figure 2: As uptake mechanism in plants (illustration by author, based on NAIDU et al. 2006)

Rhizospheric pH can differ from the surrounding soil up to two units, depending on plant species, nutrition situation (P maintenance) and local soil chemistry (high carbonate buffer can prevent soil pH decrease by exudates). As distribution in roots and shoots usually correlates with Fe (NAIDU et al. 2006). A useful parameter to express As accumulation in soil-plant system is the bioaccumulation coefficient:

Bioaccumulation coefficient = [As] in plant [mg/kg DW] / [As] growing medium [mg/kg soil] (4)

Another important and barely researched aspect is As transfer via fodder plants to livestock. The European Community released a threshold value in fodder of 2 mg As/kg DW (EG feeding stuff direction:2002/32/EG).

Toxicity:

As has influenced the human history for thousands of years, used both as poison and medicine and is known as the king of poison. Although As causes acute and chronic intoxications already at very low dose, animal experiments suggest a possible essentiality to human (SCHWEINSBERG et al. 2002). Toxicity of As is very complex, the two inorganic species arsenate and arsenite are more reactive than organic forms like MMAA and DMAA and the total As content in a sample allows no conclusion on its toxicity . One has to differ between acute and chronic poisoning and possible resorption paths. Acute As poisoning mostly appears after accidents with pesticides, rodenticides or insecticides and is furthermore sometimes used for homicidal intentions or committing suicide. Most acute toxic form of As is the gaseous arsine(AsH_3), which is primary taken up via inhalation. It reacts with haemoglobin and leads to destruction of the red blood cells by immune system. Chronic poisoning is caused by the inorganic forms As^{V} and As^{III}, which are mainly adsorbed in human gastrointestinal tract after oral ingestion (resorption of 60-90%) (SCHWEINSBERG et al. 2002). Inorganic As is supposed to act genotoxic, carcinogenic and teratogenic. Because of the similarity to phosphate, arsenate and arsenite can interact with up to 200 enzymes, most of them being part of the ATP synthesis pathway or the DNA synthesis and repair system. Transportation in human body results from As binding to enzymatic thiol-groups in blood, whereby As^{V} becomes reduced to As^{III}. As^{III} is considered to be 60 times more toxic to human organism than As^{V},while organic forms are nearly non-toxic (NAIDU et al. 2006).

Main part of As metabolism is the liver, where As^{III} becomes methylated to MMAA and DMAA, which can be easily renal excreted via urine. Clearance after resorption takes usually 4 days, but enrichment, mainly in liver, kidneys, heart and lungs, occurs easily if exposure is elevated. Studies in high As contaminated areas of Bangladesh confirm enrichment in ectodermic tissues like hair and fingernails (CHOWDHURY et al. 1999 in BHATTACHARYA et al. 2007). Acceptable daily intake (ADI) for inorganic As is qualified as 2 µg/ kg body weight (FIEDLER and RÖSLER 1993). The WHO released a provisional guideline for As in drinking water with 10µg As/l, but there is actually a discussion that it should be lowered to 0.17µg As/l, because 10µg As/l was the detection limit for As at that time (BHATTACHARYA et al. 2007). Due to the carcinogenic character of inorganic As, there exists no proper dose-response relationship and it is very problematic to assess a threshold value. Until today, there is no legislation in force in the EU for As in foodstuffs and the WHO standard is only provisional. The USEPA set a reference dose of $30x\ 10^{-4}$ mg/kg bodyweight/day as maximum acceptable daily load for man (MADL), equivalent to

220µg As per day for a 73kg person (NAIDU et al. 2006) . China replaced the old drinking water standard of 50µg As/l by 10µg As/l in 2007 (GUO et al. 2008) and in 2005 threshold values for foodstuff were released (s. table 3).

Table 3: Chinese food safety standard for inorganic As (mg/kg) in foodstuff, GB 2762-2005 (HEIKENS 2006)

Rice	Flour	Other cereals	Vegetables	Fruit	Poultry	Egg	Milk powder	Fresh milk:	Beans/pulses	Fish	Shellfish
0.15	0.10	0.20	0.05	0.05	0.05	0.05	0.25	0.05	0.10	0.10	0.5

Chronic exposure can cause amongst others diabetis melutis, cancer (esp. skin and liver cancer) and several forms of skin disease (e.g. keratosis and hyperkeratosis, pigmentation abnormality). In contrast to acute poisoning, no neurotoxic effects (affect on nerve conduction velocity) of chronic exposure to As in drinking water could be observed (FUJINO et al. 2006). The increase incident of chronic As exposure related symptoms in population is in general subscribed as arsenicosis. Main pathways of human exposure to As are digestion of contaminated drinking water and consumption of burdened foodstuff. Additional exposure is possible through air and dust inhalation, caused for example by As using facilities or coal combustion. Endemic spreading of arsenicosis is characteristic for regions with high geogenic As concentrations in groundwater. Figure 3 shows possible pathways of geogenic As uptake.

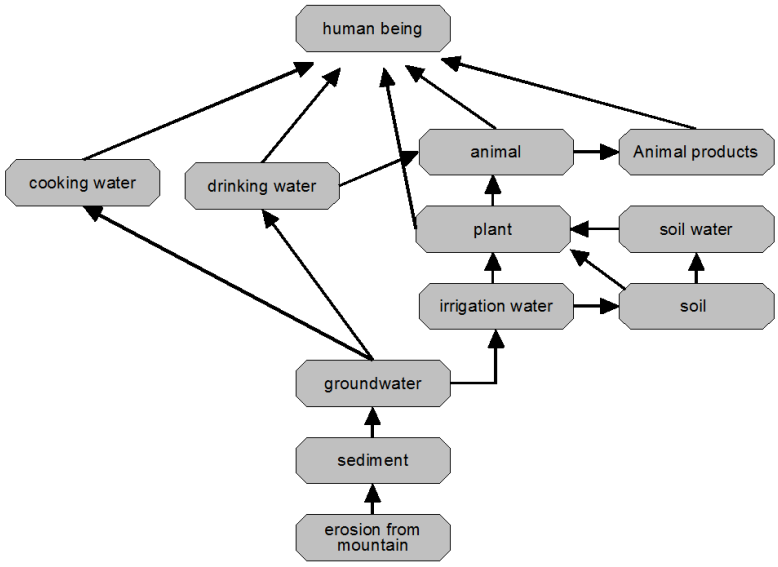

Figure 3: Possible pathways of geogenic As uptake (illustration by author)

In West Bengal and Bangladesh, the worst affected areas worldwide, arsenicosis occurred one to two decades after the installation of tube wells. Development aid in the past achieved successfully a replacement of pathogenic polluted surface water by groundwater as drinking water source. Unfortunately, no one tested the new drinking water for As contamination, provoking a creeping mass poisoning (WAGNER 2005, OLLE et al. 2007).

As concentrations in natural aquifers higher than 10 µg As/l are reported from Argentina, Australia, Bangladesh, Bolivia, Cambodia, Chile, China, Ecuador, El Salvador, Honduras, Hungary, West Bengal (India), Mexico, Nepal, New Zealand, Nicaragua, Philippines, Taiwan, Thailand, Uruguay, Vietnam and the United States. About 100 million people are used to drink water exceeding 10 µg As/l (BHATTACHARYA et al. 2007). This problem is well known among the developed countries, but in Asia this phenomenon was first reported in the early 1980s. Today, still new incidences are discovered in South America and almost nothing is known about the situation on the African continent.

Underprivileged countries are rather concerned than industrial and emerging nations. They often do not have alternative drinking water sources and the available water treatment techniques like ionic exchange, precipitation and Fe-Mn adsorption are not affordable. There are promising approaches in using simple hematite, siderite and mineral-sand columns for a small scale water purification (GUO et al. 2007 a and b). The challenge is to find out when the filter material needs to be exchanged and how to dump used material safely. Another developing country-specific problem is that malnutrition strengthens arsenicosis symptoms.

Unfortunately, no proper therapy for arsenicosis exists. Chelating agents like dimercaprol (British-anti Lewesit, BAL) are able to reduce As burden in human organism, but the treatment is expensive and not appropriate for long-term use.

As situation in China and Inner Mongolia:

During the last three decades, some widespread areas with high As contaminated groundwater have been identified in the People's Republic of China. They are mainly situated in Shanxi Province (Datong basin), Xinjiang Uygur Autonomous Region (floodplains north of Tian Mountain) and in the Inner Mongolian Autonomous Region. They are closely connected with the appearance of endemic arsenicosis in the population and are

attributable to the local geological-geochemistry environments (LIN et al. 2002).

In Inner Mongolia Autonomous Region, endemic arsenicosis and high As load in groundwater were first reported in the 1970s from Linfeng City. Later, this phenomenon also emerged in Keshenketeng County, Tumote Basin and Hetao-Plain (for more details, see chapter 2). One of the first epidemiological studies showed, that more than 400.000 people in the Inner Mongolia are used to drink water exceeding the old Chinese drinking water threshold value of 50 µg As/l with an affected area of about 3.000km². More than 3.000 cases of arsenicosis spread over 776 villages could have been confirmed (MA et al. 1995 in GUO et al. 2008). The main challenge for the local government is now to find alternative, non-contaminated water sources or affordable water conditioning treatments in order to defeat this epidemic plague.

1.3 Problem

These are the question to be answered in this diploma thesis:

1. Does horizontal or vertical enrichment take place in soil as a consequences of irrigation with high As groundwater?

2. How are quality and quantity of As burden at the sample sites?

3. What is the annual As input on the fields?

4. How is the As situation within the surroundings?

5. Is there any risk to the inhabitants there?

Modification of the questions after the field trip:

What are the consequences of irrigation with high As water for 3 years?

2. Brief introduction in the investigation area: Hetao-Plain

2.1 Geography

The Hetao-Plain, also called the Great Bend or Hetao Basin, is situated in the western part of the Inner Mongolia Autonomous Region and covers an area of about 10.000km² (GUO et al. 2008). It is restrained by the Huang He (Yellow River) in the South and by the Yinshan Mountains in the North (figure 4). About 100 villages belong to this administrative district, which is subdivided into the three counties Linhe, Hangjin and Wuyuan (LIN et al. 2002).

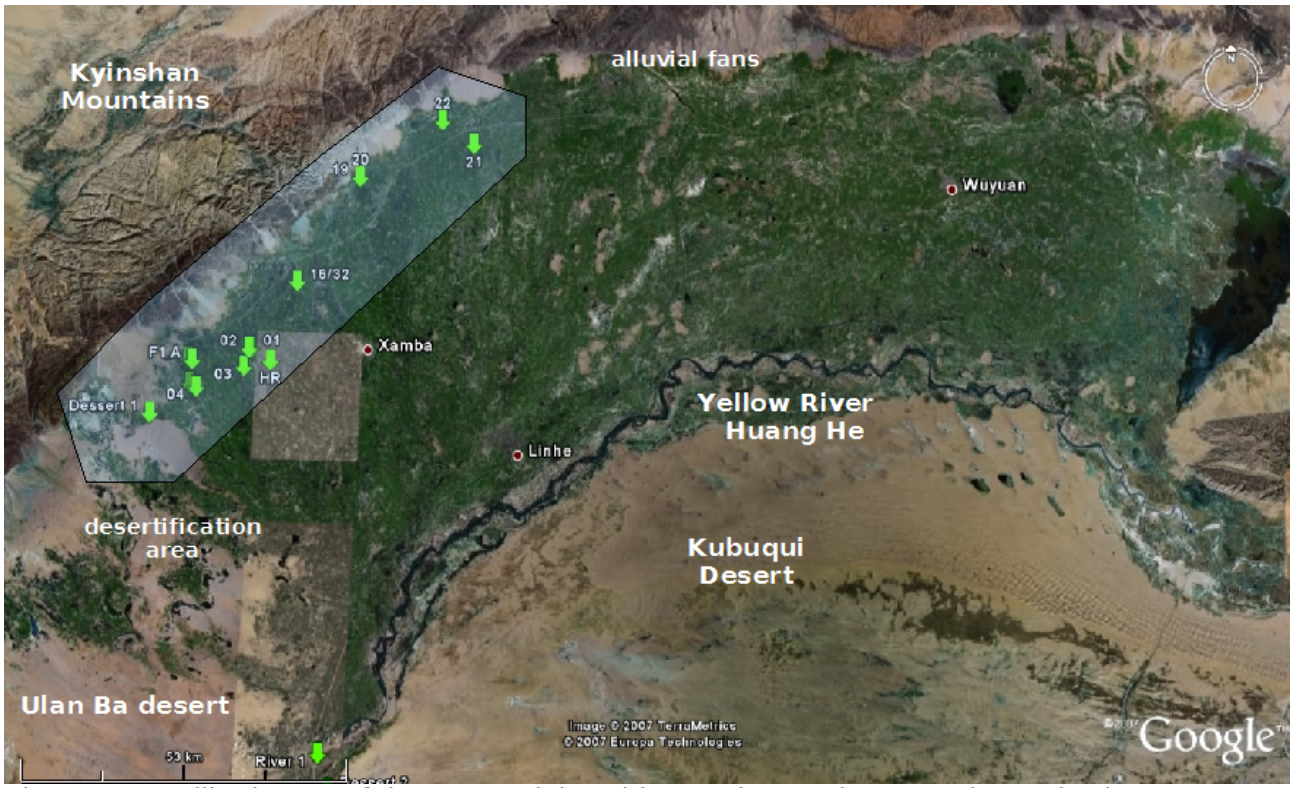

Figure 4: Satellite image of the Hetao-Plain, with sample area in NW and sample sites (Google earth™ 2008, modified)

2.2 Climate

The climate is cold and arid with average temperatures between 5.6 and 7.8°C, annual rainfall of 120 to 220mm and 2.000-2.5000mm evaporation (GUO et al. 2008, LIN et al. 2002). According to the Köppen-Geiger Climate Classification, Hetao-Plain belongs to the cold arid dessert climates, designated as Bwk type (KOTTEK et al. 2006). Figure 5 represents the annual climatic situation in Batou, main city of the neighbouring Hubao-Plain, about 250km east of the study area.

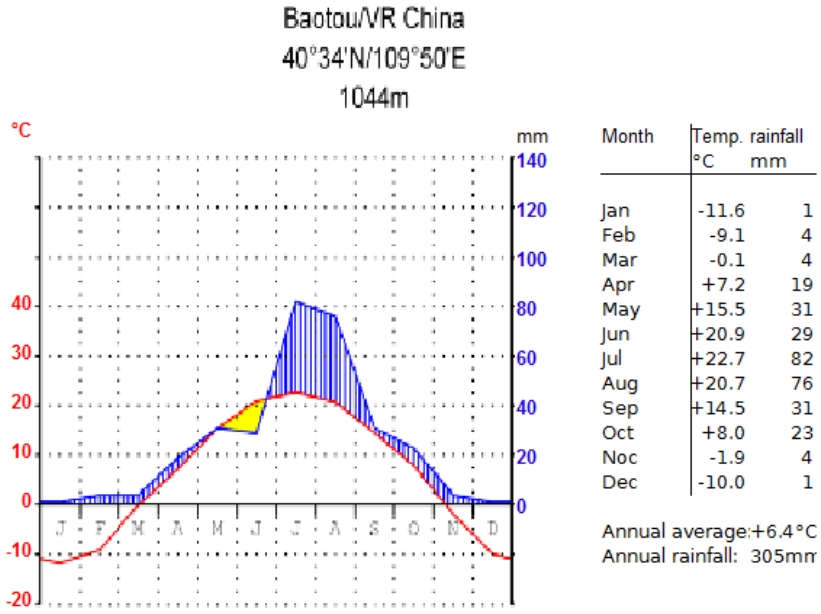

Figure 5: Climatic situation in Baotou in form of a Walther/Lieth climatic diagram (translated into english) http://upload.wikimedia.org/wikipedia/commons/thumb/5/5b/Klimadiagramm-deutsch-Baotou-VR_China.png/800px.png

2.3 Geology and morphology

Today's Hetao Basin is an alluvial plain located in a Jurassic fracture zone. In Tertiary, up to 2.000m thick red sandstone and shale layers including halite and gypsum deposits arose under oxidative and evaporative conditions (LIN et al. 2002). They became overlaid in Quaternary by deposits of heterogeneous inland lacustrine facies (in the Northwest and

East of Hetao-Plain), alluvial material from the Yellow River (mainly in the South) and alluvial-pluvial sediments from the Yinshan Mountains (in the Northern part). The lacustrine sediments of the Northwest and East are supposed to be accumulated during the late Pleistocene and consist of fine sand layers with included organic enriched clays (GUO et al. 2008). Today's Hetao-Plain is covered with Holocene alluvial sediments transported by the Huang He, reaching 20 to 50m in the North and 200 to 1.500m in the South (Zhang et al. 2002, LIN et al. 2002). This Holocene material ranges from muddy clay over silt up to fine sand and varies strong both in spatial distribution and organic content. Especially ox-bow lake systems of the Huang He are rich in organic matter (LIN et al. 2002).

In the North, the Yinshan Mountains are neighbouring (s. figure6). They are mainly composed of Jurassic to Cretaceous metamorphic rock complexes (with slate, gneiss and marble) and hold large-scale deposits of sulphur and poly-metallic sulphide ores, which are mined since 40 years (GUO et al. 2008, Zhang et al. 2002).

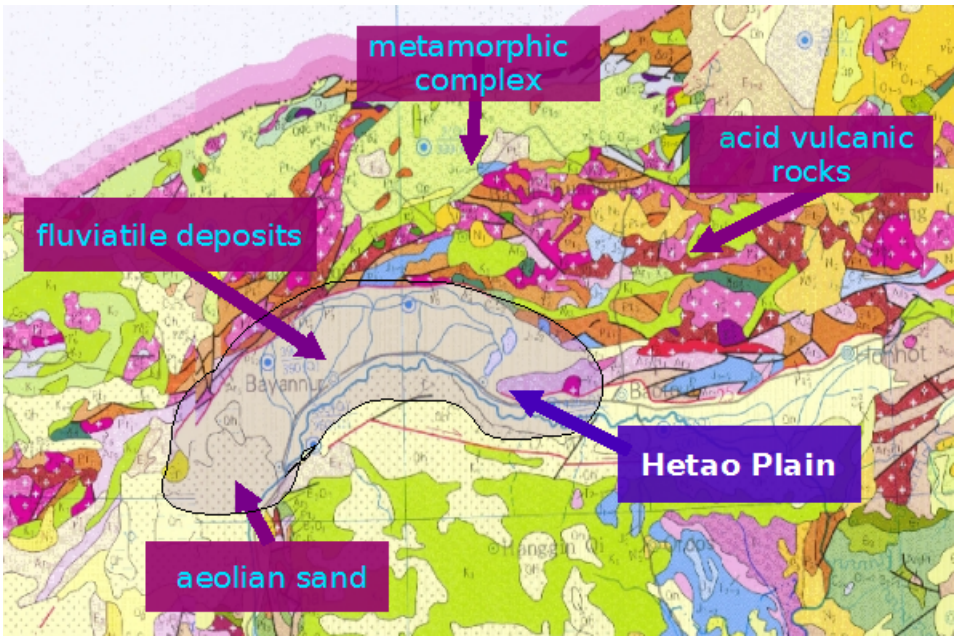

Figure 6: Geology of Hetao-Plain and surroundings (CHENG et al. 2000, modified)

2.4 Hydrology: groundwater and aquifers

Groundwater in Hetao-Plain belongs to the so called Na-Cl-HCO_3 type (GUO et al. 2008). It is characterized by high salinity, neutral to weak alkaline pH and high contents of dissolved organic matter. There are three to five different aquifer systems within a depth of 200m, strong varying both in chemical composition and water quality (LIN et al. 2002). For drinking water use and irrigation, only the shallow aquifers with up to 100m depth are used. These multi-layered groundwater aquifers are situated in the Quaternary sand sediments and show a groundwater table between 5 and 20m. In the North these aquifers are located in sediments of alluvial fans and river banks, in the rest of the plain the aquifers are mainly located in the alluvial-lacustrine deposits (GUO et al. 2008).

Predominantly negative redox potentials, high concentrations of dissolved Fe, Mn, HCO_3^-, P and S_2^- and low concentrations of NO_3^- and SO_4^- at the same time testify moderate till strong reducing conditions within the lacustrine aquifers. Especially organic rich lacustrine sediments in the Northwest exhibit strong reducing conditions, even methane and hydrogen sulphide can emerge here. The reducing conditions are a result of high microbiological oxidative decomposition, slow groundwater flow rate and disabled oxygen diffusion because of embedded clay layers (GUO et al. 2008). The direction of groundwater flow is from North to Yellow River and groundwater becomes refilled by rainfall and laterally infiltrating meteoric water from the mountainside (GUO et al. 2008, Zhang et al. 2002).

2.5 Anthropogenic changes

The entire Hetao-Plain is a strongly anthropogenic formed rural area, which has been influenced for centuries by an artificial irrigation system. Without this canal system. the areal would most likely be a desert or a half-desert as the terrain South of the Yellow River. The fertile plain is known to be one of Chinas oldest food producing area (LIN et al. 2002). Nowadays Hetao-Plain is subject to a broad structural strange. Locals began to modernize the traditional cropping system during the last decades in order to increase food productivity. This agricultural modernization mainly expresses itself in increasing mechanization and use of artificial pesticides and fertilizers. Additionally, heavy industry found its way into the few major cities and caused a rapid decrease of regional air quality.

Several serious anthropogenic environmental changes can be observed in Hetao-Plain. A serious problem is for example desertification, especially in the South, where the Ulan Ba desert is inexorable moving forward against the precious farmland. Another severe effect is soil salinization, leading to rising yield reduction up to total desertion. Caused by irrigation mismanagement and high evaporation, 35-45% of the soils within the plain are affected meanwhile (LIN et al. 2002, GUO et al. 2008).

2.6 Present results of As research in Hetao-Plain

A first important indicator for high As burden in an inhabited region is the occurrence of arsenicosis symptoms. During the early 1980s, first pathological changes like hair baldness, dermatosis and dermal cancer emerged in the local population, in particular in the north of the plain. Proximate studies showed that As caused dermatosis is widespread in Hetao-Plain, with an affected area of about 6.100km^2 and 180.000 inhabitants (LIN et al. 2002, Environmental Protection Agency of Inner Mongolia Autonomous Region 1995 in Zhang et al. 2002, GUO et al. 2001). A correlation between pathological changes in population and As contamination of the groundwater could given proof that the concerned persons are those who obtain drinking water from tube-wells (s. figure 7). Latest hydrological investigations of Hetao-Plain's groundwater display As concentrations clearly exceeding the Chinese drinking water threshold value of 10 µg/l (0.6 to 572 µg/l in GUO et al 2008; average content of 201 µg/l in Zhang et al. 2002). About 75% of the As verified is the quiet toxic trivalent form As^{III}, the rest is a mixture of As^{V} and methylated organic compounds. Further it could be shown that high As contaminated groundwater is bound to the shallow alluvial-lacustrine aquifers, which are rich in organic matter and show strong reducing conditions. GUO at al. (2008) measured an As content in these sediments between 7.3 and 73.3 ppm, with an average of 18.9 ppm. To this day, As distribution in groundwater of Hetao-Plain is poorly documented and the reasons for high concentrations are not well understood yet. There are two main theories concerning the source of the As. Zhang et al. 2002 suppose the dissolved As to be allochthonous in nature. It becomes released from Yinshan Mountain ores by mining activity and weathering and is transported into Hetao-Plain by lateral groundwater flow. He carried out isotope analysis of $^{87/86}$ Sr, $^{206/204}$ Pb and $^{207/204}$ Pb and found similarities in the isotope ratios from mine water with the As affected groundwater in Hetao-Plain. The Yellow River is considered to be a potentially source of As, too (Zhang et al. 2002, GUO et al. 2001).

In contrast, SMEDLEY et al. (2003) and GUO et al. (2008) reckon the regional geological underground and the prevailing geochemistry and hydrochemistry as the source of As release. Sequential extractions show that 60-85% of the As found in the lacustrine sediments is bound to Fe-Mn oxides, 4-20% is subdivided into exchangeable As, carbonate bound As and As fixed in organic matter and sulphides.

There are three possible different ways of As release:

1. Biological decomposition leads to a reductive environment in the lacustrine sediments and bacteria use the Fe-Mn-Oxides as electron acceptors, whereby crystal structure is destroyed and bound As (in inner-sphere complexes) becomes released -> reductive As dissolution.

2. Exchangeable As (bound in outer-sphere complexes) is affected by high pH, ionic activity and presence of other anions (e.g. HCO_3^-, PO_4^{3-})-> competitive As release .

3. Weak crystallized Fe- and Mn-Oxides alter into more complex structures because of diagenesis and loose thereby binding sites for As.

Once released, As enrichment takes place because of the slow groundwater flow rate. LIN et al. 2002 discovered, that arsenicosis symptoms in Hetao-Plain increase from east to west and are linked with local geochemical environment. Quantity and quality of arsenicosis symptoms correlate with aquifers under reducing conditions, where high contents of As and dissolved organic compounds can be found. Furthermore, distribution of the symptoms is not related to total As content in drinking water, but with As^{III} and organic As.

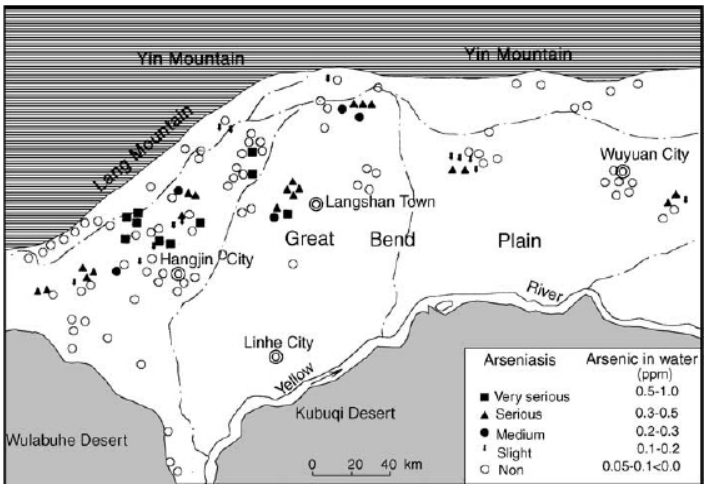

Figure 7: Distribution of As and arsenicosis (=arseniasis) in Hetao-Plain (Lin et al. 2002)

3. Methodology

3.1 Study site, sample taking and information survey

In the following, sampling and sample preparation in field are described respective for soil, plant and water.

3.1.1 Selection and short description of the study site

According to the intention of this diploma thesis, main challenge of the field work was the search for a capable and representative village within Hetao-Plain, where high As contaminated groundwater is used for field irrigation. Contrary to our expectations, it was difficult to find such groundwater irrigated fields at all, because the canal system mentioned in chapter 2 is still well-kept and widespread used. Fortunately, Prof. Guo knew a village in the Northwest called Yong-Ming (~Village of the two temples), where farmers are used to irrigate their fields with groundwater.

Yong-Ming is a typical farming village, consisting of small to middle sized homesteads with about a dozen families living there on agriculture. Farmers mainly grow sunflowers, corn (maize), wheat and vegetables and keep animals like cows, sheep, goats and chickens. Crop production exceeds by far subsistence agriculture, especially sunflowers own a key role in everyday life. The entire area is well known for its production of sunflower oil and people use the dried stems as firewood substitute for stove firing.

Finally, two fields (designated as field 1 and field 2, see figures 8 and 9) were chosen to be sampled: a sunflower (*Helianthus annuus*) field and a field with mixed culture of corn (*Zea mays*) and wheat (*Triticum spp.*). Both fields are irrigated by tube wells and the As quick test (Merckoquant® Arsen, Merck) displayed for each a total As concentration of about 200 µg/l. Air-line distance between both is about 700m.

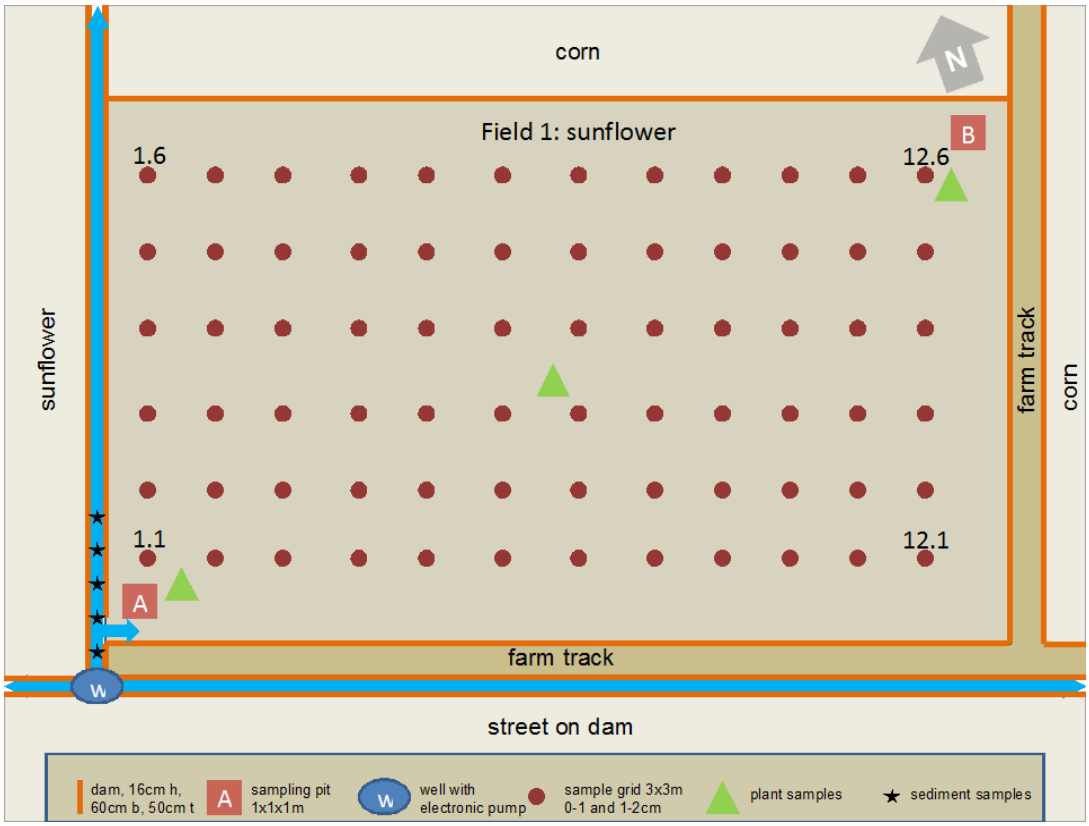

Figure 8: Sketch of field 1

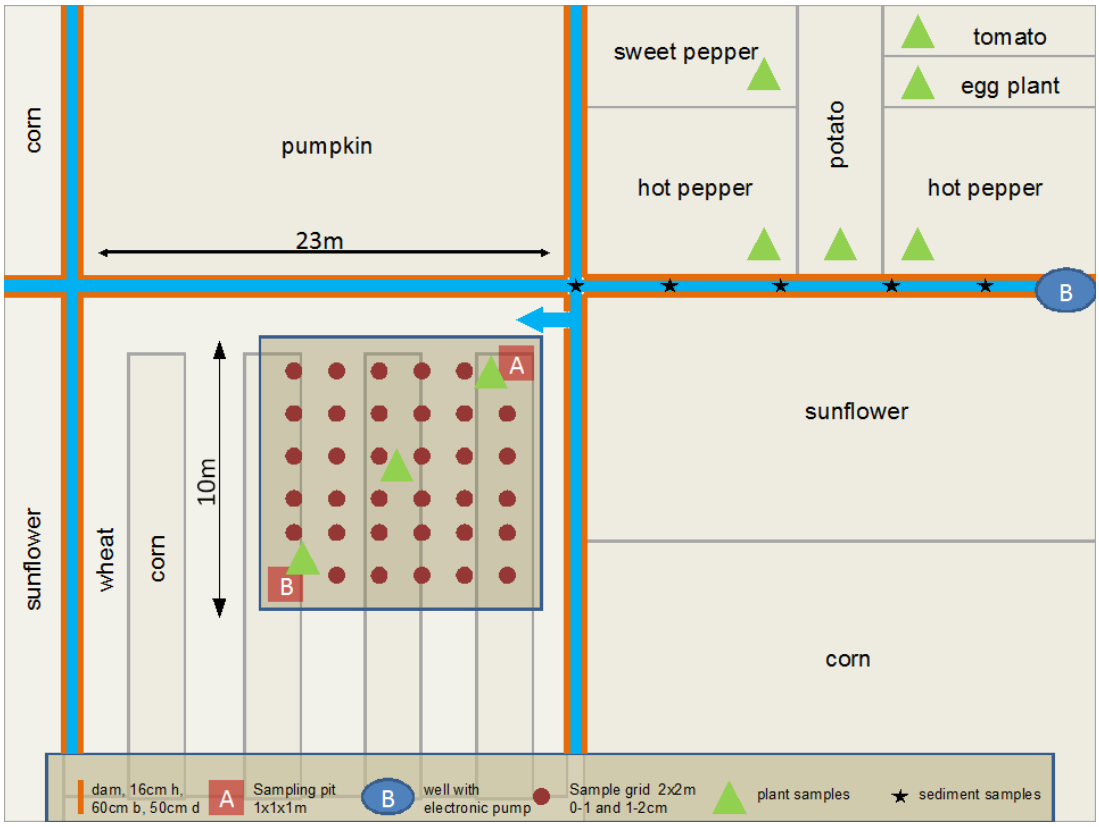

Figure 9: Sketch of field 2

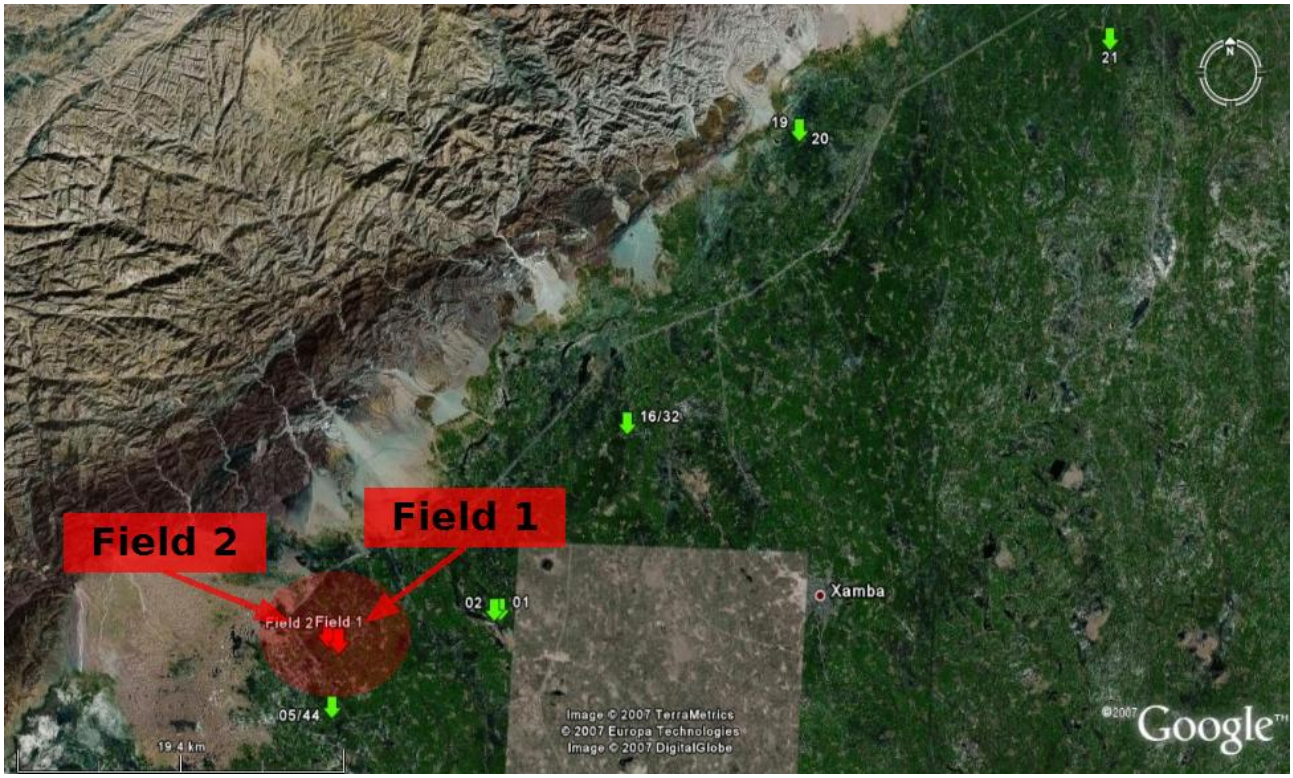

Figure 10: Location of the sample fields in the NW of Hetao-Plain (Google earthTM 2008, modified)

3.1.2 Sampling: Motivation and procedure

3.1.2.1 Water

Motivation:

Groundwater is used both as foodstuff and for irrigation and is in this case study regarded as main input factor of As in field soil, plant and human being. Arsenicosis is in Hetao-Plain straight linked with consumption of As burdened groundwater and pathological changes correlate mainly with As^{III} concentrations (LIN et al. 2002, Environmental Protection Agency of Inner Mongolia Autonomous Region 1995 in Zhang et al. 2002, GUO et al. 2001). Hence it is necessary to determine the quantitative and qualitative As load of groundwater to estimate daily human uptake and annual entry in field soils. In order to obtain further information about general groundwater quality, conditions in aquifer and As source, samples for cation and anion analyses were taken.

Procedure:

Main focus for water sampling was on the wells at field one and two, but samples were additionally taken in villages and homesteads in nearby surroundings if high As contamination was expected (s. green arrows in figure 10).

Following water samples were drawn at each location in 50ml plastic flasks:

1. Anion sample of 50ml

2. Cation sample of 50ml for trace element analysis (including total As)

3. As^{III} sample of 50ml (by using special As^{V} restraining cartridges (MetalSoft Center inc.) (WAGNER 2005)

Each sample was filtered through 0.45 µm millipore cellulose-acetate filter (Millex-HV 0,45um syrange filter units)to separate suspended matter. After sampling, cation samples were acidified with 50µl of concentrated HNO_3 to prevent precipitation occurrence. Later, filters were dried for 24h at 105°C and water samples were stored cooled until analysis.

Table 4: Overview water samples

Sample type:	Number of samples:
-Anion	10
-As_{total} (=Cation)	10
-As^{III}	10
-Suspended matter (0.45 µm filter)	10

3.1.2.2 Soil

Motivation:

Soil can be both sink and source for pollutants (in particular for heavy metals), depending on soil characteristics like mineralogical composition, organic content, geochemical surrounding, soil texture and type. In this case, anthropogenic influence is mainly manifesting in irrigation and field preparation (use of artificial fertilizers and pesticides, ploughing, firing, heavy machines) and is therefore considered to be an additional important factor for the behavior of applied As in field soil. Extensive soil examinations are necessary to evaluate in which soil compounds As appears and if there is vertical or horizontal enrichment.

Procedure:

On each field two soil pits (A and B) of $1m^3$ were excavated in order to gather the prevalent pedology. Pit A is in each case next to the water inlet located and pit B on the diagonal opposing site (see figures 8 and 9). After soil analyses (according to SPONAGEL 2005), each single horizon was sampled using a small plastic shovel. In addition, profile samples from 0-100cm depth (in depths of 0-1, 1-2, 2-5, 5-10 and then in steps of 10cm) were taken. In order to examine the horizontal As distribution in topsoil, a grid was installed and at each intersection the first 0-1 and 1-2 cm were sampled. The grid on field 1 covered the entire field and had a size of 36x18m with $3m^2$ sized meshes and smaller $1m^2$ meshes around the water inlet. Field 2 was very large-scaled (about 23x150m), so we decided to install a smaller grid of 10x10m with $2m^2$ meshes, beginning at the water inlet. A similar approach was pursued from DITTMAR et al. (2007), examining As distribution in paddy soils of rice fields in Bangladesh. Also the first centimeter of the canal sediments was taken in regular intervals in order to figure out if As precipitates together with iron oxides before reaching the field. The tube well on field 1 was located next to the inlet, but on field 2 the water had to flow 35m before it reaching the field. The situation is accurately reflected in figure 8 and 9 respectively.

Each sample was first stored in plastic or paper bags and then dried for 24h at 60°C in a drying chamber at the Department Water Resources & Environmental Science, China University of Geosciences in Beijing.

Table 5: Overview soil samples

Sample type:	Number of samples:
-Soil pit horizons	10
-Soil pit 0-100cm	52
-Topsoil sampling grid 0-1 and 1-2cm	198
-Canal sediments	15

3.1.2.3 Food chain

Motivation:

Plant analyses are an essential part of this study. Plants, acting as a link between soil and food chain, are beside drinking water a main source for As uptake in affected areas. Some plants are able to enrich As in their inner parts, even when there is little As in soil. Important are those plant parts which are eaten by human, but As can intrude the food chain as forage, too. Roots were sampled as well, because they act as an active barrier between plant and soil. Intention is to analyse the As content in different plant parts and to calculate soil-to-plant transfer coefficients. Plant samples have been taken from each field and the surrounding area. In addition, eggs and human hair samples were collected randomly to monitor the As burden.

Procedure:

Three plants were chosen in consideration of stage of maturity for sampling from each field (field 1= sunflower; field 2= maize), one at each soil pit and one from the middle of the grid. Seeds were not yet mature (one month till harvest), but the plants were almost full-grown.

From each plant, several samples from stem, leave, root and seeds were taken (stem and leave samples from varying height):

-the sunflower leaves had to be halved because of their huge size, from corn leaves equal sized pieces from the top, middle and beginning

-depending on thickness, stem sections between 10 to 20cm length

-sunflower seeds from a 2cm broad transect from edge to centre of inflorescence, maize seeds were taken randomly from corn ear

-from root both fine and coarse roots.

Vegetable had been collected from a neighbouring field to field 2. In contrast to sunflower and corn, only the edible parts were taken here. Further, eggs and hair samples were taken from other As affected villages in the surroundings.

All samples were kept stored in fridge of the public health department in Xamba during the field trip. Later, plant samples (except roots) were cleaned carefully with pure water to

remove adherent fine soil and dust, cut and dried at 105° for 24h. Root samples were dried at 40°C to protect iron-mineral coatings.

Table 6: Overview food chain samples

Sample type:	Number of samples:
-Sunflower	26
-corn	29
-Vegetable	11
-Egg	4
-Hair	7

3.1.2.4 Information survey

Various information were collected during field trip, using preassigned questionnaires and check lists with the help of professor Guo's students accompanying us as interpreters. This kind of on-site information acquisition is very important, especially for subsequent analysis understanding and interpretation. The check lists for sample site characterization and soil pit description are listed in appendix, table 38.

3.2 Analyses: methods, settings and sample preparation

While sampling was carried out corporately in a one week field trip in July, a part of the sample preparation and all subsequent analysis were done at the IMG between August and December in 2007.

3.2.1 X-ray spectroscopy: theory

X-ray spectroscopy owns a key-role position in this study. A total number of about 298 samples were analysed with three different X-ray spectroscopy methods. It is about the energy dispersive X-ray fluorescence spectroscopy (ED-XRF), the micro synchrotron X-ray fluorescence spectroscopy (µ-SyXRF) and the X-ray diffraction (XRD).

X-Ray spectroscopy theory:

X-rays are in the electromagnetic spectrum situated between gamma rays and extreme ultraviolet, with a wavelength of 0.1 to 300 Å and an energy of about 0.125 to 125 keV (NAIK 1999). The relation between the radiations wavelength λ and energy E is described as

$$E\ [keV] = 12.4 / \lambda\ [Å] \qquad (5)$$

The two most important ways of generating X-ray photons are atomic inner shell transitions and emissions by free electrons.

Atomic inner shell transition occurs, when an electron from the inner shell of an atom is removed by photon excitation exceeding its binding energy and an outer shell electron with higher energy jumps in that vacancy. This act is called photoelectric effect or photoeffect (KRAMAR 1999). The energy difference of the electron transferred is compensated during this process by releasing energy in form of an X-ray photon with a certain wavelength. This secondary or fluorescence radiation is characteristic both for each atom and each orbital transition. Inner shell transitions are described through the Siegbahn notation as K- and L-series (NAIK 1999). For example, the $K_{\alpha 1}$-line of the As K-series features an energy of 10.54 keV (PFENNIG et al. 1995).

The correlation between the emitted X-ray's wavelength λ, the atomic number Z and the line transition is shown by Moseley's law:

$$\lambda = K_1/(Z-K_2)*2 \qquad (6)$$

with K_x as a line depending constant (PAVICEVIC et al. 2000).

By measuring the emitted characteristic energy spectra of a sample with X-ray fluorescence spectrometer (XRF), it is possible to determine its qualitative and quantitative elemental composition.

Emission by free electrons is another important source of X-rays. It occurs, when free electrons become accelerated with an intensity being proportional to the acceleration^2. This primary X-ray is used for sample excitation in XRF.

There are three main sources used for creation of primary X-ray, X-ray tubes, synchrotron accelerators and plasma generators (NAIK 1999). If a beam of primary X-rays hits matter, it can cause atomic inner shell transitions and so called bremsstrahlung. Bremsstrahlung appears if an electron slows down strongly and its kinetic energy becomes transformed to electromagnetic radiation.

3.2.1.1 ED-XRF

Introduction:

The energy dispersive X-ray fluorescence spectroscopy (ED-XRF) is a widely-used, physical based and non-destructive method for multi-elemental analyses. Samples can be qualitatively and quantitatively analysed, from sub-ppm up to high percentage concentrations (KRAMAR 1999). The ED-XRF is used to determine the fluorescence radiation emitted by the sample after exciting it with primary X-ray.

Components:

A typical ED-XRF consists of several complex elements as shown in figure 11. The XRF (spectrace 5000, spectrace instruments) used for sample analyses in this study features an X-Ray tube as primary photon source. Free electrons are generated by a heated tungsten filament and become accelerated in a strong electromagnetic field (NAIK 1999,

KRAMAR 1999). X-Ray characteristics can be influenced by anode material, connected voltage and current. In order to optimize signal-to-noise ratio, primary filters can be used like palladium filter, which reduces high-energy bremsstrahlung. Beam and sample collide in the so called sample unit by an angle of 45°. The detector system is attached here in order to determine spectral distribution and intensities of fluorescence radiation emitted by the sample. This is done by a semiconductor detector based on lithium drifted silicon, converting fluorescence radiation into electrical signals. The signal passes both pre- and main-amplifier, pile-up rejector, analogue-to-digital converter and finally a multichannel analyser (KRAMAR 1999). Data conversion and evaluation were done with programs written by U. Kramar at the IMG.

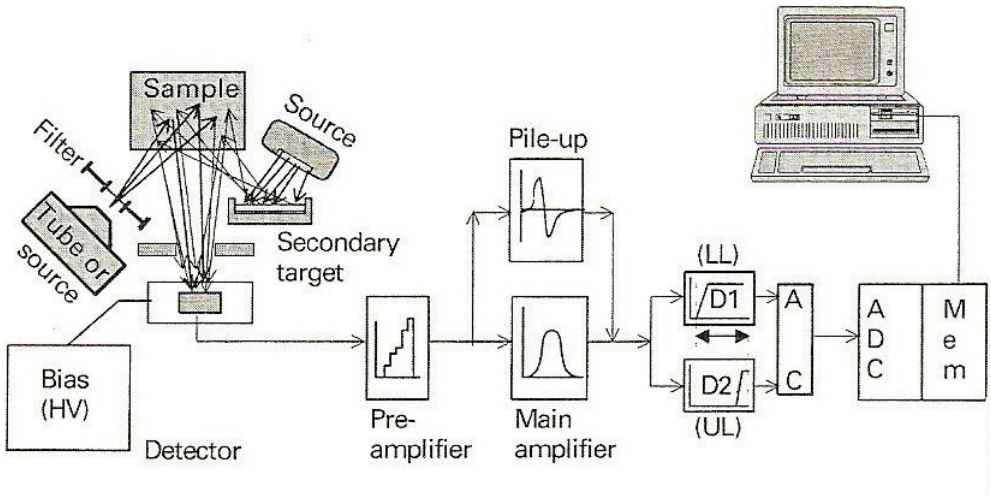

Figure 11: Layout of an ES-XRF (KRAMAR 1999)

Sample description and preparation technique:

The XRF was used to get qualitative and quantitative information about the main and trace elemental composition of the soil and sedimentary samples. In total, 280 samples were analysed with the ED-XRF in the form of bulk powder samples. Due to sample composition, X-Ray penetration depth varied between some µm for light and up to 100µm for heavy elements (STRELI et al. 1999). This high surface sensitivity requires very homogeneous samples and a thin carrier foil. To achieve this, the dried soil samples were milled with an oscillating agate stone disc mill and filled in spectro-cups with 6µm thin Mylar foil as carrier.

Settings, standards and detection limits:

Table 7: Used settings, ED-RFA

Filter:	Pd	Al
Tube voltage:	50kV	15kV
Tube current:	0.05mA	0.15mA
Lifetime:	1000sec.	600sec.
Max. energy:	40keV	10keV

Table 8: Measured components, instrumental detection limits (IDL), used standards with reference, recommended and information values (GOVINDARAJU 1994)*

Standard	**K2O** [%]	**CaO** [%]	**TIO_2** [%]	**MNO** [%]	**FE_2O_3** [%]	**NI** [PPM]	**CU** [PPM]	**ZN** [PPM]
Soil 5	2,24	3,10	0,78	0,11	6,36	13,0	77,00	370
Soil 7	-	-	-	0,08	-	-	11,00	104
GXR 5	1,06	1,17	0,37	0,04	4,84	75,0	354	49,0
GXR 2	1,65	1,30	0,50	0,13	2,66	21,0	76,0	530
IDL	<0.5	<0.1	<0.02	<0.02	<0.02	<20	<7	<5

Standard	**AS** [PPM]	**BR** [PPM]	**RB** [PPM]	**SR** [PPM]	**Y** [PPM]	**ZR** [PPM]	**NB** [PPM]	**PB** [PPM]
Soil 5	94,0	5,00	140	330	21,0	220	9,00	130
Soil 7	13,4	-	51,0	108	21,0	185	-	60,0
GXR 5	11,2	7,80	41,0	110	16,0	140	6,70	21,0
GXR 2	25,0	3,20	78,0	160	17,0	269	11,0	690
IDL	<5	<3	<2	<2	<3	<5	<2	<5

3.2.1.2 µ-SyXRF

Introduction:

Micro-synchrotron X-ray fluorescence analysis (µ-SyXRF) uses similar to ED-XRF fluorescence radiation to determine qualitative and quantitative elemental composition of unknown samples. It is a non-destructive, multi-element analysis method based on X-Ray excitation, too, but there is an important difference (HEINRICH 2007). Synchrotron radiation is used as photon source instead of an X-Ray tube. Synchrotron radiation, including among all kinds of radiation X-ray, occurs when accelerated electrons with high energies are forced into a circular path. This can be achieved in a storage ring of a synchrotron by using strong bending magnets. Synchrotron radiation is emitted highly

concentrated in form of a narrow cone in tangential direction of the electrons' movement. The beam can be focused to a micro-beam with just a few µm in diameter using focusing optics like slits, attenuator, multilayer monochromator and x-ray-lenses (NAIK 1999). Another advantage is that synchrotron radiation is polarized in the orbital plain, so scattering is reduced and detection limits decrease (STRELI 1999). These qualities allow combining trace elemental detection at sub-ppm level with high spatial resolution. By moving the sample in respect of the beam, an elemental mapping can be performed. µ-SyXRF is used in the geosciences now for many years (KICZKA 2005; KRAMAR et al. 2007, for example) and can be considered as a state-of-the art technology, although handling is quiet complex.

FLUO-beamline at ANKA:

The µ-SyXRF examinations of this study have been carried out at the FLUO-beamline of the Angströmquelle Karlsruhe (ANKA) at Forschungszentrum Karlsruhe (FZK). Table 9 describes beamline characteristics and figure 12 represents experimental set-up.

Table 9: Characteristics of the FLUO beamline (HEINRICH 2007)

Energy range	1.5keV - 33keV
Energy resolution [ΔE/E]	$2x10^{-2}$ or white light
Source	1.5 T Bending magnet (EC = 6.2keV)
Optics	Double multilayer monochromator with W-Si multilayers in 2.7 nm period Focusing optics: compound refractive lenses (CRL); poly-capillaries
Flux at sample position	Poly-capillary: $1x10^{11}$ph/s @ 17keV (12µm x 12µm) CRL: $2x10^{9}$ph/s @ 17keV (5µm x 2µm)
Beam size at sample	5mm (horizontal) x 2mm (vertical) down to 2µm x 1µm
Experimental setup/ sample environment	Vacuum (10^{-2}mbar, inert gas, air)
Experimental setup/ detector	1 Ionization chamber, 1 PIN-Diode for monitoring Si(Li)-energy dispersive detector 133eV average resolution at 5.9keV, 52µs sharing time Silicon multicathode detector, 50mm^2 area throughput > 100kcps
Software / Data treatment/Evaluation:	SPEC, AXIL, Spectran, MC-simulation (MSIM), newplot, PyMCA

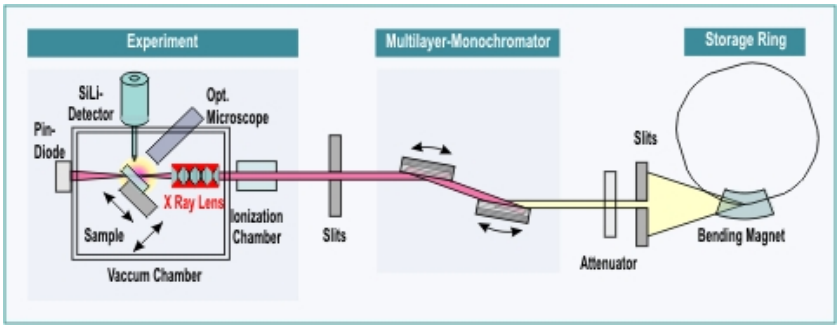

Figure 12: Set-up of the FLUO-beamline (HEINRICH 2007)

Sample description and preparation technique:

From each field a root (from sample pit A, carefully cleaned considering possible mineral coatings) and soil sample (0-1cm depth, sample pit A) were analysed by µ-SyXRF. The first step of thin-section preparation is to embed dried sample material in epoxy casting resin (3:1 mixture of epoxy and curing agent) and set it under vacuum for 30 minutes to remove air bubbles. After drying for 12 hours at 60°, the sample pieces were cut with a stone saw, lapped with silicon carbide (grain size of 600 and then 1000) and attached to microscope slides with heat-removable quartz resin. To reduce matrix effects and improve detection limits, samples should be as thin as possible (at least 100µm), have a constant thickness and a plane and wave-less surface (KRAMAR et al. 2007). Therefore the slides were lapped again with silicon carbide of 600 and 1000 grain size to a final thickness of 100µm. The surface was polished with poly-chrystaline diamonds of 3 and 1µm grain size afterwards (DP-spray®, Sommer). Thin-sections were finally removed from slides by heating and transferred to sample holder with sticky Mylar foil as carrier. The thin section preparation was carried out with support of K. Nikoloski, preparator at the IMG.

Measuring at FLUO-beamline:

Measuring of the 4 samples was done from November 12. to 16. in 2007. Samples and used settings are described in table 10 and 11. A certified standard named StHs6 (St Helens andesitic ash glass) was used for calibration (described in JOCHUM et al. 2000). Like ED-XRF, detection limits depend on atomic number, beam energy and measuring time. In case of As, detection limit is about 1-1.5 ppm (by 12,5keV and 10-25sec.) and has to be considered as a semi-quantitative method. For data evaluation and spectra fitting, the program PyMCA (Vers. 4.2.1), developed by the Beamline Instrumentation Software

Support group (BLISS) of the European Synchrotron Radiation Facility (ESRF) was utilized (s. figure 13).

Table 10: Used settings at ANKA

excitation energy:	12,5keV
measuring time:	10-25sec.
resolution:	horizontal 2 to 10µm, vertical 28 to 62µm
detector:	Si(Li)-energy dispersive detector, 133 eV average resolution at 5.9 keV

Table 11: Scan overview ANKA

sample	ID	type	horiz.res. [µm]	vert.res [µm]	vert.extent [µm]	horiz.extent [µm]	meas.time [sec.]
Root F1	N031qa P2	mesh	2,98	61,8	540	680	17
	N031qa P1	transect	2,97		330		
	N031qa P3	transect	5,94		600		
Root F2	N067L P3	transect	9,88		830		10
	N67qb P1	transect	6,93		700		15
	N67qb P3	mesh	2,00	60,0	570	420	16
Soil F1	B025a P20	mesh	4,96	31,3	650	500	20
Soil F2	B51 Q P6	mesh	3,88	28,7	330	689	22

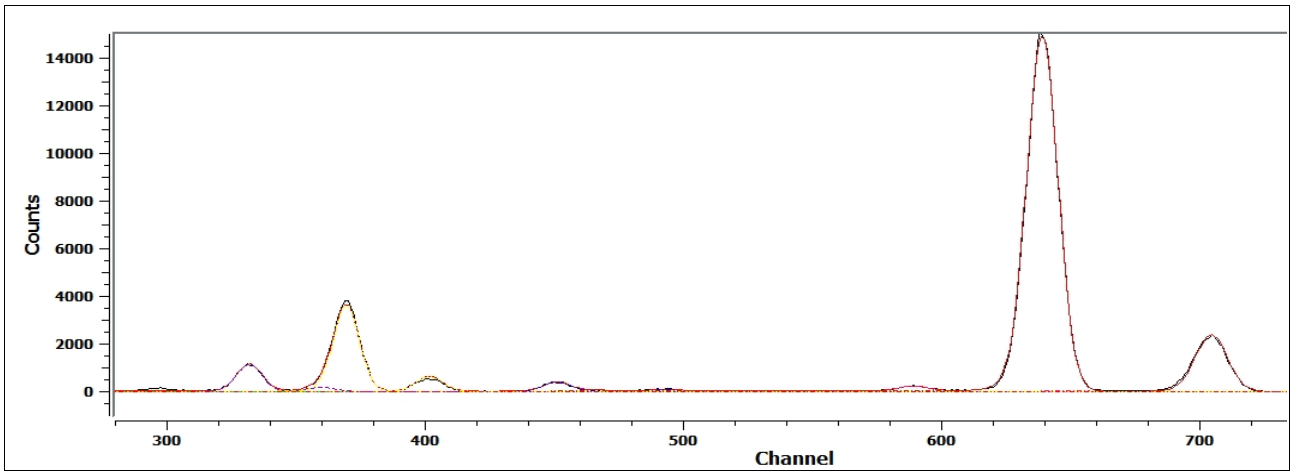

Figure 13: Example of a spectra fitted with PyMCA

3.2.1.3 XRD

Introduction:

Powder X-Ray diffraction (XRD) is used to determine the mineral content of crystalline materials using monochromatic X-rays with a wavelength comparable to distance of atoms in crystal lattice. X-rays hitting a crystal structure become scattered according to the law of Bragg:

$$\lambda = 2d * \sin\Theta \qquad (7)$$

with λ= X-ray wavelength, d= lattice distance, Θ= scattering angle (LOUËR 1999)

A detector is used to measure the intensities of scattered X-ray under altering diffraction angle. Applying the law of Bragg, lattice distance *d* can be calculated, which is used together with the referring observed relative intensity *I* to identify mineral compounds.

Components and used settings:

The XRD used for sample analyses was a SIEMENS Kristalloflex D 500 with Bragg-Brentano geometry and a copper X-Ray tube. Measurement was carried out in 0.01° step sizes and 0.5 sec. measuring time from Θ=3° to 63°.

Sample description and preparation technique:

XRD investigation was used to characterize mineral composition of 22 representative soil samples from each field, with focus on the soil horizons. The samples had to be in form of a fine powder consisting of single crystalline grains, which is achieved by milling corresponding to ED-XRF sample preparation.

3.2.2 Optical and mass spectrometry based methods

3.2.2.1 FIAS

Introduction:

The flow injection atom absorption spectrometry (FIAS) is used for As detection in liquid phases. It combines an atomic adsorption spectrometer (AAS) with a flow injection system, separating As as gaseous hydride from sample solution (PAVICEVIC et al.2000). According to the Marsh test, As compounds become reduced in an acid medium to volatile arsine gas (AsH_3). Instead of zinc, sodium borate solution (1%$NaBH_4$, diluted in 0.1 M sodium hydroxide) is used together with hydrochloride acid (HCl, 1.2 M):

$$3BH_4^- + 3H^+ + 4As(OH)_3 <=> 4AsH_3 + 3B(OH)_3 + 3H_2O \quad (8)$$

(HEINRICHS et al. 1998).

Before this reaction, As^V needs to be reduced to As^{III} by a solution of 10% potassium iodide and 10% ascorbic acid and 2.4 M hydrochloride acid, otherwise hydride formation is interfered.

Components and procedure:

After pre-reduction, 500µl of sample solution become separated by an injection loop and transported with 1.2 M HCl as carrier into the reaction well, where hydride generation with sodium borohydride ($NaBH_4$) takes place. The generated AsH_3 is transferred into a gas/liquid separator and from thereon with a constant flow of argon gas into the AAS.

An AAS consists of light source (electrode-less discharge lamp, EDL), atomizer (900°C heated quartz cell), monochromator and detector (photomultiplier). The high temperature in the quartz cell atomizes the AsH_3 molecules and liberates As atoms:

$$a)\ 4AsH_3 + 3O_2 <=> 4As + 6H_2O \quad (9)$$

$$b)\ AsH_3 + 3H^+ <=> As + 3H_2 \quad (10)$$

Free gaseous As absorbs the radiation emitted by an As EDL at a wavelength of 193.70nm, which is measured with the detector. The relation between As concentration and absorption is specified by the law of Beer-Lambert:

$$A = \log I_0 / I \qquad (11)$$

with A=sample absorption, I_0 =intensity of incident light, I= light intensity after absorption. For interpretation, sample absorption is compared to a calibration curve, performed with a certified As standard.

Table 12: Used settings

Producer and model:	FIAS: FIAS 400 flow injection system,Perkin-Elmer AAS: AAnalyst 200 spectrometer, Perkin-Elmer
Evaluation software:	WinLab32™ for AAS, Perkin-Elmer
Calibration curve range:	0.1 to 10.0µg As/l
Calibration standard:	AAS-standard As 1,000 g As/l, Bernd Kraft GmbH
Instrumental detection limit:	0.33µg As/l
Limit of quantification:	0.66µg As/l

Sample description and preparation technique:

FIAS was used to qualify the As content of 72 food chain samples and therefore is another important method used in this study. As prerequisite the sample material had to be completely dissolved in a microwave acid digestion, using hydrofluoric acid (HF) in order to digest hardly soluble siliceous compounds.

250 mg of dried (105°C for 12 hours) and milled sample material was put into a microwave teflon flask, adding 3ml of twice distilled water (Milli-Q water), 5 ml of 65% nitric acid s.b. (HNO_3, subboiled quality), 1ml of 30% hydrogen peroxide (H_2O_2, per analysis quality, Merck) and 0.5ml of 40% HF s.p. (suprapur quality, Merck). The sample-acid mixture was then heated up in a laboratory microwave (MW system start 1500, MLS GmbH) with a special program adapted to plant material (s. table13). In the next step digestions were transferred into small teflon cups and heated up to 200°C, to fume off remaining HF. After evaporating the digestions to the size of a small drop, 2ml of 1% HNO_3 s.b. were added. Having repeated this evaporation step twice, digestions were transferred finally into 25ml volumetric flasks and diluted with 1% HNO3 s.b. to a total volume of 25ml. Digestions were stored in fridge until analysis.

Table 13: Used microwave settings

Elapsed time (min.)	E (W)	Temp. (°C)
3	700	75
8	650	130
10	1000	200
12	1000	200

Table 14: Microwave digested samples and used standards(described in table 16) [number]*

Field 1	**Field 2**	**Next to field 2**	**Surroundings**	**Standards*:**
sun flower: grains [3] stems [9] leave [9] roots [3]	Maize: grains [3] stems [9] leave [11] roots [3]	Vegetables: potato [2] paprika [2] egg-plant [1] tomato [4] hot pepper [2]	Other: egg [4] hair [7]	rice unpolished [5] citrus leaves [5] hay 10 [9]

3.2.2.2 HR-ICP-MS

Components and procedure:

The double focusing high resolution inductively coupled plasma mass spectrometer (HR-ICP-MS VG AXIOM, VG Elemental) is used for multi-element analysis of liquid samples. It consists of high frequency generator, plasma torch, double-focusing high resolution mass spectrometer and a computer based control system (s. figure 14). The plasma is generated by collision of inductively accelerated free electrons with argon gas atoms and reaches temperatures of about 10000° K (HEINRICHS et al. 1998). Sample material is injected into plasma as a nebulized droplet, whereby its compounds become atomized and ionized. The induced ions are separated by a double-focussing electro-magnetic field in the spectrometer according to their mass-to-charge ratio. A single-detector system consisting of electron multiplier and Faraday cup (PAVICEVIC et al 2000; VG Axiom user manual) records the incoming signals. In order to avoid dust contamination and enable high resolution, the HR-ICP-MS is situated in a separated clean room.

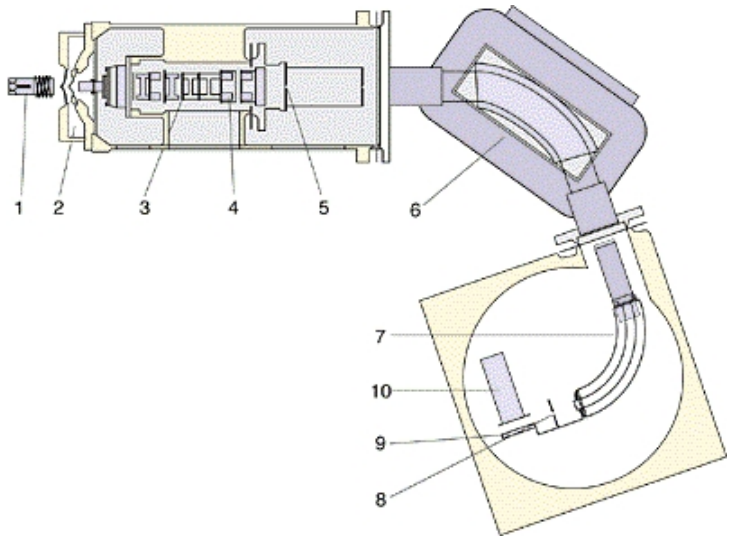

1) ICP ion source
2) Interface, including sampler and skimmer cones
3) Transfer and focusing optics
4) Acceleration and beam focusing
5) Entrance slit
6) Electromagnet
7) Electric sensor
8) Exit slit
9) Conversion dynode
10) Electron multiplier

Figure 14: Sketch of a HR-ICP-MS (MOENS et al. 1998)

Table 15: Detected elements, instrumental detection limits (IDL) and used standards for water sample analysis

Standard:	**Na** [mg/L]	**Mg** [mg/L]	**K** [mg/L]	**Ca** [mg/L]	**Al** [µg/L]	**V** [µg/L]	**Cr** [µg/L]	**Mn** [µg/L]	**Fe** [µg/L]	**Co** [µg/L]	**Ni** [µg/L]
HPS standard	1,2	1,8	0,5	7,0	24,0	6,0	4,0	8,0	20,0	5,0	12,0
Trace Elem. Std.	315	37,8	231	1554	46,2	37,8	16,8	16,8	12,6	25,2	29,4
IDL	0,009	0,002	0,003	0,006	0,430	0,008	0,004	0,038	0,459	0,021	0,024

Standard:	**Cu** [µg/L]	**Zn** [µg/L]	**As** [µg/L]	**Rb** [µg/L]	**Sr** [µg/L]	**Mo** [µg/L]	**Cd** [µg/L]	**Ba** [µg/L]	**Tl** [µg/L]	**Pb** [µg/L]
HPS standard	4,0	14,0	16,0	2,0	50,0	20,0	2,0	10,0	2,0	8,0
Trace Elem. Std.	29,4	12,6	-	-	58,8	37,8	42,0	273	54,6	29,4
IDL	0,032	0,637	0,172	0,003	0,050	0,244	0,005	0,057	0,052	0,060

Sample description and preparation technique:

a) Water samples

A total number of 20 water samples were analysed, consisting of ten As_{total} and ten As^{III} samples. Depending on the salt load (measured with IC), samples were diluted with 1% HNO3 s.b.. Because of insufficient acidifying in field, some samples had to be analysed twice after adding additional 65% HNO_3 s.b. and shaking for 12 hours (s.b.).

The referring suspended load was separately collected by using 0.45µm cellulose-acetate filters. After drying (12 h, 105°C) and weighing, a digestion of the 10 filters was done by an employee of the IMG. Therefore, filter material and 2ml 65% HNO3 s.b. were filled in small teflon cups and evaporated at 175-200°C to the size of a small drop. Than 1.5ml 40% HF s.p. and 0.3ml 70% perchloric acid ($HCLO_4$, s.p.) were added and fumed off. This step was repeated twice with 0.5 ml HF and 0.5ml $HCLO_4$. Residues were absorbed with 1% HNO_3 s.b. and transferred into 10ml volumetric flasks. Finally, each digestion was diluted with 1% HNO_3 s.b to a total volume of 10ml.

b) Food chain samples

HR-ICP-MS was also used to characterize the 7 hair samples, with focus on heavy metal load. Sample preparation is identical to plant samples as described in 3.2.2.1. As a cross-check, the FIAS samples were additionally tested for As content with HR-ICP-MS.

Table 16: Used standards for HR-ICP-MS analysis

Calibration standard: -ICP multi element standard VI (Merck) **Internal standard:** -Defined rhodium-indium solution **Water samples:** -Certified Reference Material: Trace Metals In Drinking Water (High Purity Standards) -Water Quality Control Reference Material: Trace Metals ICP, QCP 050-1 (Promochem GmbH) **Filter samples:** -GXR2 (s. 3.2.1.1) **Food chain samples:** -Certified Reference Material: IAEA/V-10 HAY (Powder) (International Atomic Energy Agency) -NIES Certified Reference Material: No.10.b “Rice Flour – Unpolished, Medium level” (National Institute for Environmental Studies Japan Environment Agency) -Standard Reference Material 1572: Citrus Leaves (National Bureau of Standards, U.S. Department of Commerce)

3.2.2.3 IC

Ion chromatography (IC) separates ions in liquid phase according to their mass-to-charge ratio. In this study, anions of the water samples were determined with a DIONEX ICS 1000 system. It consists of a sample injection system (peristaltic pump and carrier eluate, a $NaHCO_3/Na_2CO_3$mixture), injection valve, separation column (DIONEX AS 4 SC) with stationary phase, detector including conductivity measuring cell and suppressor system. Separation process takes place in the solid stationary phase, where positively charged functional groups (ammonium bases) are located. These groups retain anions of the liquid phase depending on their charge and mass, resulting in a temporal separation. Anions reaching the detector increase measured conductivity according to their concentration. The suppressor system is necessary to decrease basic conductivity of the eluate by transmuting sodium hydrogen carbonate ($NaHCO_3$) into weak conductive carbonic acid (H_2CO_3).

Sample description and preparation technique

IC was used to analyze the unaltered anion water samples. The only preparation step was dilution with MilliQ water to keep within calibration range (s. table 19).

Table 17: Used settings for IC

Calibration standard:	SPEC PURE™ Multi Ion IC Standard Solution (Alfa-Aesar)
Basic conductivity:	~16µS
Suppressor current:	43mA
Detection limit:	10ppb for each anion

Table 18: Range of used calibration curve

Calibration standard	F^- [mg/l]	Cl^- [mg/l]	Br^-, NO_3^{2-},SO_4^2 [mg/l]	HPO_4^{3-} [mg/l]
Std. 1	0.2	0.4	0.8	1.2
Std. 2	1.0	2.0	4.0	6.0
Std .3	2.0	4.0	8.0	12.0
Std. 4	4.0	8.0	16.0	24.0
Std. 5	10.0	20.0	40.0	60.0

3.2.2.4 CSA

Total carbon and sulphur can be detected with non-dispersive IR-spectroscopy in an elemental analyser. Carbon and sulphur are removed from a solid sample as gaseous CO_2 and SO_2 by calcination. The molecules created this way are transferred together with an inert gas in a metering chamber, where they become excited by absorption of low energetic IR radiation. The remaining IR radiation is detected and used to calculate the molecules concentration:

$$A = \log(I_0/I) \qquad (12)$$

A=Absorption, I_0 =initial intensity of IR radiation, I=remaining radiation

CSA consists of IR source, optical interrupter, measuring and comparison cuvette, receiver and membrane condenser.

Sample description and preparation technique:

Only a few representative soil samples, mainly soil horizon samples, were analysed with CSA. 100-150µg of dried and milled sample material was mixed with 500µg of iron swarf and 1000µg of elemental tungsten. For calibration, an iron-tungsten-mix was used with +/- 3% range of tolerance.

3.3 Geostatistics: Kriging

Kriging is a geostatistical method to get the best (with least variance) unbiased linear estimates of spatial distributed measuring values (ARMSTRONG 1998, SCHAFMEISTER 1999). It includes the theoretical variogram,which describes the spatial variability of a measured variable and is used to fit a spatial correlation model. Altogether, the number, position and distances between samples and the spatial continuity of the observed variable are in the complex calculation included. Kriging was used to interpolate spatial As distribution in topsoil based on the ED-XRF results of the grid samples. In addition, µ-SyXRF results of soil and root mesh scans were interpolated. Gridding was done with program Surfer® (version 8, Golden Software inc.) using the default linear variogram (settings: slope=1; anisotropy with ratio=1 and angle=0) with point Kriging algorithm by what best results were produced.

4.Results

4.1 Information survey

Table 19: Results of field survey

Aspect	Field 1	Field 2
Title data:		
Position	fields of Yong-Ming	
Date of survey	26.07.2007	28.07.2007
Field dimensions	35 x 16m	23 x 150m
Cultivation details:		
Cultivated crop	corn	sunflower; wheat
Stage of maturity	~6 weeks before harvest	~6-8 weeks before harvest
Crop rotation	corn, wheat, sunflower	
Fertilizer application	natural + artificial (NPK)	
Pesticides	yes	
Machine use	use of light tractors and harvesters	
Field preparation methods	plough use, firing and flooding after harvest	
Irrigation details:		
Type of irrigation	flood irrigation using groundwater from tube well	
Deliver depth	83m	80m
Result of As quick test	~200µg As/l	~200µg As/l
Age of well	3 years	
Distance well to field intake	5m	38m
Duration of irrigation	early April - middle of October	
Irrigation frequency	twice per month	
Further information and observations:		
➔ high soil quality, only one fallow of 2 years during last 13 years on field 2 ➔ before tube well installation, irrigation with Huang He surface water ➔ farmer do not own the land, they have only the right of use ➔ no flooding influence from yellow river ➔ 6cm water table on field after flood irrigation, lasting for 2-7 days on field ➔ irrigation of vegetables only once per month ➔ corn and wheat in mixed cultivation for yield increase ➔ corn is used as feeding stuff, sunflower seeds for oil production, wheat and vegetables as foodstuff, sunflower stems for cooking and heating		

4.2 Water samples

Table 20 shows available results of field measurements, IC and HR-ICP-MS for water samples taken at fields 1 and 2. Table 21 figures out the most important results for water samples from the surroundings, further values are listed in table 39, 40 and 41 (appendix). Figure 15 and 16 picture both soil pits with horizontal partition. Figure 17 and 18 show µ-SyXRF mesh scan results for topsoil samples (0-1cm) from soil pit A and B, interpolated with Kriging.

Table 20: Water samples results

Parameter	Field 1	Field 2
Field parameter		
GPS-coordinates	40°51'39.60"N; 106°48'13.30"O	40°51'49.90"N; 106°47'48.20"O
pH	9.1	-
Ox.-red.-potential [mV]	-162	-
Electrical conductivity [µS/cm]	2150	
IC, anions		
Cl^- [mg/l]	383	1100*
NO_3^- [mg/l]	<IDL	<IDL
SO_4^{2-} [mg/l]	3*	593
PO_4^{3-} [mg/l]	<IDL	<IDL
HR-ICP-MS, As		
Measuring pH	0.38	0.31
As_{total} dissolved [µg/l]	154	238
As^{III} (%)	false	92%
As suspended [µg/l]	0.37	3.12
HR-ICP-MS, cations (dissolved/suspended matter)		
Measuring pH	7.52	7.96
Na [mg/l]	441	0.89
Mg [mg/l]	16.3	0.01
K [mg/l]	3.88	<IDL
Ca [mg/l]	8.41	0.03
Al [µg/l]	5.10	27.4
V [µg/l]	0.47	<IDL
Cr [µg/l]	0.11	<IDL
Mn [µg/l]	34.2	0.35
Fe [µg/l]	296	19.7

Continuation of table 20:

Parameter	Field 1		Field 2	
HR-ICP-MS, cations (dissolved/suspended matter)				
Ni [µg/l]	2.25	<IDL	1.37	<IDL
Cu [µg/l]	1.15	0.28	1.07	0.14
Zn [µg/l]	2.94	<IDL	3.69	<IDL
Sr [µg/l]	474	1.71	3180	4.04
Mo [µg/l]	25.4	<IDL	14.4	<IDL
Cd [µg/l]	0.03	0.01	0.03	<IDL
Ba [µg/l]	446	8.49	280	3.78
Tl [µg/l]	<IDL	1.41	<IDL	<IDL
Pb [µg/l]	<IDL	0.04	<IDL	<IDL
*Out of calibration range				

Table 21: Groundwater As load in the surroundings of Xamba, NW of Hetao-Plain

Location:	Position	Well depth [m]	pH	ORP [meV)	As dis. [µg/l	As susp. [µg/l
1	40°52'35.70"N, 106°55'4.10"O	17-18	8.2	-	345	14.4
16 (32)	40°58'1.80"N, 107° 0'31.40"O	20	8.3	-173	959	0.97
19	41° 6'38.10"N, 107° 7'59.60"O	22	8.2	-164	301	5.39
20	41° 6'36.50"N, 107° 7'57.90"O	25	7.7	-138	191	4.97
Huang He River	40°18'48.80"N, 107° 2'4.70"O	-	-	-	6.70	46.8
Hotel Xamba	-	-	-	-	14.7	3.38

4.3 Soil samples

4.3.1 Soil pits

There are two different approaches to realise vertical elemental distribution in soil pits. A pedological orientated procedure includes continuous sampling of the soil horizons, while a geochemical approach designates a static sampling in predefined depths. The ED-XRF results are illustrated in condensed form in tables 22 and 23, detailed results are listed in table 44 and 45 in appendix. Interpolations of µ-SyXRF results are illustrated in figure 17 and 18, while the raw data are located at the data cd attached because of large extent.

Table 22: Vertical As [ppm] distribution in depth profiles of 0-100cm, measured with ED-RFA

Depth [cm]	Field 1, pit A	Field 1, pit B	Field 2, pit A	Field 2, pit B
0-1	16	16	19	18
1-2	16	15	20	14
2-5	16	14	20	18
5-10	14	15	16	17
10-20	14	13	18	17
20-30	19	14	15	17
30-40	12	15	18	22
40-50	16	12	24	17
50-60	16	12	19	15
60-70	14	14	23	11
70-80	16	13	12	13
80-90	14	13	12	15
90-100	13	14	11	13

Table 23: Soil horizon characterisation of both soil pits

Horizontation: Field 1, pit A

horizon symbol	Boundary [cm]	munsell colour	agg. shape	bulk density	soil texture	As [ppm]	CaO [%]	MnO [%]	Fe2O3 [%]	C_{total} [%]	S [%]
Ap1	0 – 7,5	10 YR 4/4	crumb	2	Uu	15	8,18	0,06	3,57	1,93	0,02
Ap2	7,5 – 37	10 YR 4/4	subpolyhed.	3	Uu	13	8,44	0,06	3,53	1,72	0,02
ael C	37 – 48	10 YR 4/6	polyedral	4	Tu3	17	9,64	0,09	4,96	2,15	0,02
ael II C	48 – 82	10 YR 5/4	subpolyhed.	3	Slu	13	7,24	0,06	3,04	1,36	0,01
ael III C	82 – 100	10 YR 5/4	platy	4	Lu	14	8,23	0,07	4,06	1,83	0,02

Horizontation: Field 2, pit A

horizon symbol	Boundary [cm]	munsell colour	agg. shape	bulk density	soil texture	As [ppm]	CaO [%]	MnO [%]	Fe2O3 [%]	C_{total} [%]	S [%]
Ap1	0 – 10,5	10 YR 5/3	crumb	1	Uls	19	9,36	0,08	4,54	2,68	0,04
Ap2	10,5 – 35	10 YR 5/3	subpolyhed.	3	Uls	14	9,06	0,07	4,12	2,23	0,03
ael C	35 – 65	10 YR 5/3	polyedral	3	Tu4	18	9,43	0,11	4,96	2,29	0,03
ael II C	65 – 84	10 YR 5/4	platy	4	Lu	12	8,71	0,08	3,99	1,71	0,02
ael III C	84 – 100	10 YR 5/3	subpolyhed.	3	Slu	10	7,69	0,05	3,01	1,40	0,01

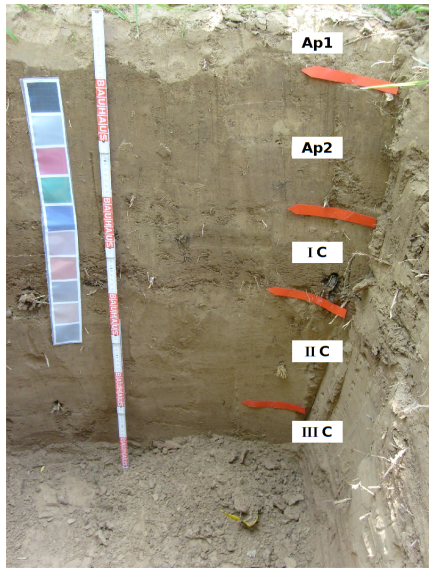

Figure 16: F1 A

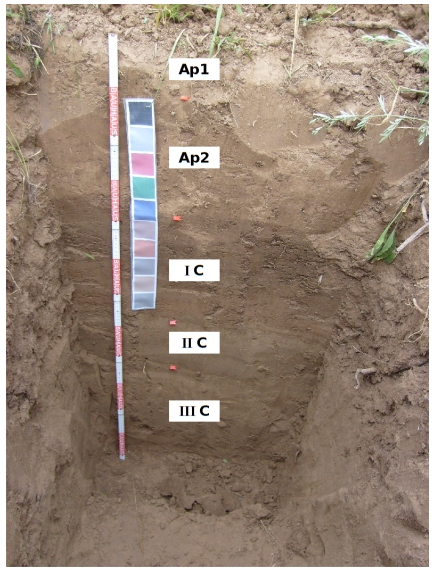

Figure 15: F2 A

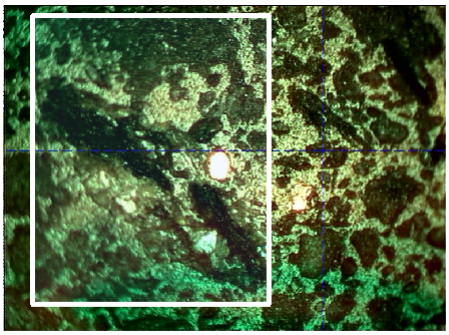

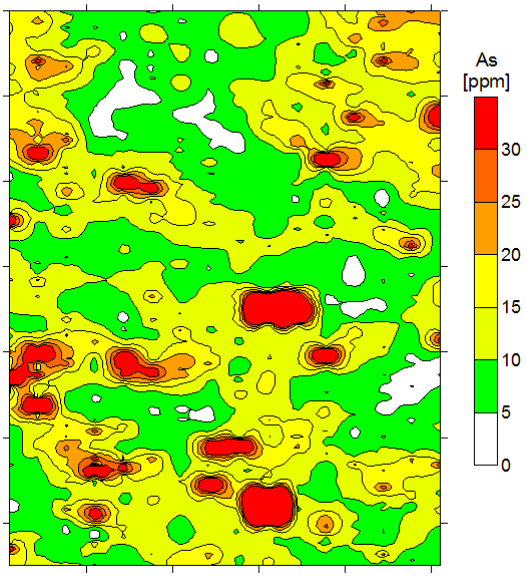

Field 1, pit A, 0-1cm

Settings mesh

Dimensions:	500 x 650µm
Resolution:	4.96 x 31.3µm
Measuring points:	2096
Measuring time:	20 sec.

As [ppm]

Minimum:	0.00
25%-tile:	7.42
Median:	10.8
75%-tile:	14.9
Maximum:	263
Average:	13.5

Figure 17: µ-SyXRF mesh scan results for topsoil (0-1cm) from soil pit A

Field 2, pit A, 0-1cm

Settings mesh

Dimensions:	330 x 689µm
Resolution:	3.88 x 28.7µm
Measuring points:	2040
Measuring time:	22 sec.

As [ppm]

Minimum:	0.00
25%-tile:	9.12
Median:	12.8
75%-tile:	17.8
Maximum:	198
Average:	15.6

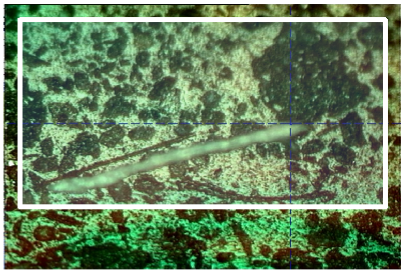

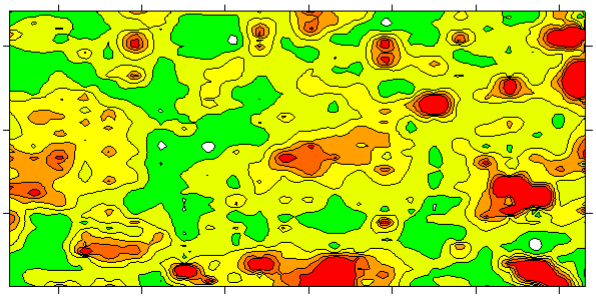

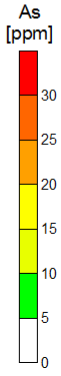

Figure 18: µ-SyXRF mesh scan results for topsoil (0-1cm] from soil pit A, field 2

4.3.2 Grid sampling, canal sediments and root soil

Table 24: RFA results of the grid samples

		As ppm	K_2O %	CaO %	TiO_2 %	MnO %	Fe_2O_3 %	Ni ppm	Cu ppm	Zn ppm	Br ppm	Rb ppm	Sr ppm	Y ppm	Zr ppm	Nb ppm	Pb ppm
Field 1 0-1cm-	Min.	11	2.14	7.94	0.41	0.06	3.21	22	15	58	3	89	258	18	146	8	10
	Max.	22	2.82	10.6	0.53	0.10	4.72	36	31	91	6	118	367	28	223	14	22
N=65	Mean	15	2.46	8.94	0.47	0.07	3.80	26	24	68	4	99	303	23	186	11	14
Field 1 1-2cm-	Min.	12	2.22	8.20	0.42	0.06	3.46	22	18	59	3	92	270	20	151	9	11
	Max.	18	2.72	9.81	0.53	0.09	4.34	31	29	83	6	111	330	26	209	13	33
N=65	Mean	15	2.43	8.87	0.46	0.07	3.83	26	24	69	4	100	304	23	184	11	15
Field 2 0-1cm-	Min.	15	2.42	8.61	0.43	0.07	4.03	22	16	65	4	101	300	21	143	9	12
	Max.	22	2.92	10.1	0.53	0.10	4.80	37	37	97	8	120	352	26	171	15	20
N=34	Mean	18	2.60	9.22	0.48	0.08	4.36	28	26	80	6	109	326	24	156	12	16
Field 2 1-2cm-	Min.	14	2.42	8.65	0.45	0.07	4.05	23	14	71	4	102	297	21	144	9	14
	Max.	21	2.76	9.92	0.52	0.10	4.73	36	38	99	7	120	349	26	182	14	23
N=34	Mean	17	2.58	9.22	0.48	0.08	4.36	29	27	80	6	110	317	24	158	12	17

Table 25: RFA results for canal sediments

Field 1	Dist. well-field [m]	1	2	3	4	5	6	7	8	9	10
0-1cm	As [ppm]	17	17	15	12	15	16	12	14	13	14
	Fe [%]	3.68	3.70	3.71	3.60	3.52	3.44	3.00	3.27	3.01	3.16

Field 2	Dist. well-field [m]	2	5	12	15
0-1cm	As [ppm]	74	13	19	36
	Fe [%]	2.97	4.10	3.69	2.91

Table 26: As contents of root soil

Root soil samples	AS [PPM]
F1 A	13
F1 B	15
F1 Middle	20
F2 A	17
F2 B	18
F2 Middle	16

Soil horizon	Field 1	Field 2
Ap1	mica, quartz, smectite, calcite, feldspar	mica, smectite, calcite, quartz, feldspar,
Ap2	mica, smectite, calcite, quartz, feldspar	mica, smectite, quarz, calcite, feldspar
IC	mica, smectite, calcite, quartz	mica, smectite, calcite, feldspar, quartz
IIC	mica, quartz, calcite, feldspar	mica, smectite, quartz, calcite
IIIC	mica, smectite, feldspar, quartz, calcite	mica, smectite, calcite, feldspar

Figure 19: XRD: Main mineral phases with relative Intensity > 10% in decreasing order

4.4 Food chain samples

4.4.1 Sunflowers and maize

Table 21 expresses the As load of sunflower and maize samples measured with HR.ICP-MS, figures 20, 21 and 22 show the µ-SyXRF results for root sections.

Table 27: HR-ICP-MS results of As concentration in plant tissues (dry weight related)

F1: Sunflower

Plant location:	**Leaves**		**Stems**		**Seeds**	**Roots**
	height [cm]	As [ug/kg]	height [cm]	As [ug/kg]	As [ug/kg]	As [ug/kg]
A	125 151 180	<MDL 173 189	120-130 145-155 175-185	<MDL 53,4 53,0	<MDL	1260
Middle	44 100 133	489 212 196	38-48 95-105 125-135	81,3 48,0 <MDL	<MDL	2290
B	45 150	457 173	40-50 107-117 145-155	100 66,9 78,6	117	1220

F2: Maize

Plant location:	**Leaves**		**Stems**		**Seeds**	**Roots**
	height [cm]	As [ug/kg]	height [cm]	As [ug/kg]	As [ug/kg]	As [ug/kg]
A	28 110, tip 110, middle 110, beginning 110, basement 180	1020 774 547 209 178 188	25-35 105-125	146 66,0	<MDL	777
Middle	10 110 190	1210 322 146	0-20 105-125 170-200	508 <MDL 121	<MDL	3210
B	22 78-90 182-196	52,6 609 637	10-20 100-120 180-200	657 52,07 241	74,2	2520

MDL=51,8 [ug As/kg] for 250mg DW

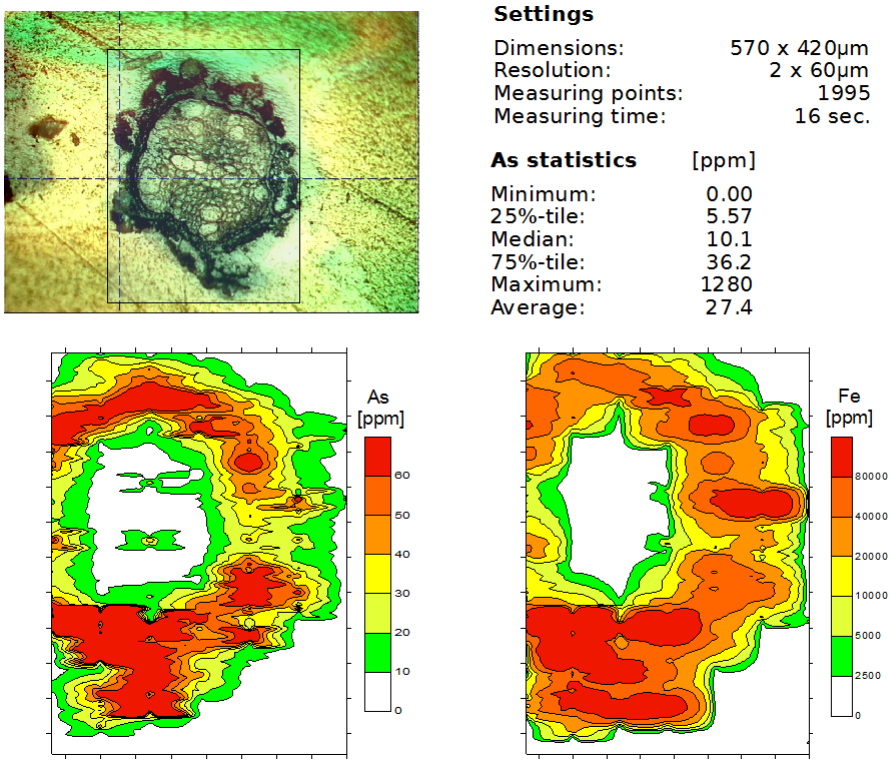

Figure 20: 19:µ-SyXRF mesh scan results for corn root, interpolated by Kriging

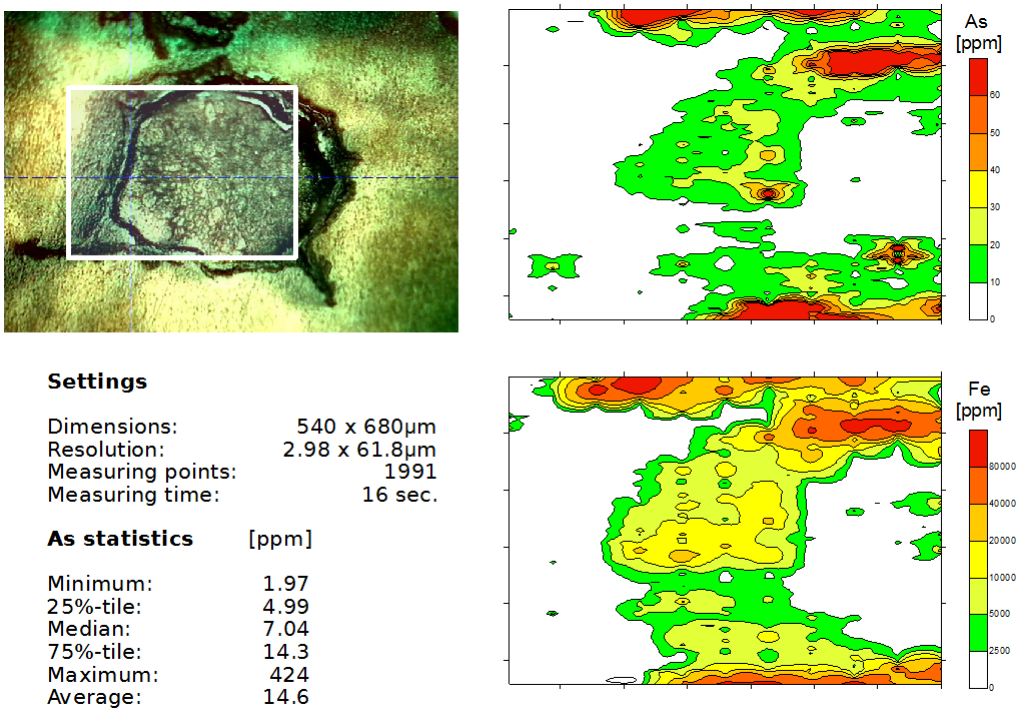

Figure 21: SyXRF mesh scan results for sunflower root, interpolated by Kriging

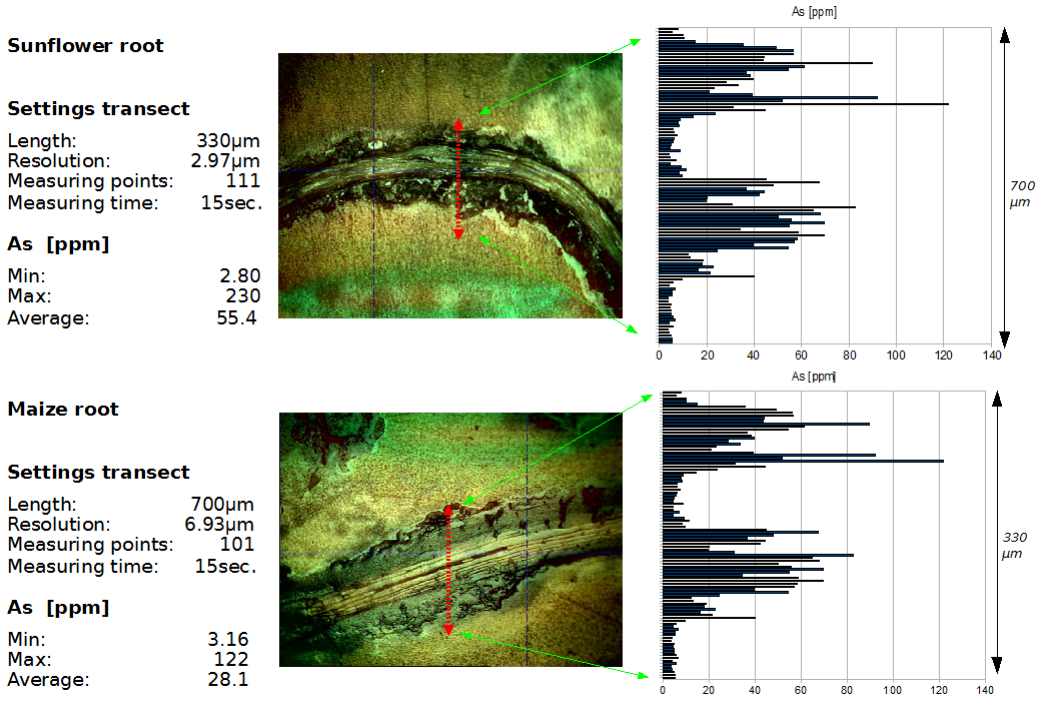

Figure 22: µ-SyXRF transect scans on corn and sunflower roots

4.4.2 Foodstuff

Table 28 shows the As burden of vegetable samples taken from a field next to F2 and eggs from location 20, measured with FIAS.

Table 28: As burden of vegetable (grown next to field 2) and eggs (taken at sample site 20), measured with HR-ICP-MS, dry weight related

Sample:	As [ug/kg]
Hot pepper 1	121
Hot pepper 2	96,6
Tomato 1	<MDL
Tomato 2	<MDL
Tomato 3	60,9
Tomato 4	68,4
Sweet pepper 1	<MDL
Sweet pepper 2	63,5
Egg plant 1	184
Potato 1	<MDL
Potato 2	<MDL

Sample:	As [ug/kg]
Egg 1, yolk	195
Egg 1, egg white	108
Egg 2, yolk	214
Egg 2, egg white	85,5

MDL=51,8 [ug As/kg] for 250mg DW

4.4.3 Hair

Results of hair samples measured with HR-ICP-MS combined with water sample results and information from survey are given in table 29.

Table 29: As concentrations in hair from locals combined with additional information

Sample	**Location**	**As**	**Well**	**Subject****			
		[mg/kg]	As dis. [µg/L]	age	sex	smoker	consumption of well water
Hair 1	1	5,33	345	50	m	n	y
Hair 2	2	0,79	21,5***	62	m	y	y
Hair 3	field 1	1,72	154	61	m	y	y
Hair 4	16 (32)	6,23	959	65	m	y	n
Hair 5	19	3,44	301	63	m	y	y
Hair 6	20	0,53	191	45	f	n	y
Hair 7	21	1,3	0,9***	48	m	y	y

* all wells older than 3 years and depth>10m
**all subjects living for more than 10 years at location and with short hair
*** values submitted from Prof. GUO

5. Discussion

In this chapter the questions raised in 1.3 shall be responded using the analysis results. Although the different analysis methods used in this field study delivered numerous data and results, main focus of the discussion is on As and compounds related to As. Other issues are only mentioned if they are remarkable.

5.1 Consequences of irrigation with As burdened water related to field soil

5.1.1 Vertical distribution of As

Table 23 expresses soil horizon characterisations of both soil pits A, each situated next to water inlet . Soil type is according to FAO nomenclature (REINHOLD 2006) an agricultural affected *fluvisol* respectively. A and C horizons were distinguished according to bulk density and soil textures, with agriculture as only identifiable soil forming processes. Ap_1 and Ap_2 differ in bulk density, most likely a result of field work and root penetration. Soil parent material is formed of alternating alluvial sediment layers of loamy sand, silt, loamy silt, silty loam and silty clay. This could be a sign of eroded loess matter, transported and sedimented by the Huang He.

Comparing ED-XRF results for Ap_1 to Ap_2 , As seems to be enriched in topsoil (F1: 15 opposite to 13ppm; F2: 19 opposite 14ppm), supposable as a result of irrigation with high As contaminated groundwater during the last three years, as calculated in 5.3. The values are in excess of mean content for uncontaminated alluvial soils given in KABATA-PENDIAS et al. 1984 (mean 8.2ppm, range 2.1 to 22ppm), and exceed USEPA soil limit of 10mg As/kg soil (NAIDU et al. 2006). Nevertheless, measured concentrations are not that serious and are by far not comparable to high contaminated soils appearing near mining sites or historical burdens. One can perhaps conclude that As is related to grain size and soil texture within the mineral (C-) horizons, as maxima occur each together with silty clays and minima with loamy sands. The same applies to other heavy metals like copper, zinc and lead, s. table 44 and 45 in appendix.

Elemental distributions in depth profiles (F1 and 2, A+B) shown in table 22 are similar to the soil horizon related, but figure 23 pictures a more accurate resolution, especially in topsoil. Here one can see a decrease in As concentrations inside the first 5 to 10cm, readily identifiable at both soil pits on F2. Related to the entire profiles, vertical As

distribution diversifies moderately at F2 (from 11 to 24ppm) and only weak within F1 (12 to 19ppm). Linear regression indicates decreasing As concentrations with increasing depth in general, but it is not possible to specify a background value for As that could be compared to the horizontal topsoil results. Comparing both soil pits (A+B) on each field, it is difficult to say if differences in As spreading are naturally or a consequence of human activities.

Correlation coefficients between As and other soil constituents are listed in table 30. Conspicuous are correlations between As and the potential adsorptive compounds calcium-, iron- and manganese-minerals (specified as CaO, Fe_2O_3.and MnO), in particular at F2. Ca- and Fe-compounds are a matter of particular importance, with percentages of 8 to 11% for CaO and 3 to 6% for Fe_2O_3 (s. table 44 and 45 in appendix). Correlations between As and other trace elements vary strongly and do not provide further conclusions.

XRD analysis shown in figure 19 that the main mineral phases in soil horizons are composed of mica, clay minerals (smectite), calcite, quartz and feldspars. High intensities measured for calcite coincide with high contents of CaO measured with ED-XRF. Smectites seem to be the dominating clay minerals, important as possible As adsorbents. Fe- and Mn-oxyhydroxides could not have been identified doubtless.

Table 30: Correlation coefficients matrix between As and other soil constituents

Correlations:	**vertical**				**horizontal**			
	F1 A, 0-100	**F1 B, 0-100**	**F2 A, 0-100**	**F2 B, 0-100**	**F1,0-1**	**F1, 1-2**	**F2, 0-1**	**F2, 1-2**
As-K_2O:	0,59	0,80	0,94	0,91	0,56	0,50	0,27	0,22
As-CaO:	0,49	0,82	0,94	0,91	0,65	0,43	0,31	0,29
As-TIO_2 :	-0,04	0,26	0,85	0,49	0,62	0,34	0,21	0,41
As-MnO:	0,38	0,44	0,85	0,86	0,45	0,41	0,35	0,16
As-Fe_2O_3:	0,38	0,63	0,93	0,91	0,64	0,54	0,42	0,37
As-Ni:	0,52	0,42	0,56	0,78	0,11	0,09	0,38	0,04
As-Cu:	0,45	0,29	0,70	0,48	0,21	0,23	0,06	0,32
As-Zn:	0,44	0,80	0,93	0,91	0,47	0,39	0,15	0,35
As-Br:	0,45	-0,15	-0,41	0,16	-0,22	-0,02	-0,05	0,02
As-Rb:	0,46	0,53	0,91	0,90	0,60	0,43	0,32	0,28
As-Sr:	0,57	0,83	0,88	0,83	0,62	0,48	0,24	0,35
As-Y:	-0,18	0,05	0,76	0,19	0,58	0,47	0,36	0,23
As-Zr:	-0,46	-0,13	-0,69	-0,63	0,38	0,39	0,16	0,05
As-Nb:	0,04	0,19	0,25	0,10	0,27	0,06	0,32	0,09
AS-Pb:	-0,19	-0,33	0,52	0,93	-0,22	-0,19	-0,35	-0,14

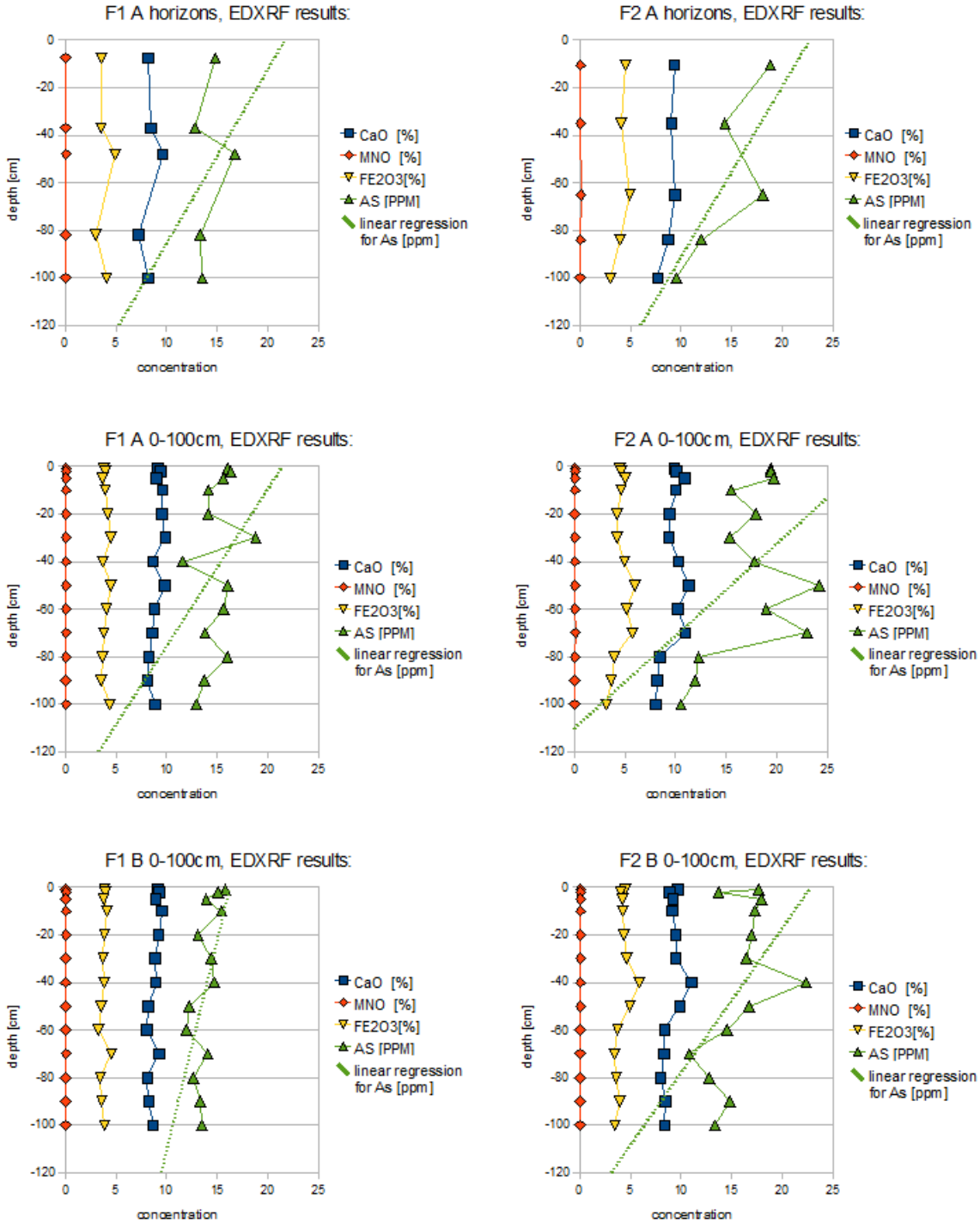

Figure 23:Vertical distribution of As, CaO, MnO and Fe_2O_3 in soil pits on field 1 and 2, for pedological and geochemical approach respectively

5.1.2 Horizontal distribution of As

A concise comparison of horizontal As distribution in first two centimetres of topsoil on F1 and F2 is given in figure 24 in form of a box-and-whisker plot, while detailed results are listed in table 24 and tables 46 to 51. A resultant conclusion is that F2 features in average higher As concentrations than F1, possibly emerging from the differing As burden in irrigation water (F1:154, F2: 241µgAs/l).

Grid sample results are illustrated in figure 25 and 26, using Kriging for spatial interpolation. Contrary to expectations, it is difficult to say if there are significant differences in As spreading within topsoil that can be attributed to their position in relation to water inlet. Minimum concentrations of As rather occur around the inlets and high concentrations are more likely a reflection of micro-relief, related to sinks where water accumulates during evaporation. Such sinks could be indicated by algae crusts spreading over soil surface as shown in picture 1. Statistic variables (quartiles and median) show no significant differences in As distribution between 0-1 and 1-2cm, but there seems to be an enrichment in 0-1cm on closer examination at the Kriging interpolations, especially at F2.

By the high clay contents, drying cracks appear in topsoil surface when evaporation is increased (s. picture 1). This can cause relocation of matter from the surface into deeper sections of Ap_1 and could distribute potential As enrichments.

In contrast to depth profiles, As correlations with other soil compounds (in particular for Ca- and Fe-oxides) are weak at F2 (Cor. As-Fe2O3=0.41/0.37; As-Ca=O 0.31/0.29) and moderate at F1 (Cor. As-Fe_2O_3=0.64/0.54 and CaO=0.65/0.43) (s. figure 25 and 26).

As burden of topsoil within both irrigation canals varies from 12-17ppm at F1 and from 13 to 74ppm at F2, with maxima appearing close to the wells (s. table 26). While As Situation in F1 canal is similar to the field, two very high values appear with 74 and 36ppm at F2. These differences remain unclear as distances to wells are similar and As contents of well waters are not that significantly high. Further conclusions, in particular possible relations to Fe and other soil constituents, can not be made because the total number of canal sediment samples is too low for statistics.

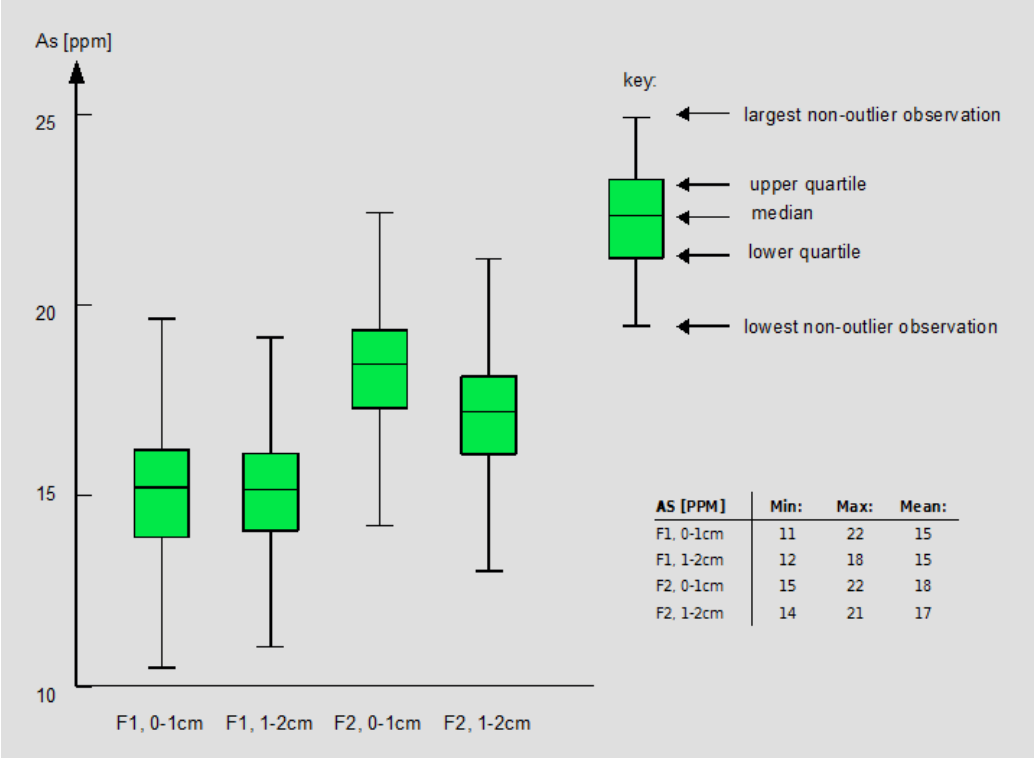

AS [PPM]	Min:	Max:	Mean:
F1, 0-1cm	11	22	15
F1, 1-2cm	12	18	15
F2, 0-1cm	15	22	18
F2, 1-2cm	14	21	17

Figure 24: Comparison of horizontal As distribution in topsoil on field 1 and 2

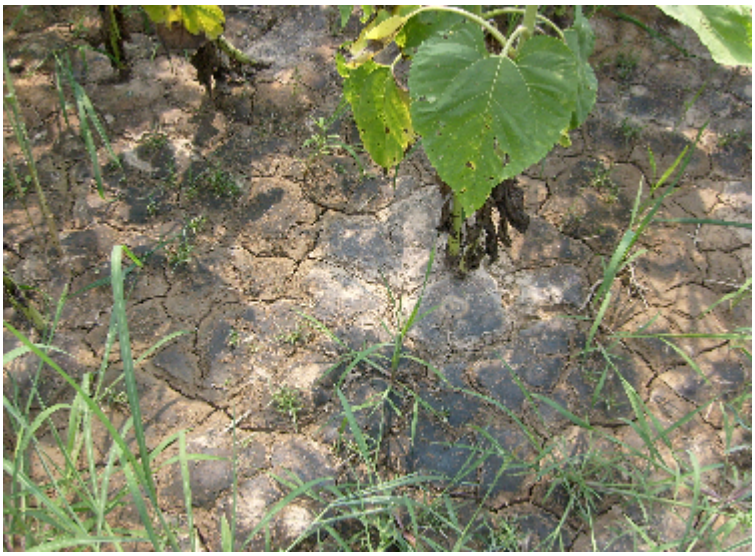

Picture 1: Bio-crust on soil surface at field 1

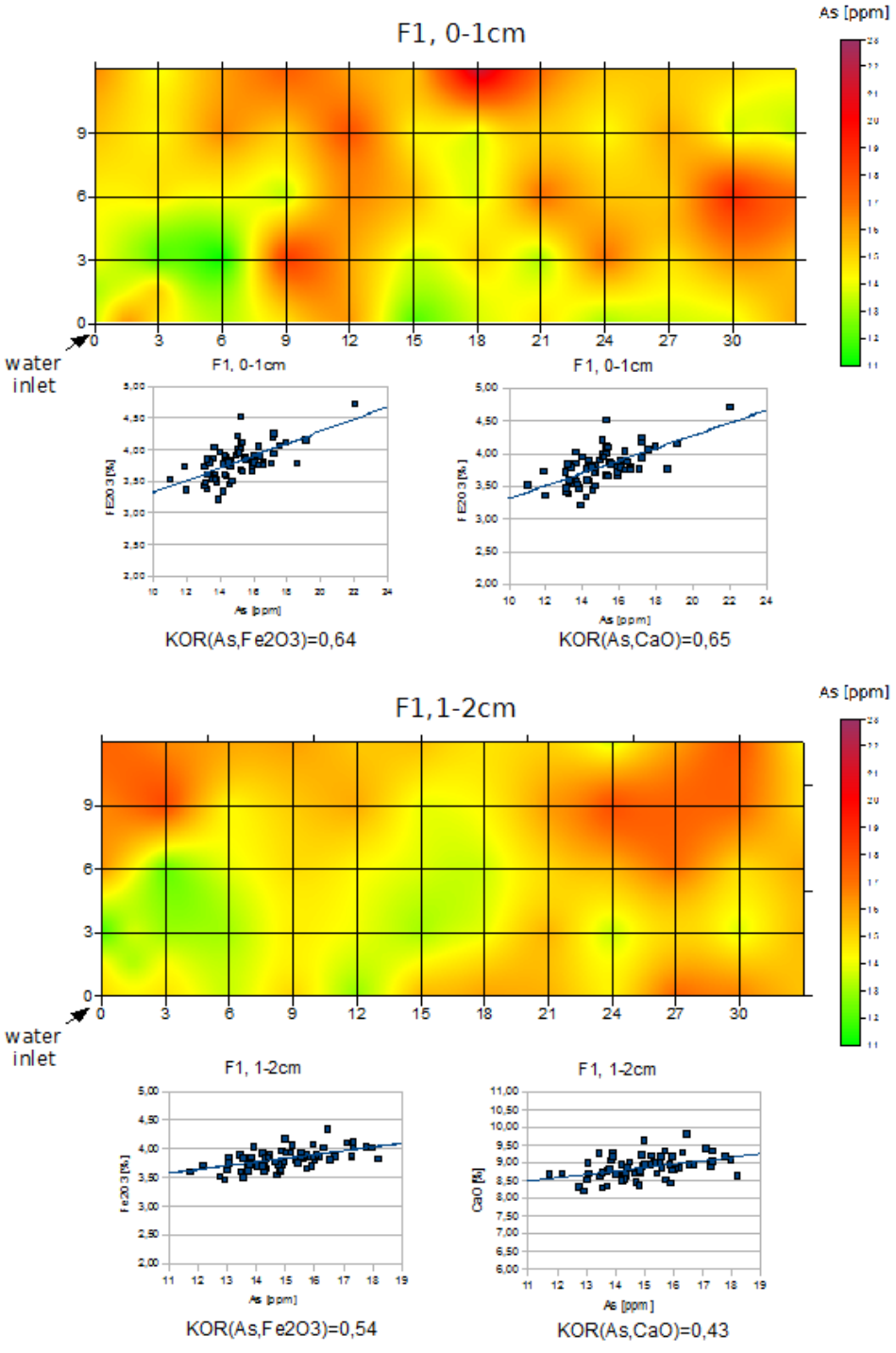

As [ppm]	F1, 0-1cm n=65	F1, 1-2cm n=65
minimum	11	12
25%quartile	14	14
median	15	15
75%quartile	16	16
maximum	22	18

Correlation coefficients:		K_2O	CaO	TIO_2	MNO	FE_2O_3	NI	CU	ZN
F1, 0-1cm	-As	0,56	0,65	0,62	0,45	0,64	0,11	0,21	0,47
F1, 1-2cm	-As	0,50	0,43	0,34	0,41	0,54	0,09	0,23	0,39
		BR	RB	SR	Y	ZR	NB	PB	
F1, 0-1cm	-As	-0,22	0,60	0,62	0,58	0,38	0,27	-0,22	
F1, 1-2cm	-As	-0,02	0,43	0,48	0,47	0,39	0,06	-0,19	

Figure 25: With Kriging interpolated horizontal As distribution on F1

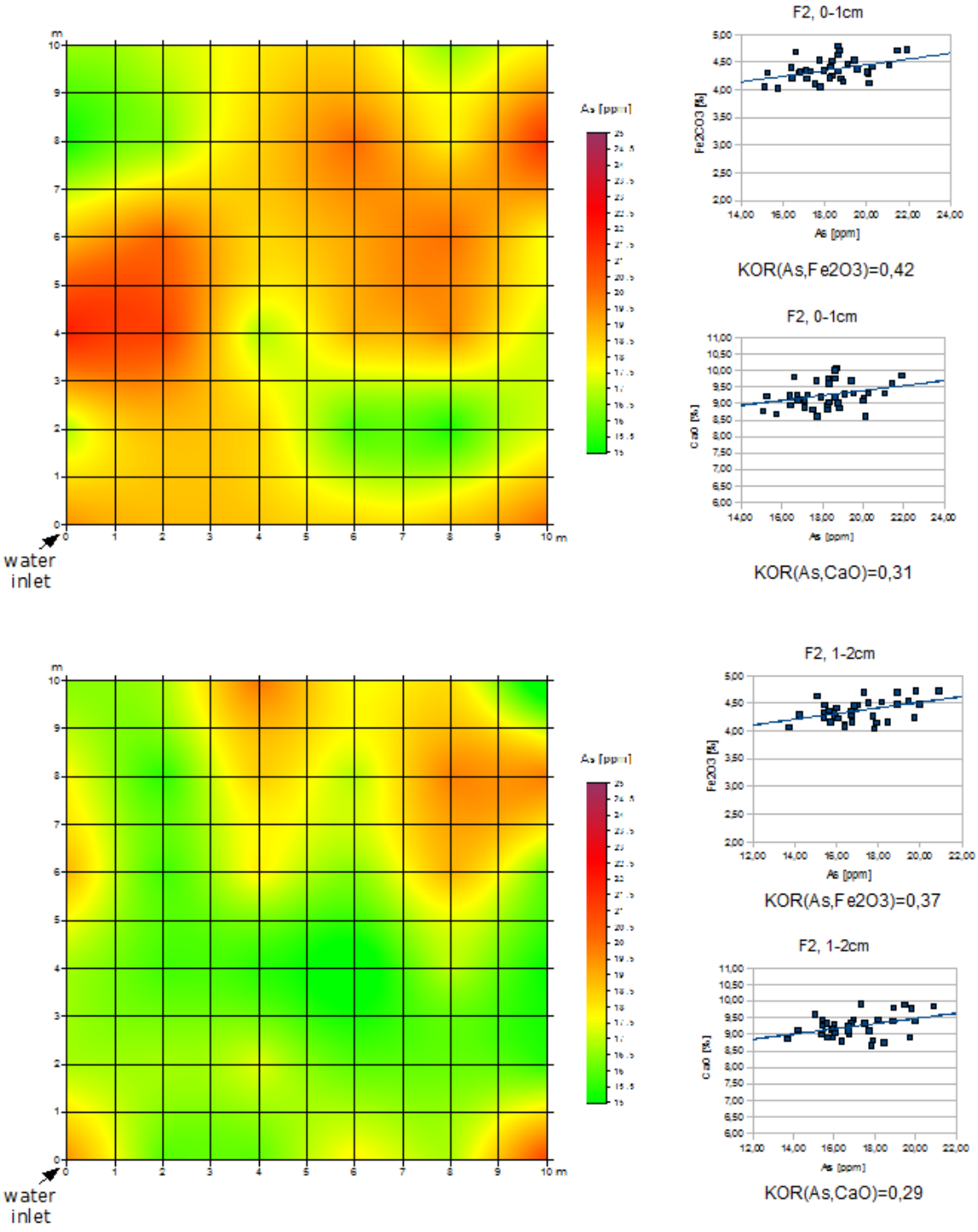

As [ppm]	F2, 0-1cm n=34	F2, 1-2cm n=34
minimum	15	14
25% quartile	17	16
median	18	17
75% quartile	19	18
maximum	22	21

Correlation coefficients:		K_2O	CaO	TIO_2	MNO	FE_2O_3	NI	CU	ZN
F2, 0-1cm	-As	0,27	0,31	0,21	0,35	0,42	0,38	0,06	0,15
F2, 1-2cm	-As	0,22	0,29	0,41	0,16	0,37	0,04	0,32	0,35
		BR	RB	SR	Y	ZR	NB	PB	
F2, 0-1cm	-As	-0,05	0,32	0,24	0,36	0,16	0,32	-0,35	
F2, 1-2cm	-As	0,02	0,28	0,35	0,23	0,05	0,09	-0,14	

Figure 26: With Kriging interpolated horizontal As distribution on F2

5.1.3 Soil characteristics at micro-scale

The results for the two mesh scans done with µ-SyXRF (presented in figure 17 and 18) display a quite inhomogeneous distribution of As amongst analysed soil compounds with only a few spots of high As deposits (>30ppm). Although µ-SyXRF is a semi-quantitative method, average As concentrations measured for both sections (14 and 16ppm) mainly coincide with ED-XRF results.

A common assumption is that As is primary fixed within Fe-coatings around mineral grains. Figure 27 contrasts As distribution to Fe- and Ca-spreading. For Fe, both correlation coefficients (F1:0.54, F2:0.64) and plots reveal a spatial relation to As. In case of Ca, correlation coefficients are weak (F1:0.19, F2:0.36), but the mappings show that relatively high As deposits are linked with high Ca concentrations. These micro-scaled observations strengthen the prior assumption and emphasize further a relevance of Ca-compounds in this soil.

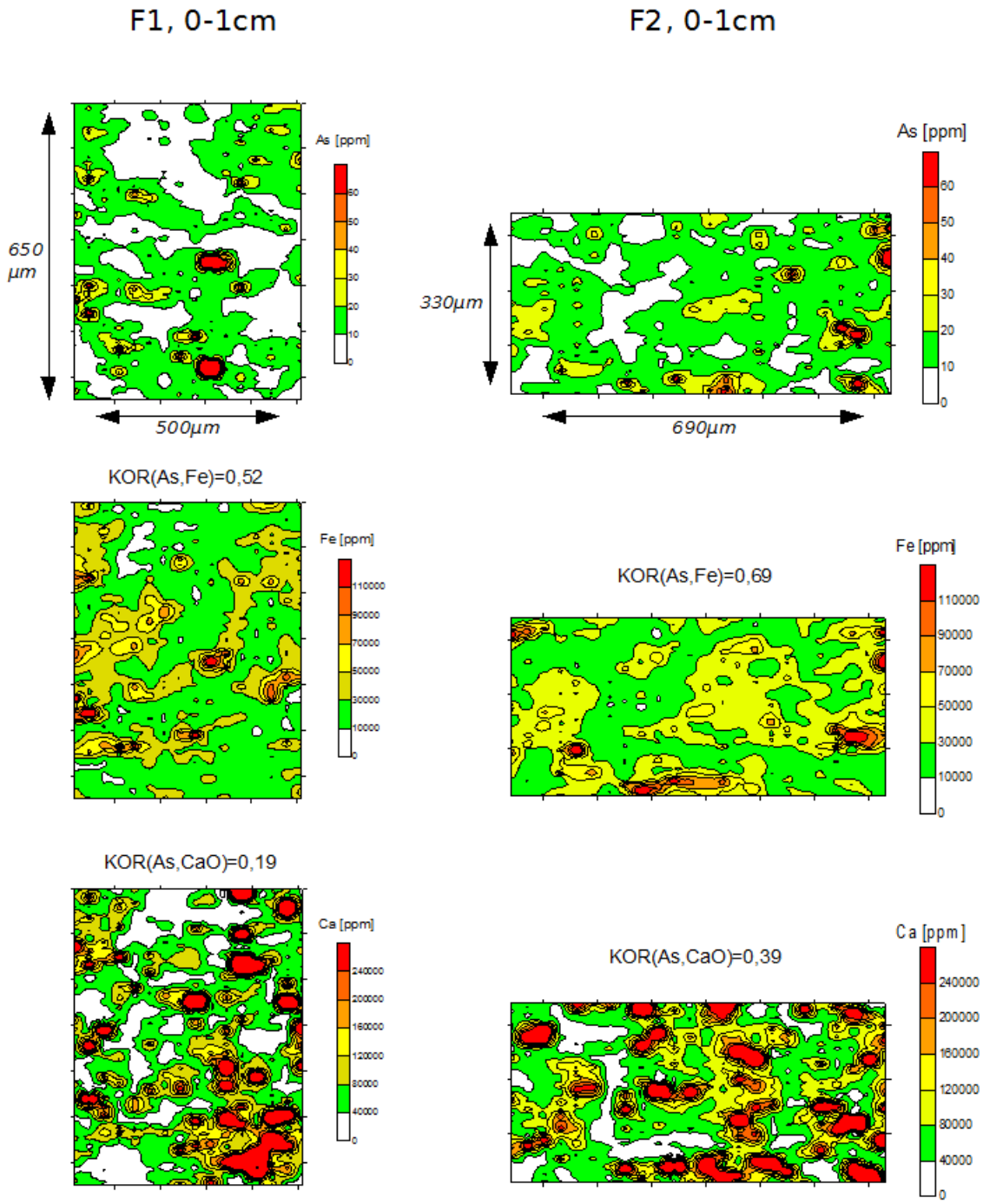

As [ppm]	F1, 0-1cm B25 A P20 n=2096	F2, 0-1cm B51 Q P6 n=2040
minimum	0,00	0,00
25%quartile	7,42	9,12
median	10,8	12,8
75%quartile	14,9	17,8
maximum	263	198

Correlation coefficients:

		Al	Si	S	K	Ca	Ti	V
F1, soil 0-1cm	-As	0,41	0,18	0,26	0,35	0,19	0,19	0,21
F2, soil 0-1cm	-As	0,41	0,18	0,42	0,20	0,39	0,13	0,22
		Cr	**Mn**	**Fe**	**Ni**	**Cu**	**Zn**	**Ga**
F1, soil 0-1cm	-As	0,10	0,28	0,52	0,32	0,42	0,56	0,60
F2, soil 0-1cm	-As	0,22	0,37	0,69	0,39	0,37	0,59	0,42

Figure 27: µ-SyXRF results for soil mesh scans, interpolated with Kriging

5.2 Quality and quantity of As burden at the sample sites

5.2.1 Irrigation water

The wells at field one (F1) and field two (F2) are in central of this study. They are used for flood irrigation of the fields and act therefore as primary As source. Although both wells are nearby (about 700m air-line distance) and deliver nearly from the same depths (83 and 80m), there are some obvious differences in hydro chemistry, especially pertaining salinity. F2 well has a 102x load of sulphate, calcium and magnesium, 7x strontium and about a 2.5x higher chloride and sodium content than F1 (s. table 20). Major differences in trace elemental composition occur only regarding manganese cations, while remaining measured elements range within similar dimensions.

Total As concentrations reach 154 (F1) and 241µg/l (F2) respectively, confirming the quick test results measured on-site of about 200µg/l. As appears predominantly in dissolved and trivalent form, with little share in suspended matter (<1,3%). It seems that suspended As is related to iron particles, both show a difference of factor 10 at the two fields (F1: 0.37µg As/l and 19.7µg Fe/l; F2: 3.12µg As/l and 194µg Fe/l)

Another important aspect is the fact that the irrigation water usually lasts up to one week on field surface before seepage. This causes a change from oxidic to reductive milieu, and could be associated with re-solution and reduction of As, leading finally to an increased bio-availability and plant uptake. Later, redox potential switches to oxidic conditions for one to two weeks, before next flood irrigation is done. On soil surface algae crusts appeared (see picture 1 in chapter 5.1) and in C-horizons of all four soil pits rust was observed, a clear indication of frequent changes between aerobic and anaerobic conditions (SCHEFFER at al. 2002).

In context of As co-precipitation under oxidic conditions, secondary water samples were taken from the inlets after several hours. The results shown in table 31 indicate a decrease of dissolved total As with time and an increase of As^{V} at the same time. The abrupt rise of suspended matter at F2 after 4h is related to a heavy rainfall, causing massive input of suspended matter from soil erosion by splash.

Table 31: As in relation to time

Sample:	**As $_{total}$ dis [µg/l]**	**As^{III} dis.[µg/l]**	**As $_{total}$ susp [µg/l]**
Field 1	154	238	0,37
Field 1 +6h	134	16,5	4,26
Field 2	238	219	3,12
Field 2 +4h	109	70,8	107

5.2.2 Plants grown at the sample sites

5.2.2.1 Sunflower and maize

FIAS analysis was replaced by HR-ICP-MS because of analytical problems as described in chapter 5.6, analytical problems. Results for sunflower and maize samples listed in table 27 indicate a characteristic decrease of As from roots to leaves and stems to seeds. Roots exhibit by far the highest As contents (770 to 3210µg/kg) and form the crucial link within the soil-plant system. They were therefore further examined by µ-SyXRF (s. 5.2.2.3). Both sunflower and maize leaves vary strong in As burden (<MDL to 481µg/kg for sunflower and 52.6 to 1210µg/kg for maize). One maize leaf was divided into 4 parts (tip, middle, beginning and basement) that were analysed separately, showing a permanent As increase towards the tip where growth mainly proceeds. As contents in sunflower stems are lower than in leaves, while maize stems show higher values, similar to the leaves. Regarding the seed, only two out of six samples hold a detectable amount of As (sunflower: 117, maize: 74µg/kg) , still below the Chinese food safety standard for cereals of 200µg/kg. Due to strong varying concentrations, there are no relations between As and sampling height (in case of leaves and stems) noticeable. In compare of As concentrations in roots to surrounding soil (presented in table 26), a relation is unlikely, too.

The bioaccumulation coefficient (mentioned in chapter 1.2) was calculated for one plant respectively, s. table 32. In case of leaves and stems, results for one sample height (F1: 40-50cm , F2: 180-200cm) with representative As concentrations was included.

Table 32: Calculation of bioaccumulation coefficients

	bioaccumulation coefficient	
Seed	0,008	0,004
Stem*	0,007	0,013
Leaf*	0,030	0,035
Root	0,081	0,140
Soil	1,0	1,0
	Sunflower, soil pit B	Maize, soil pit B

*related to leafe and stem from same height

Main criticism is that plants were not mature yet by the time of sampling. They would have probably accumulated more As in the remaining 3-4 weeks until harvest, especially in seeds.

5.2.2.2 µ-SyXRF results for root samples

µ-SyXRF results shown in figure 20, 21 (mesh scans), 22 and 28 (transects scans) reveal strong spatial correlations between As and Fe. Especially transect scans (s. figure 28 below) indicate that As is mainly accumulated around the rhizodermis (=root epidermis) within Fe-coatings, and appears only in lower concentrations within the root itself.

Illustrations of Kriging interpolations displaying As- and Fe-distribution are in comparison to microscope pictures of the scanned sections obviously disproportionate, but they give a goof idea of the coatings surrounding the rhizodermis. Most other measured elements like Al, Mn, Ga, and Zn seem to be included within the coatings as well (s. table 33 below). Results evidence further that preparation removed adherence soil successfully without destroying mineral coatings around the fine root epidermis.

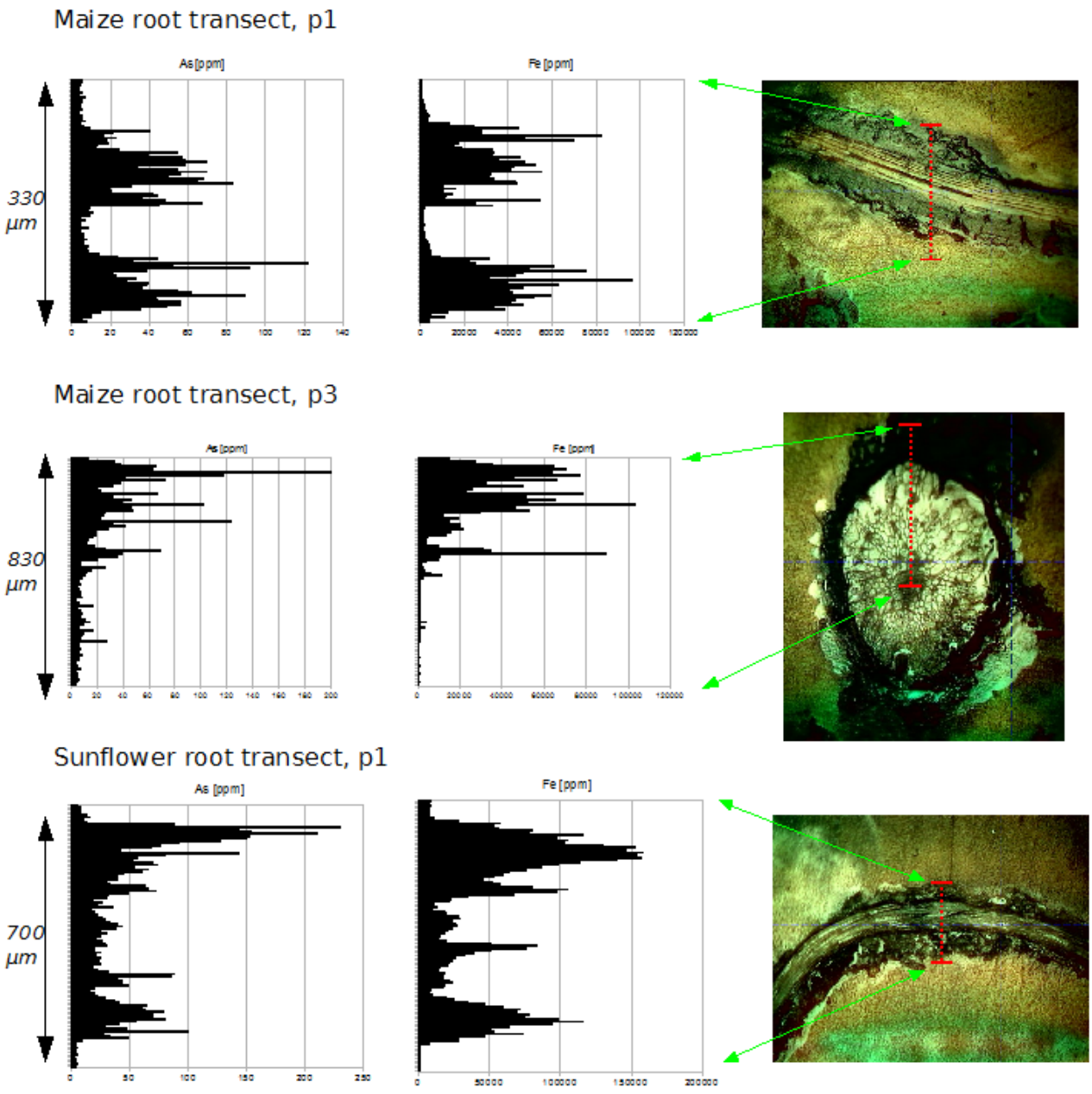

Correlation coefficients:		Al	Si	S	K	Ca	Ti	V
F1, sunflower root 1	-As	0,60	0,59	0,27	0,75	0,50	0,60	0,74
F1, sunflower root 2	-As	0,60	0,41	0,27	0,61	0,60	0,39	0,53
F2, maize root 1	-As	0,51	0,21	0,27	0,25	0,62	0,42	0,28
		Cr	**Mn**	**Fe**	**Ni**	**Cu**	**Zn**	**Ga**
F1, sunflower root 1	-As	0,06	0,22	0,57	0,21	0,39	0,54	0,53
F1, sunflower root 2	-As	0,44	0,67	0,64	0,56	0,52	0,49	0,61
F2, maize root 1	-As	0,28	0,64	0,64	0,68	0,56	0,68	0,55

Figure 28: Root transect results for µ-SyXRF

Table 33: Correlation coefficients between Fe and other measured elements

			Al	**Si**	**S**	**K**	**Ca**	**Ti**	**V**
transects	F1, sunflower root 1	**-Fe**	0,86	0,71	0,13	0,54	0,35	0,47	0,38
	F1, sunflower root 2	**-Fe**	0,85	0,66	0,32	0,92	0,78	0,66	0,83
	F2, maize root 1	**-Fe**	0,74	0,43	0,34	0,58	0,47	0,46	0,32
meshs	F1, sunflower root	**-Fe**	0,72	0,18	0,49	0,74	0,51	0,37	0,52
	F2, maize root	**-Fe**	0,71	0,31	0,59	0,7	0,45	0,64	0,43
			Cr	**Mn**	**Ni**	**Cu**	**Zn**	**Ga**	**As**
transects	F1, sunflower root 1	**-Fe**	0,25	0,5	0,51	0,35	0,82	0,92	0,57
	F1, sunflower root 2	**-Fe**	0,82	0,81	0,85	0,47	0,55	0,96	0,64
	F2, maize root 1	**-Fe**	0,38	0,78	0,86	0,46	0,75	0,8	0,64
meshs	F1, sunflower root	**-Fe**	0,67	0,84	0,71	0,55	0,85	0,87	0,57
	F2, maize root	**-Fe**	0,35	0,84	0,28	0,57	0,76	0,54	0,53

5.2.2.3 Vegetables

Total As matter in half of the vegetable random samples is below the HR-ICP-MS MDL of 52 ug/kg (s. table 28). The samples with detectable As range below average values for plants grown on uncontaminated soils published in NAIDU et al. (2006), s. table 2. Although total As fraction was measured, it is very likely that the samples with detectable As exceed the Chinese threshold value for inorganic As in vegetables of 50µg/kg (table 3) as main fraction of As in plants is present in inorganic form (NAIDU et al. 2006). In order to make a statistically based statement about As enrichment in vegetables, more samples are necessary.

5.3 Annual As input on the fields

In combination with the survey results (s. table 19), total As input per square metre and year could be calculated for each field.

Assumptions:

- irrigation with groundwater for 6 months per year and twice a month;
- water input for each irrigation about 60mm/m2 (a very discreet assumption);

→ total input of 720l/m^2 and year

As input::

F1= 720l/m^2*year * 154µgAs/l= 111 mg As/year*m^2

F2= 720l/m^2*year * 241µgAs/l= 174 mg As/year*m^2

This input would cause an annual increase of about 3.3 (F1) and 5.1ppm (F2) in topsoil, acting on the theoretical assumption that all As is accumulated in the first two centimetres of topsoil ,featuring a density of 1,7kg/cm^3. This calculation is only an example and shall give an idea about the input dimensions. As infiltration ranges in reality of course deeper than only two cm.

Although being off-topic, it should be mentioned that at the same time more than 0.6 (F1) and 2.1kg (F2) respectively of salts (Na^+, Mg^{2+}, Ca^{2+}, Cl^- and $SO4_3^-$) are being brought onto each square metre field soil per year, clearly provoking soil salinization. Such a massive presence of anions could further induce As release by anion replacement from Fe-oxyhydroxides and other soil constituents. The farmers should reconsider to return to irrigation with surface water from Huang He instead of using groundwater.

5.4 Supplementary examinations within the surroundings

5.4.1 Water examinations

Groundwater samples (described in tables 20, 21 and 39 to 41 in appendix) are in general characterised by weak to moderate alkalinity (pH 7.7-9.1) and negative redox potentials (between -138 and -178 meV), indicating reducing conditions within the respective aquifers. Deliver depth of sampled wells ranged from 17 to 83m, so groundwater was taken from different aquifers. Strongly varying values for sulphate (below IDL up to 1040 mg/l), chloride (172-1100mg/l), sodium (119-1010mg/l) and magnesia (16.3-188 mg/l) reflect differences in salinity and geochemical conditions in subsurface.

Major total As is present in dissolved form, ranging from 154 up to 959µg/l, as suspended fraction (>0.45µm) reaches only 0.97-14.4µg As/l. Dissolved As is mainly present in the toxic form $As^{III,}$ another reference to reducing environments in aquifer sediments. These values explicitly exceed the Chinese drinking water threshold value of 10µg As/l and form a strong hazard to human health if used as drinking water.

In comparison to dissolved contents, suspended matter seems to be of little importance, only location 20 exhibits elevated concentrations for most elements (s. table 41, appendix).

Measured contents in water samples coincide with results from Guo et al. (2008) and suggest that geochemistry in aquifers varies at small scale and reflects inhomogeneous and complex sediment composition in underground like described in chapter 2.6. Positive facts are the absence of phosphate (below IDL) and low contents of nitrate (<IDL to 8.17mg/l), both indicators for extensive fertilizer application. Some bacteria are able to reduce nitrate to elemental nitrogen by denitrification in anaerobic conditions. The results give reason to consider biological activities under reducing conditions within the aquifer sediments as a possible source of As release, but concentrations of dissolved iron (16.8-1330µg/l) are low (compared to other high As contaminated groundwater, for example in West Bengal, described in STÜBEN et al. 2008) and it is questionable if dissolution of Fe-oxyhydroxides leads to As release. Due to the high salinity, anion exchange processes (as postulated in GOH and LIM 2004) are rather imaginable, but this problem is not subject to this case study.

The sample taken from Huang He River differs strongly from the groundwater samples. Conditions are aerobic and according to its name, Yellow River water is characterised by a high suspended load of clayey and silty material. Total As content reaches 53.5µg/l, with remarkable 87.5% belonging to particular phase. Due to the Huang He's huge size and load with particulate matter, his sediments could form an important source for As. This circumstance also applies to all other elements. Suspended material forms usually a multiple of the dissolved compounds, except for sodium, magnesium, strontium and molybdenum. Regarding the high iron content of 80.2mg/l, it is very likely that As is transported bound to Fe-oxyhydroxides. Nevertheless, it is quite unlikely that surface water conveyed in the canal system for irrigation purposes still examines that much As when reaching the fields as most of the suspended matter should have sedimented before.

Tap water sampled at our Hotel in Xamba can be considered as a kind of reference material in comparison to the groundwater samples. It contains furthermore a reference to As elimination quality of the local drinking water treatment. Total As amounts 18.1µg/l with 81.2% in dissolved form, still slightly exceeding the Chinese drinking water threshold value

5.4.2 Hair samples

Hair composition in respect to burden with As and other heavy metal elements is shown in table 29. Similar to high As contaminated areas of Bangladesh (CHOWDHURY et al. 1999 in BHATTACHARYA et al. 2007), As is enriched in hair of local residents in Hetao-Plain with 0,53 up to 6.3mg/kg. According to NAIDU et al. (2006), hair sample between 0.1-0.5 mg/kg indicate chronic As poisoning, whereby all sample donors are concerned. In addition, there seems to be a relationship between As burden in hair and well water (used as drinking water) in samples 1,3, 5 and 6. By contrast, samples 2 and 7 show high contents in hair but low in well water, indicating that there are other sources of As besides drinking water. Same applies to sample 4 showing the highest As load both in hair and well water, but the subject does not consume the well water. Other heavy metals appear to be enriched as well. Even though the use of hair samples for human biomonitoring is not indisputable (s. DREXLER and SCHALLER 1999) and the implementation in this study is limited to random samples being not representative, they are a possible evidence for As enrichment in human being. The public health authority started recently to make preparations for a area-wide urine biomonitoring within Hetao-Plain to manage the As problem. During our field campaign, a medical scientist accompanying us collected urine samples as reference background for further investigations.

5.5 Estimation of As situation in Hetao-Plain

Analysis results show that the direct consumption of As burdened groundwater as drinking water forms the main input into human being within Hetao-Plain. The toxic dissolved As^{III} species dominates and the Chinese drinking water threshold value is at some locations exceeded in a threatening extent (for example location 16/32 with 959µg As/l) The USEPA reference dose of 30x 10^{-4} mg/kg bodyweight/day as maximum acceptable daily load for man (MADL) can be exceeded easily if the groundwater is consumed. One litre of water from the well at F1 for example, is sufficient to meet the MADL for a person of 50kg. Additionally, As can be taken up via foodstuff as results for vegetables and eggs reveal, but in lesser extent. Further studies should be carried out to confirm these results and to estimate As input via foodstuff more precisely.

Soil samples taken at the sample sites at Yong-Ming indicate that irrigation with As loaded water can cause enrichment in topsoil already after a short time. Annual input was calculated in a discreet estimation with 111 and 174 mg As/m^2, causing in worst case an increase in topsoil of some ppm. However, As contents in topsoil are not critical yet, but could rise middle-term. On the other hand, it is very likely that agriculture will not exist any longer if irrigation continues with such enormous salt inputs causing soil salinization.

The crucial question is the bioavailability of As when brought onto field and the influence of permanent changing redox potentials in soil caused by flood irrigation. Additionally, As mobility could be affected by the strong salinity and alkaline pH of the irrigation water and high clay mineral and calcite contents in soil. Because of these complex feasible interactions, it is very difficult to assess the fate of As in field soil in this special case. Therefore, further research is required as described in chapter 7, outlook.

5.6 Analytical problems

5.6.1 Water analysis

During analysis, some unexpected problems appeared. First of all, acidifying of the water samples in field (adding 50µl HNO_3 conc.) was in some cases insufficient as pH measurements in lab revealed. This is important, As solubility is strongly correlated to pH and precipitation effects can occur under neutral conditions. To adjust this, a second acidifying was done for the most important samples (as described in chapter 3.2.2.2) and measurements were repeated. As a consequence, measuring pH value is quoted in all results. Table 34 and figure 29 illustrate the different pH values (measured on-site in field and in lab, before and after secondary acidifying) and changes in detected As. It is incomprehensible why there is such a different in the two samples (As total and As^{III}) at location 16(32) after first acidifying, because sample and acid volumes were equal.

Another problem is, that some AsIII contents exceed the total As concentrations, what should not be possible. Concerned locations are highlighted red in table 35. Small differences below 10% are explainable with natural and analytical fluctuations, but everything else is incomprehensible. There are no problems reported in relation to the AsV restraining cartridges we used. Only possible explanation is a mix-up of the respective samples in field, but this is hardly imaginable.

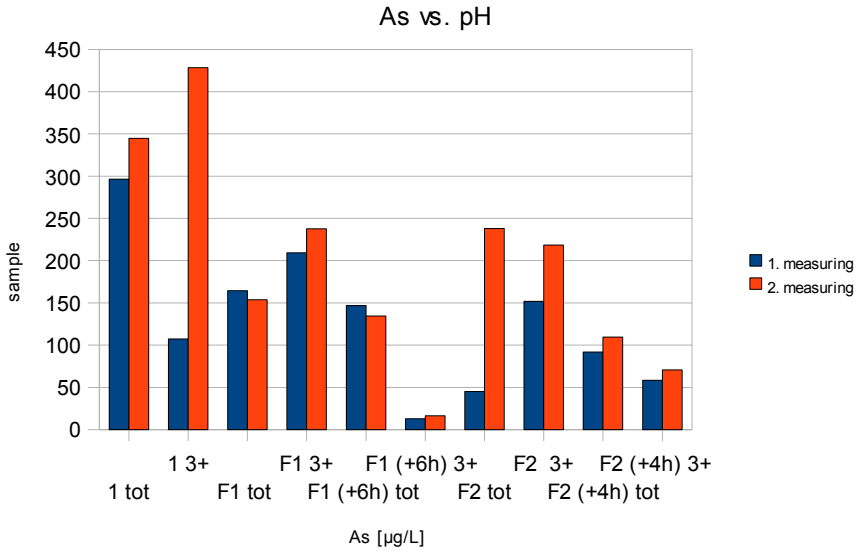

Figure 29: pH related measuring problems

Table 34: Problems concerning pH

Sample:	**pH** no acid	**pH** 1. acidif.	**pH** 2. acidif.	**As [µg/L]** after 1. acidif.	**As [µg/L]** after 2. acidif.	**Change 1. to 2.** pH decrease	As increase %
1 As tot	8,2	7,5	0,36	296	345	7,1	16,3
1 AsIII	8,2	7,5	0,38	107	428	7,1	299
16 (32) As tot	8,3	7,3	-	959	-	-	-
16 (32) As^{III}	8,3	4,8	-	841	-	-	-
19 As tot	8,2	2,7	-	301	-	-	-
19 As^{III}	8,2	2,6	-	248	-	-	-
20 As tot	7,7	2,9	-	191	-	-	-
20 As^{III}	7,7	2,7	-	157	-	-	-
F1 As tot	9,1	7,5	0,38	165	154	7,1	-6,6
F1 50ml As^{III}	9,1	7,5	0,4	209	238	7,1	13,5
F1 +6h As tot	-	7,7	0,32	147	134	7,3	-8,52
F1 +6h As^{III}	-	7,1	0,36	12,8	16,5	6,7	28,5
F2 As tot	-	8,0	0,31	45,0	238	7,7	429
F2 As^{III}	-	8,0	0,42	152	218,5	7,6	43,8
F2 +4h As tot	-	8,3	0,39	92,0	109	7,9	19,0
F2 +4h As^{III}		-	0,46	58,5	70,8	-	-
Huang He As tot	-	1,9	-	6,70	-	-	-
Hotel As tot	-	6,3	-	14,7	-	-	-

Table 35: Differences between AsIII and AsV contents in relation to measuring pH

HR-ICP-MS: As^{III} vs As^{V} n= neutral a=acid						
Location:	pH:	As tot **As [µg/L]**	As 3+ **As [µg/L]**	As 5+ **As [µg/L]**	As 3+ %	As 5+ %
1	n	296,38	107,43	188,95	36,25	63,75
	a	344,67	428,27	-83,61	124,26	-24,26
16 (32)	n	958,63	840,78	117,85	87,71	12,29
19	a	301,23	247,93	53,3	82,31	17,69
20	a	190,58	157,18	33,4	82,47	17,53
Field 1	n	164,53	209,38	-44,85	127,26	-27,26
	a	153,67	237,65	-83,98	154,65	-54,65
Field 1 (+4h)	n	146,88	12,85	134,03	8,75	91,25
	a	134,36	16,51	117,85	12,29	87,71
Field 2	n	44,96	151,92	-106,95	337,86	-237,86
	a	237,97	218,5	19,46	91,82	8,18
Field 2 (+6h)	n	91,98	58,48	33,5	63,58	36,42
	a	109,47	70,81	38,66	64,68	35,32

5.6.2 Soil analysis

Major problem of As analysis done with ED-XRF is that most measured values are close to the IDL of 5ppm, causing statistical variances of about ± ½ IDL (~±2.5ppm). This variance corresponds unfortunately with most concentration differences, especially with regard to the question of vertical and horizontal enrichment in topsoil. Only high numbers of samples provide statistically firm conclusions, as in comparison of F1 to F2 in form of a box-whisker-plot.

Results for used soil standards (GXR 2 and 5, soil 5 and 7) differ for some elements, but deviations related to As contents are in average only 8% below the certified value. ED-RFA results were corrected regarding the average deviations to the reference values, see table 54 in appendix.

A specific problem related to correlation coefficients are so called spurious relationships. To avoid false conclusions, all possible appearing correlations were reviewed in literature and mentioned as far as possible in chapter 1.2, geochemistry of As.

5.6.3 Plant analysis

A cross-check with several microwave digestions (mainly rice and citrus leave standards) revealed significant differences between analysis results of FIAS and HR-ICP-MS. As consequence, all plant samples and standards analysed with FIAS were measured again by HR-ICP-MS. Table 36 emphasizes the differences in case of used standards. FIAS results are constant lower (about 40%) compared to HR-ICP-MS, while HR-ICP-MS values are rather consistent with the given reference values and show lower standard derivations (except for the HAY standard). Table 55 in appendix opposes FIAS to HR-ICP-MS results. There are several possible causes for this phenomenon. Rüde (1996) and Welz (1990) describe interferences in hydrate generation induced by acid residues. HF is particularly significant, signal reductions already appear at HF concentrations of about 0.01%. Although all digestions were fumed off for three times, it is thinkable that there are still marginal HF residues remaining. Another possible reason for decreased arsine generation are matrix effects caused by cations (like Cu, Fe, Ni,Co), as hydrides can co-precipitate with or adsorb to metallic deposits (HEINRICHS 1998). This effect seems to apply to the root samples, which are characterised by high Fe contents and strong deviations between FIAS and HR-ICP-MS results (FIAS values reach only 1/3 of HR-ICP-MS) at the same time, represented in table 37. Methodical detection limits of FIAS and HR-ICP-MS are not as low as the

instrumental detection limits, because microwave digestion blanks vary slightly as a result of inaccuracies in sample preparation. Due to a higher analytical accuracy, HR-ICP-MS features a little higher MDL than FIAS (s. table 36 below).

Table 36: Comparison of HR-ICP-MS with FIAS

Detection limits*:	**HR-ICP-MS**	**FIAS**	
	As [ug/kg]	As [ug/kg]	
IDL	23	12	
MDL	52	33	
*related to 250mg net weight DW and 25ml volume			
Standards:	**HR-ICP-MS**	**FIAS**	**Reference val.**
	As [ug/kg]	As [ug/kg]	As [ug/kg]
Rice 2	89,02	56,24	110
Rice 4	81,74	79,16	
Rice 6	99,68	75,82	
Rice 8	81,65	<MDL	
average:	88,02	70,4	
std. derev.:	8,51	12,38	
Citrus 1	3068,5	2132,32	2800-3400
Citrus 3	2952,96	2208,18	
Citrus 5	3017,13	2457,67	
Citrus 7	3070,97	2596,73	
Citrus 9	2905,28	2432,95	
average:	3002,97	2365,57	
std. derev.	72,74	190,81	
Hay 1	160,43	43,39	not specified
Hay 3	139,22	53,1	
Hay 4	105,25	46,2	
Hay 5	136,84	55,02	
Hay 6	126,74	56,05	
Hay 7	101,88	57,53	
Hay 8	86,4	<MDL	
Hay 9	121,97	<MDL	
Hay 10	77,22	<MDL	
average:	96,87	57,53	
std. dev.:	26,87	5,74	

Table 37: Relationship between Fe content in root and deviation between FIAS and HR-ICP-MS

Sample location:	**As measured FIAS/HR-ICP-MS**	**Fe in digestion [µg/L]**
F1 A	0,24	17400
F1 B	0,25	16400
F1 middle	0,24	35300
F2 A	0,34	8940
F2 B	0,41	44200
F2 middle	0,21	37600
average root samples:	0,28	26600
average of remaining samples*:	0,59	2020

*with As> MDL

6. Summary

Research design and methodology:

Subject of this case study were the consequences of irrigation by As contaminated water in the Hetao-Plain, part of the Inner Mongolia Autonomous Region in China. Therefore, the arsenic (As) distribution within the food chain was examined in a representative farming village named Yong-Ming in the North-West of the plain. Field survey revealed that the farmers in Yong-Ming village substituted Huang He River water by high As burdened groundwater for irrigation purposes three years ago, providing the opportunity to assess the influence of As on field soil since this time.

Two fields (field 1 and 2) were chosen to be sampled, a sunflower and a maize field, both irrigated by tube wells. The As quick test displayed for each a total concentration of about 200 µg As/l, hence multiple water samples were taken. In order to examine the spatial As distribution within both field soils, four soil pits were excavated and two sample grids installed to enable extensive sampling. Representative samples from plants grown on the two fields were also taken to be checked for potential As burden. To complete the survey, water and hair samples were additionally taken in villages and homesteads in nearby surroundings to improve the estimation of As situation within Hetao-Plain.

Analytics:

Water samples were analyzed using HR-ICP-MS for cation and trace elemental detection and IC to determine anion composition. Soil samples were characterized by ED-XRF, XRD and CSA. µ-SyXRF at the ANKA provided an insight into total As distribution within topsoil at micro-scale and was also used to scan sunflower and maize roots sections. For interpretation of spatial data, Kriging interpolation was applied. The total As content of food chain samples was first quantified with FIAS, then by HR-ICP-MS.

Results:

-Water samples:

The groundwater samples taken in the surroundings and at the sample sites are characterized by varying consistences related to pH, salinity and As content. This reflects moderate to strong reducing conditions and a complex, inhomogeneous hydro geochemistry within the aquifers.

All groundwater samples exceed the Chinese drinking water threshold value of 10µg As/l by far and form a strong hazard to human health if used as drinking water. The toxic form As^{III} dominates in dissolved matter, while suspended matter contains only marginal contents of As. Based on the survey results and total As concentrations measured in well water at both sample sites (154µg/l at F1 and 241µg/l at F2), the annual input in topsoil per square meter was approximately calculated as 111mg and 174mg respectively. Remarkable are the differences in salinity as both wells are located nearby and deliver almost from the same depths (80 and 83m). In contrast, moderate As concentrations are transported in Huang He surface water mainly in form of suspended matter.

-Soil samples:

Vertical distribution of As in soil pits indicates a slight enrichment in topsoil and a possible relation to grain size and soil texture in mineral horizons of both fluvisols. Spatial spreading within topsoil (11.0 to 22.0 mg As/kg) varies strongly and there is no relation between As accumulation and position to inlet noticeable. It rather seems that As enrichment reflects the surface micro-relieve. ED-RFA and µ-SyXRF analysis reveal that mainly Fe- and Ca-compounds appear to have an important effect on As mobility in soil as there are the dominating components and important possible As adsorbents at the same time. Mesh scans done with µ-SyXRF display further a quite inhomogeneous distribution of As amongst analysed soil compounds, limited to a few spots of deposits with >30mg As/kg.

-Food chain:

Although As concentrations in soil are not that serious, As could have been detected in micro wave digestions of plant parts with up to 3210µg/kg DW by HR-ICP-MS. Results for sunflower and maize samples indicate a characteristic decrease of As from roots to leaves and stems to seeds, in which roots feature by far the highest contents. With regard to human uptake, one third of the seeds and half of the vegetable random samples taken next to F2 accumulated As in detectable amounts (74.2-184µg As/kg DW), but still in concentrations that are in the range of plants grown on uncontaminated soils. Evaluation of µ-SyXRF results for root transect and mesh scans of sunflower and maize plants reveal that most of the As is associated with Fe-coatings around the rhizodermis and appears only in lower concentrations within the root itself. Random hair samples taken from locals in the surroundings indicate with contents ranging from 0.53 up to 6.3mg/kg chronic As poisoning.

-Conclusion:

As can be detected in food chain in varying concentrations. The USEPA reference dose of 30x 10^{-4} mg/kg bodyweight/day as maximum acceptable daily load for man (MADL) can be exceeded easily if the groundwater is consumed. Additional As can be taken up in lesser extent via foodstuff as results of vegetable and egg samples reveal.

The crucial question is the bioavailability of As in field soil in this special case respective the complex prevailing means. As contents in topsoil are not critical yet, but could rise middle-term if irrigation is continued. On the other hand, it is very likely that agriculture will not exist any longer because of soil salinization, caused by the enormous salt input. Hence the farmers should as quickly as possible try to deliver irrigation water from a less problematic aquifer or return to Huang He surface water if possible.

Finally, further research on the As burden of foodstuff and the fate of As brought on field are required, as described in chapter 7, outlook. It is an essential challenge to assure the supply with uncontaminated drinking and irrigation water within this ancient and unique man-made environment of the Hetao-Plain.

7. Outlook

In spite of all extensive research done in this study, there are still many questions remaining unanswered in context of As situation in Hetao-Plain and in general.

In Hetao-Plain, science provides an opportunity to examine a complete different environment of As release and manner than in the extensive investigated areas of West-Bengal and Bangladesh, as prevailing geochemistry, climate and land use differ strongly. Isotope analysis of precipitated sulphate from water samples of Hetao-Plain were recently carried out at IMG to provide an indication of As release mechanisms in subsurface, but results were not yet interpreted.

Soil monitoring should continue during the next years on both sample sites, carrying out control measurements each two or three years to examine As enrichment in topsoil and plants, but it is very likely that soil salinization is going to interfere with crop cultivation soon. Moreover, it is very important to spot out for other fields that are also irrigated with groundwater and to check the contamination level. Sequential extractions, lysimeter and column experiments could additionally help to estimate As ad- and desorption processes in topsoil. Other possible As input sources like pesticide and fertilizer application should be identified and qualified as well.

Further studies on As release and enrichment in food chain within Hetao-Plain are essential, as many thousands of people are affected here and in other similar areas of the Inner Mongolia Autonomous Region. Therefore, exact maps of As distribution within groundwater aquifers are required that can be used as base for human biomonitoring, which is already scheduled. More studies on the As burden of foodstuff (especially vegetables and animal products) should be done as random food chain samples indicated partially moderate As loads. One should also pay more attention to As transfer via fodder plants to livestock.

Finally, an integrated control and management system that plans and coordinates all actions based on present research results of groundwater, foodstuff and arsenicosis distribution could be a crucial tool to contain As burden in population. The well established cooperation between local public authorities and scientists should be extended and local agents from affected villages should be included.

In February 2008, I availed myself of the opportunity of carrying out some additional

measurements at the newly established SUL-X beamline at the ANKA. Here are three synchrotron radiation based analysis methods combined, X-ray diffraction (XRD), fluorescence analysis (XRF) and X-ray absorption spectroscopy (XAS), all operating in µm dimensions. The root thin-sections were analysed again in order to get more detailed information about elemental (XRF) and mineral (XRD) composition of the root coatings and the ratio of As^{III} to As^{V} (XAS). Results will be published at the earliest possible date.

8. LITERATURE

ALLOWAY, B.J. (1999): Schwermetalle in Böden. Berlin, Heidelberg: Springer Verlag

ARMSTRONG, M. (1998): Basic linear geostatistic. Berlin, Heidelberg: Springer Verlag

BARNES, M., CORRELL, R., SMITH, E., NAIDU, R., HUQ, S.M. (2005): Assessing dietary uptake of arsenic by villagers in Bangladesh. International Statististical Institute. 5 pp.

BHATTACHARYA, P., MUKHERJEE, A.B., BUNDSCHUH, J., ZEVENHOVEN, R., LOEPPERT, R.H. (2007): Arsenic in soil and groundwater environment: Biogeochemical Interactions, Health Effects and Remediation (Trace Metals and Other Contaminants in the Environment). Amsterdam: Elsevier

CHENG, Y., JIANG X., GAO S. (2000): Concise regional geology of china. Beijing: Geological Publishing House

DITTMAR, J., VOEGELIN, J., ROBERTS, L.C., HUG, S.J., SAHA, G.C., ALI, M.A., BOHRAN, M., BADRUZZAMAN, M., KRETZSCHMAR, R. (2007): Spatial Distribution and Temporal Variability of Arsenic in Irrigated Rice Fields in Bangladesh. 2. Paddy Soil. Environ. Sci. Technol. 41, 5967-5972

DREXLER, H., SCHALLER, K.-H. (1999): Haaranalysen in der klinischen Umweltmedizin: Eine kritische Betrachtung. Dtsch Ärztebl. 99, 45, A 3026–3029

FAYIGA, A.O., MA, Q.L., ZHOU, Q. (2007): Effects of plant arsenic uptake and heavy metals on arsenic distribution in an arsenic-contaminated soil. Environmental Pollution Kidlington. 147, 3, 737-742

FIEDLER, H.J., RÖSLER, H.J. (1993): Spurenelemnte in der Umwelt. 2. Aufl. Jena; Stuttgart: Gustav Fischer Verlag

FUJINO, Y., GUO, X., SHIRANR, K., LIU, J., WU, K., MIYATAKE, M., TANABE, K., KUSUDA, T., YOSHIMURA, T., JAPAN INNER MONGOLIA ARSENIC POLLUTION STUDY GROUP (2006): Arsenic in Drinking Water and Peripheral Nerve Conduction Velocity among Residents of a Chronically Arsenic-affected Area in Inner Mongolia. Journal of Epidemiology. 16, 5, 207-213

GOH, Kok-Hui, LIM, Teik-Thye (2005): Arsenic fractionation in a fine soil fraction and influence of various anions on its mobility in the subsurface environment. Applied Geochemistry. 20, 2, 229-239

GOVINDARAJU, K. (1994): Compilation of working values and sample description for 383 geostandards. Geostandards Newsletter. 18, Special Issue, 1-158

GUO, H. , YANG, S., TANG, X. LI, Y., SHEN, Z. (2008, in press): Groundwater geochemistry and its implications for arsenic mobilization in shallow aquifers of the Hetao Basin, Inner Mongolia. Science of the Total Environment.

GUO, H., STÜBEN, D., BERNER, Z. (2007 a): Arsenic removal from water using natural iron mineral-quartz sand columns. Science of the Total Environment. 377, 142-151

GUO, H., STÜBEN, D., BERNER, Z. (2007 b): Removal of arsenic from aqueous solution by natural siderite and hematite. Applied Geochemistry. 22, 1039-1051

GUO, X., FUJINO, Y., KANEKO, S., WU, K:, XIA, Y., YOSHIMURA, T. (2001): Arsenic contamination of groundwater and prevalence of arsenical dermatosis in the Hetao-Plain area, Inner Mongolia, China. Molecular and Cellular Biochemistry. 222, 137-140

HEIKENS, A. (2006): Arsenic contamination of irrigation water, soil and crops in Bangladesh: Risk implications for sustainable agriculture and food safety in Asia. Bangkok: Food and Agriculture Organization of the United Nations, regional office for asia and the pacific

HEINRICH, J. (2007): ANKA Instrumentation Book. Eggenstein-Leopoldshafen: ANKA Angstroemquelle Karlsruhe, ISS Insitute for synchroton radiation, Forschungszentrum Karlsruhe GmbH

HEINRICHS, H. HERRMANN, A.G. (1998): Praktikum der Analytischen Geochemie. 1. Aufl. Berlin: Springer

JOCHUM, K.P., DINGWELL, D.B., ROCHOLL, A., STOLL, B., HOFMANN, A.W., BECKER, S., BESMEHN, A., BESETTE, D., DIETZE, H.-J., DULSKI, P., ERZINGER, J., HELLEBRAND, E., HOPPE, P., HORN, I., JANSSENS, K., JENNER, G.A., KLEIN, M., MC DONOUGH, W.F., MAETZ, M., MEZGER, K., MUENKER, C., NIKOGOSIAN, I.K., PICKHARDT, C., RACZEK, I., RHEDE, D., SEUFERT, H.M., SIMAKIN, S.G., SOBOLEV, A.V., SPETTEL, B., STRAUB, S., VINCZE, L., WALLIANOS, A., WECKWERH, G., WEYER, S., WOLF, D., ZIMMER, M. (2000): The Preparation and Preliminary Characterisation of Eight Geological MPI-DING Reference Glasses for In-Situ Microanalysis. Geostandards Newsletter. 24, 1, 87-133

KABATA-PENDIAS, A., PENDIAS, H. (1985): Trace elements in plants and soils. Boca Raton, Florida: CRC Press Inc.

KEON, N.E., SWARTZ, C.H., BRABANDER, D.J., HARVEY, C., HEMOND, H.F. (2001):Validation of an Arsenic Sequential Extraction Method for Evaluating Mobility in Sediments. Environmental Science & Technology. 35, 13, 2778-2784

KICZKA, M. (2005): Verteilung, Trägerphasen und Spezies von Arsen aus Bewässerungswasser in Reisböden und -pflanzen : eine Fallstudie in West Bengalen, Indien am Institut für Mineralogie und Geochemie der Universität Karlsruhe. Karlsruhe (unpubl.)

KOTTEK, M., GRIESER, J., BECK, C., RUDOLF, B., RUBEL, F. (2006): World map of the Köppen-Geiger climate classification updated. Met. Z. 15, 3, 259-263

KRAMAR, U., HARTING, M, RICKERS, K., STÜBEN, D. (2007): µ-Synchrotron radiation excited X-ray fluorescence microprobe trace element studies on spherules of the Cretaceous/Tertiary boundary transitions of NE-Mexico and Haiti samples. Spectrochimica Acta. Part B62, 824-835

KRAMAR, U. (1999): X-Ray Fluorescence Spectrometers. In LINDON, C.J., TRANTER, G.E., HOLMES, J.L (2000): Encyclopedia of spectroscopy and spectrometry, Vol.3. Academic Press

LIN, N.-F., TANG, J., BIAN, J.-M. (2002): Characteristics of Environmental Geochemistry in the Arseniasis Area of the Inner Mongolia of China. Environmental Geochemistry and Health. 24, 3, 249-259

LOUËR, D. (1999): Powder X-Ray Diffraction, Applications. In In LINDON, C.J., TRANTER, G.E., HOLMES, J.L (2000): Encyclopedia of spectroscopy and spectrometry, Vol.2. Academic Press

MOENS, L., JAKUBOWSKI, N. (1998): Double-Focusing Mass Spectrometers in ICPMS. Analytical Chemistry News & Features. 70, 251A-256A

NAIK, P.A. (1999): X-Ray Spectroscopy, Theory. In LINDON, C.J., TRANTER, G.E., HOLMES, J.L (2000): Encyclopedia of spectroscopy and spectrometry, Vol.3. Academic Press

NORRA, S., BERNER, Z., AGARWALA, P., WAGNER, F., CHANDRASEKHRARAM, D., STÜBEN, D. (2005): Impact of irrigation with As rich groundwater on soil and crops: A geochemical case study in West Bengal Delat Plain, India. Applied Geochemistry. 20, 1890-1906

NAIDU, R., EUAN, S., OWENS, G., BHATTACHARYA, P., NADEBAUM, P. (2006): Managing Arsenic in the Environment: From Soil to Human. Enfield NH: Science Publishers

OBERACKER, F., MAIER, D., MAIER, M. (2002): Arsen und Trinkwasser, Teil 1-Ein Überblick über Vorkommen, Verteilung und Verhalten von Arsen in der Umwelt. Vom Wasser. 99, 99, 79-110

SCHEFFER, F.; SCHACHTSCHABEL, P., BLUME, H.-P. (2002): Lehrbuch der Bodenkunde. 15. Aufl. Heidelberg ; Berlin : Spektrum, Akad. Verl.

PAVICEVIC, M. K., Amthauer, G. (2000): Physikalisch-chemische Untersuchungsmethoden in den Geowissenschaften, Band 1: Mikroskopische, analytische und massenspektrometrische Methoden. Stuttgart : Schweizerbart

PFENNIG, G., KLEWE-NEBENIUS, H., SEELMANN-EGGEBERT, W. (1995): Karlsruher Nuklidkarte. Karlsruhe: Forschungszentrum Karlsruhe, Technik und Umwelt

REINHOLD, J. [Red.] (2006): Guidelines for soil description. 4. edition. Rom : Food and Agriculture Organization of the United Nations

RÜDE, T.R. (1996): Beiträge zur Geochemie des Arsens. Karlsruher Geochemische Hefte. Karlsruhe: Schriftenreihe des Instituts für Petrographie und Geochemie

SCHAFMEISTER, M.-Th. (1999): Geostatistik für die hydrologische Praxis. Berlin: Springer

SCHEFFER, F.; SCHACHTSCHABEL, P., BLUME, H.-P. (2002): Lehrbuch der Bodenkunde. 15. Aufl. Heidelberg ; Berlin : Spektrum, Akad. Verl.

SCHWEINSBERG, F., SCHWEIZER, E., KOSMUS, W. (2002): Toxikologische Bewertung der Arsen-Aufnahme mit Trinkwasser. Vom Wasser. 99, 99, 1-20

SMEDLEY, P.L., ZHANG, M., ZHANG, G., LUO, Z. (2003): Mobilisation of arsenic and other trace elements in fluviolacustrine aquifers of the Huhhot Basin, Inner Mongolia. Applied Geochemistry. 18, 1453–1477

SPONAGEL, H. (2005): Bodenkundliche Kartieranleitung . Ad-hoc-Arbeitsgruppe Boden der Staatlichen Geologischen Dienste und der Bundesanstalt für Geowissenschaften und Rohstoffe. Stuttgart: Schweizerbart

STRELI, C., WOBRAUSCHECK, P., KREGSAMER, P. (1999): : X-Ray Fluorescence Spectroscopy, Applications. In LINDON, C.J., TRANTER, G.E., HOLMES, J.L (2000): Encyclopedia of spectroscopy and spectrometry, Vol.3. Academic Press

STÜBEN, D., BERNER, Z., CHANDRASEKHRARAM, D, KARMAKAR, J. (2008, in press): Arsenic enrichment in groundwater of West Bengal, India: geochemical evidence for mobilization of As under reducing conditions. Applied Geochemistry. 18 , 1417–1434

WAGNER, F. (2005): Prozessverständnis einer Naturkatatstrophe : eine geo- und hydrochemische Untersuchung der regionalen Arsen-Anreicherung im Grundwasser West-Bengalens (Indien). Karlsruhe : Universitätsverlag

WELZ, B. (1990): Atomabsorptionsspektrometrie. 3. Aufl. Weinheim [u.a.]: Wiley-VCH

WENZEL, W. W., KIRCHBAUMER, N., PROHASKA, T., STINGENDER, G., LOMBI, E., ADRIANO C. (2001): Arsenic fractionation in soils using an improved sequential extraction procedure. Analytica Chimica Acta. 436, 2, 309-324

ZHANG, H., MA, D., Hu, X. (2002): Arsenic pollution in groundwater from Hetao Area, China. Environmental Geology. 41, 638-643

ZEIEN, H., BRÜMMER, G.W. (1989): Chemische Extraktionen zur Bestimmung von Schwermetallbindungsformen in Böden. Mitteilungen der Deutschen Bodenkundlichen Gesellschaft. 1, 59, 505-510

APPENDIX

Table 38: Check list used for for field survey

Check list field campaign, Inner Mongolia, China, July-August 2007

Title data check list, field-nr.:												
Position	Date	Editor	GPS-nr.	Weather	Photo-nr.	Field dimension	Owner/ Leaseholder		Utilization of the neighbor fields			

Cultivation information									
Cultivated crop	Cultivar(s)	Stage of maturity	Harvests per year	Crop rotation	Crop kg/ha	Duration of cultivation	Fallow cycle	Fertilizer	Pesticides

Irrigation details						
Kind of irrigation	Deliver depth	Duration of irrigation	Irrigation frequency	Distance to yellow river	Flood water influence [d per year]	Comment

Miscelanious			
Use of crop residues	Salinization aspect	Knowledge of As-problem (farmer)	Practiced field preparation method

Comments/sketch:

Diploma thesis „Study on the arsenic contamination of the food chain in an agricultural affected area of the Inner Mongolia, Datong-Basin, China" by Harald Neidhardt

Table 39: Water analysis results, part A

Field parameter, IC results and As load:

Location:	Position	pH	ORP [mV]	Cl⁻ [mg/L]	NO_3^- [mg/L]	SO_4^{2-} [mg/L]	PO_4^{3-} [mg/L]	meas pH	As_{total} dis. [µg/L]	As^{III} dis. %	As susp. [µg/L]
Field 1	.60"N; 106°4	9,1	-162,3	383	<IDL	2,99*	<IDL	0,38	154	mistake	0,37
Field 1 (+6h)	.60"N; 106°4	-	-	476	<IDL	65,6	<IDL	0,32	134	12,3	4,26
Field 2	.90"N; 106°4	-	-	1100*	<IDL	593	<IDL	0,31	238	91,8	3,12
Field 2 (+4h)	.90"N; 106°4	-	-	954*	2,49*	505	<IDL	0,39	109	64,7	107
1	5.70"N, 106°	8,2		912*	<IDL	<IDL	<IDL	0,36	345	mistake	14,4
16 (32)	.80"N, 107° 0	8,3	-173	233	8,17*	<IDL	<IDL	7,32	959	87,7	0,97
19	.10"N, 107° 7	8,2	-164	172	<IDL	327	<IDL	2,70	301	82,3	5,39
20	.50"N, 107° 7	7,7	-138	385	<IDL	1030	<IDL	2,85	191	82,5	4,97
Huang He, river	3.80"N, 107°	-	-	102	13,2*	162	<IDL	1,89	6,70	-	46,8
Hotel in Xamba	-	-	-	233	<IDL	251	<IDL	6,30	14,7	-	3,38
Huan He, canal	.20"N, 106°5	8,9	107	-	-	-	-	-	-	-	-

*out of calibration range

Table 40: Water analysis results, part B

Dissolved cations: **Location:**	**meas pH**	**Na** [mg/L]	**Mg** [mg/L]	**K** [mg/L]	**Ca** [mg/L]	**Al** [µg/L]	**V** [µg/L]	**Cr** [µg/L]	**Mn** [µg/L]	**Fe** [µg/L]	**Co** [µg/L]
Field 1	7,52	441	16,3	3,87	8,41	4,53	0,46	0,1	34,1	296	0,15
Field 1 (+6h)	7,66	586	23,5	11,1	19,5	1410	13,8	2,15	44,7	1100	0,94
Field 2	7,96	1011	188	9,2	98,8	1,48	0,34	0,17	347	159	0,50
Field 2 (+4h)	8,26	992	178	10,6	96,3	38,0	1,63	0,28	139	121	0,59
1	7,50	474	110	6,4	47,6	14,5	0,13	0,06	144	16,8	0,09
16 (32)	7,32	345	29,5	6,26	23,0	6,22	0,65	0,15	51,85	322	0,21
19	2,7	119	64,8	9,91	84,4	7,78	0,05	0,04	50,47	1160	0,04
20	2,85	529	188	12,6	157	64,5	0,49	1,81	518	1330	0,25
Huang He River	1,89	81,6	26,9	3,6	66,7	163	3,43	0,39	12,0	185	0,23
Hotel in Xamba	6,3	240	74,6	3,54	60,2	3,25	0,07	0,17	114	11,5	0,13

	Ni [µg/L]	**Cu** [µg/L]	**Zn** [µg/L]	**Rb** [µg/L]	**Sr** [µg/L]	**Mo** [µg/L]	**Cd** [µg/L]	**Ba** [µg/L]	**Tl** [µg/L]	**Pb** [µg/L]
Field 1	2,23	1,00	2,63	1,47	474	25,3	0,03	446	< IDL	< IDL
Field 1 (+6h)	4,45	8,24	4,75	5,35	523	29,9	0,07	221	< IDL	1,20
Field 2	1,35	0,93	3,38	3,82	3180	14,2	0,02	280	< IDL	< IDL
Field 2 (+4h)	2,02	3,33	8,37	4,08	2960	12,8	0,07	317	< IDL	< IDL
1	0,18	1,32	3,28	3,09	2010	2,04	< IDL	1280	< IDL	< IDL
16 (32)	0,36	9,25	4,3	3,5	746	0,56	0,01	690	< IDL	< IDL
19	0,18	0,85	2,18	2,31	987	3,62	0,01	27,4	< IDL	< IDL
20	0,83	1,17	9,93	1,44	2220	3,4	0,02	19,2	< IDL	< IDL
Huang He River	1,72	2,95	4,35	1,16	859	3,01	0,02	109	< IDL	0,38
Hotel in Xamba	0,78	1,41	16,4	1,8	1380	7,18	0,01	50,7	< IDL	< IDL

Table 41: Water analysis results, part C

Suspended matter: **Location:**	**Na** [µg/L]	**Mg** [µg/L]	**K** [µg/L]	**Ca** [µg/L]	**Al** [µg/L]	**V** [µg/L]	**Cr** [µg/L]	**Mn** [µg/L]	**Fe** [µg/L]	**Co** [µg/L]	**Ni** [µg/L]
Field 1	894	47,5	< IDL	30,8	27,3	< IDL	< IDL	0,35	19,7	0,01	< IDL
Field 1 (+6h)	2100	1770	1710	4500	6320	8,34	6,69	58,4	2900	1,28	3,1
Field 2	425	91,7	< IDL	93,7	49,9	0,08	< IDL	1,03	194	0,01	< IDL
Field 2 (+4h)	37800	40700	21400	146000	162700	176	155	1300	57100	28,5	74,04
1	269	96,3	< IDL	91,4	42,7	< IDL	< IDL	1,1	246	< MDL	< IDL
16 (32)	117	19,1	< IDL	29,2	29,1	0,02	< IDL	0,53	69,2	0,01	< IDL
19	76,8	35,3	< IDL	112	11,1	< IDL	< IDL	0,23	131	< MDL	< IDL
20	831	1090	837,4	2230	3340	4,31	7,68	36,8	2460	0,76	1,25
Hotel in Xamba	154	74,8	< IDL	144	50,3	0,07	< IDL	1,15	382	0,01	< IDL
Huang He River	24700	55500	58200	142000	219000	272	216	2050	80200	43,6	108

Location:	**Cu** [µg/L]	**Zn** [µg/L]	**As** [µg/L]	**Rb** [µg/L]	**Sr** [µg/L]	**Mo** [µg/L]	**Cd** [µg/L]	**Ba** [µg/L]	**Tl** [µg/L]	**Pb** [µg/L]
Field 1	0,28	< IDL	0,37	0,06	1,71	< IDL	0,01	8,49	1,41	0,04
Field 1 (+6h)	2,93	8,01	4,26	11,3	34,2	0,2	0,05	58,9	0,05	2,14
Field 2	0,14	< IDL	3,12	0,1	4,04	< IDL	< IDL	3,78	< IDL	< IDL
Field 2 (+4h)	55,5	168	107	116	801	1,53	0,71	1350	1,34	48,5
1	5,71	1,41	14,4	0,01	4,96	< IDL	< IDL	16,6	< IDL	0,33
16 (32)	0,12	0	0,97	0,04	0,74	< IDL	< IDL	1,87	< IDL	0,10
19	5,03	5,83	5,39	0,01	1,62	0,05	< IDL	0,26	< IDL	0,37
20	2,99	11,9	4,97	5,61	16,1	< IDL	0,01	20,3	0,03	1,39
Hotel in Xamba	0,05	< IDL	3,38	0,1	3,53	< IDL	< IDL	1,48	< IDL	0,08
Huang He River	90,0	291	46,8	405	679	2,07	1,16	1290	1,52	56,4

Table 42: Check list F1, soil pit A

Field 1, soil pit A													
Title data				Terrain situation									
Date	Position	GPS- coordinates	Pit size	Relief		Vegetation cover	Anthropo-genic changes						
				Decli-nation	Relieftype/ form								
26.07. 2007	Yong-Ming	40°51'39.60"N 106°48'13.80"O	1x1x1m	N1	TS	Sunflower	BS,T						
Horizon referring data													
Nr.	Horizon-tation	Horizon symbol	Pedogenic attributes						Bulk density	Roots		Criteria substrate composition	
	Under/ upper boundary (cm)		Hydro-morphic attributes		Struc-ture	Soil colour				fine	coarse	Soil texture	∑ Skeleton (%)
			ox.	red.	Agg. shape	Hue	Chroma	Value					
1	0-7.5	Ap1	-	-	crumb	10	YR	4/4	2	4	1	Uu	-
2	7.5-37	Ap2	-	-	sub	10	YR	4/4	3	4	1	Uu	-
3	37-48	ael C	e h+(s)	-	pol	10	YR	4/6	4	3	1	Tu3	-
4	48-82	ael II C	e h+(s)	-	sub	10	YR	5/4	3	2	1	Slu	-
5	82-100	ael III C	-	-	platy	10	YR	5/4	4	0	0	Lu	-

Table 43: Check list F2, soil pit A

Field 2, soil pit A													
Title data				Terrain situation									
Date	Position	GPS- coordinates	Pit size	Relief		Vegetation cover	Anthropo-genic changes						
				Decli-nation	Relieftype/ form								
28.07. 2007	Yong-Ming	40°51'49.90"N 106°47'48.20"O	1x1x1m	N0	TS	Maize and wheat	BS,T						
Horizon referring data													
Nr.	Horizon-tation	Horizon symbol	Pedogenic attributes						Bulk density	Roots		Criteria substrate composition	
	Under/ upper boundary (cm)		Hydro-morphic attributes		Struc-ture	Soil colour				fine	coarse	Soil texture	∑ Skeleton (%)
			ox.	red.	Agg. shape	Hue	Chroma	Value					
1	0-10.5	Ap1	-	-	crumb	10	YR	5/3	1	3	2	Uls	-
2	10.5-35	Ap2	-	-	sub	10	YR	5/3	3	3	1	Uls	-
3	35-65	ael C	e h+(s)	-	pol	10	YR	5/3	3	2	0	Tu4	-
4	65-84	ael II C	e h+(s)	-	platy	10	YR	5/4	4	1	0	Lu	-
5	84-100	ael III C	-	-	sub	10	YR	5/3	3	0	0	Slu	-

Table 44: Vertical elemental distribution in soil pits on F1

Field 1, soil pit A	AS [PPM]	K_2O [%]	CaO [%]	TIO_2 [%]	MNO [%]	FE_2O_3 [%]	NI [PPM]	CU [PPM]	ZN [PPM]	BR [PPM]	RB [PPM]	SR [PPM]	Y [PPM]	ZR [PPM]	NB [PPM]	PB [PPM]
0-1cm	16,1	2,58	9,17	0,46	0,08	3,82	29,7	25,3	79,0	<IDL	98,2	302	24,1	163	12,5	14,4
1-2cm	16,4	2,62	9,38	0,49	0,08	3,96	23,6	27,5	74,9	<IDL	100	312	23,8	171	13,4	13,8
2-5cm	15,6	2,50	9,02	0,47	0,08	3,67	22,7	22,1	68,8	3,61	94,3	288	22,0	154	11,8	10,9
5-10cm	14,1	2,58	9,58	0,48	0,08	3,93	<IDL	22,8	72,7	<IDL	103	291	23,0	159	10,4	13,7
10-20cm	14,1	2,66	9,58	0,50	0,09	4,20	25,7	27,0	89,4	3,72	107	275	22,9	155	13,5	18,8
20-30cm	18,8	2,79	9,88	0,52	0,09	4,51	29,6	29,7	81,4	5,12	114	283	24,4	171	12,3	19,4
30-40cm	11,6	2,40	8,65	0,53	0,08	3,70	23,2	22,1	59,5	4,06	92,1	225	28,2	362	12,5	14,5
40-50cm	16,1	2,60	9,83	0,55	0,09	4,51	23,6	30,4	81,9	3,26	111	265	26,1	212	12,6	16,9
50-60cm	15,6	2,48	8,83	0,52	0,08	4,06	<IDL	20,3	71,3	<IDL	105	251	25,4	203	12,9	18,9
60-70cm	13,8	2,39	8,58	0,50	0,08	3,79	27,5	23,2	60,9	<IDL	101	229	23,8	205	11,7	24,3
70-80cm	16,0	2,43	8,28	0,47	0,08	3,72	<IDL	23,4	63,8	<IDL	100	229	21,8	160	12,8	21,2
80-90cm	13,7	2,38	8,11	0,44	0,07	3,54	21,8	28,2	58,7	<IDL	99,2	223	20,9	154	11,2	19,9
90-100cm	12,9	2,60	8,86	0,53	0,09	4,36	23,2	23,6	76,9	<IDL	107	235	24,3	160	14,3	26,3
Field 1, soil pit B																
0-1cm	15,9	2,54	9,15	0,48	0,07	3,90	28,1	20,3	69,8	3,52	100	309	23,6	188	12,9	11,6
1-2cm	15,1	2,58	9,29	0,46	0,08	3,99	26,8	23,5	78,2	3,89	100	315	22,6	187	11,9	15,3
2-5cm	14,0	2,40	8,96	0,46	0,07	3,79	<IDL	27,9	70,9	3,86	96,5	297	22,8	171	12,0	16,8
5-10cm	15,4	2,61	9,58	0,50	0,08	4,10	23,5	27,0	74,1	4,19	105	319	23,1	185	11,4	32,1
10-20cm	13,1	2,50	9,21	0,47	0,08	3,88	<IDL	21,1	64,7	5,76	98,5	306	22,4	181	10,9	22,0
20-30cm	14,4	2,42	8,87	0,46	0,07	3,77	24,7	22,5	66,4	5,15	97,2	284	21,4	184	11,3	18,8
30-40cm	14,7	2,47	8,93	0,49	0,07	3,86	23,3	20,8	64,2	<IDL	100	278	23,3	192	11,4	16,2
40-50cm	12,3	2,26	8,21	0,48	0,06	3,55	24,4	23,7	56,0	<IDL	93,7	232	23,0	208	13,0	45,6
50-60cm	12,0	2,13	8,02	0,47	0,06	3,26	23,6	18,6	51,1	<IDL	86,6	219	23,3	213	10,5	13,2
60-70cm	14,1	2,65	9,24	0,51	0,09	4,56	26,4	29,3	77,5	<IDL	111	262	24,1	148	14,1	24,9
70-80cm	12,7	2,30	8,10	0,45	0,07	3,48	<IDL	19,9	53,8	3,01	94,8	226	23,8	177	12,7	23,2
80-90cm	13,3	2,34	8,23	0,44	0,06	3,62	25,9	23,4	63,1	<IDL	102	239	20,6	140	10,1	23,4
90-100cm	13,5	2,47	8,69	0,48	0,07	3,90	24,2	16,4	65,3	<IDL	106	256	23,0	164	10,1	23,8

Field 1, soil pit A	AS [PPM]	K_2O [%]	CaO [%]	TIO_2 [%]	MNO [%]	FE_2O_3 [%]	NI [PPM]	CU [PPM]	ZN [PPM]	BR [PPM]	RB [PPM]	SR [PPM]	Y [PPM]	ZR [PPM]	NB [PPM]	PB [PPM]
Horizon 1 , 0-7,5cm	14,8	2,32	8,18	0,43	0,06	3,57	32,1	23,3	71,6	<IDL	97,1	265	19,2	157	13,5	17,1
Horizon 2 , 7,5-37cm	12,8	2,35	8,44	0,47	0,06	3,53	22,8	24,2	58,7	3,79	92,8	226	22,5	257	11,3	19,2
Horizon 3 , 37-48cm	16,7	2,71	9,64	0,55	0,09	4,96	31,3	30,5	93,9	<IDL	121	275	28,9	204	14,4	21,9
Horizon 4 , 48-82cm	13,3	2,01	7,24	0,44	0,06	3,04	21,8	18,8	44,9	<IDL	84,8	204	22,5	276	11,1	11,7
Horizon 5 , 82-100cm	13,5	2,36	8,23	0,48	0,07	4,06	27,1	28,5	75,8	<IDL	105	235	24,4	188	12,2	15,5

Table 45: Vertical elemental distribution in soil pits on F2

Field 2, soil pit A	AS	K_2O	CaO	TIO_2	MNO	FE_2O_3	NI	CU	ZN	BR	RB	SR	Y	ZR	NB	PB
	[PPM]	[%]	[%]	[%]	[%]	[%]	[PPM]	[PPM]	[PPM]	[PPM]	[PPM]	[PPM]	[PPM]	[PPM]	[PPM]	[PPM]
0-1cm	19,4	2,78	9,89	0,50	0,09	4,54	22,9	24,2	89,5	5,32	112	338	23,9	148	12,4	20,6
1-2cm	19,5	2,75	10,1	0,51	0,10	4,66	25,9	30,4	87,9	5,08	112	333	24,8	142	11,9	19,1
2-5cm	19,7	2,90	10,9	0,55	0,10	5,08	<IDL	32,4	101	5,07	125	357	25,4	161	11,5	19,9
5-10cm	15,5	2,72	10,0	0,49	0,10	4,61	30,2	28,4	83,5	6,07	115	317	24,0	145	10,1	18,9
10-20cm	18,0	2,62	9,39	0,48	0,08	4,28	26,0	21,8	73,8	4,37	107	301	22,3	154	12,4	12,9
20-30cm	15,4	2,63	9,37	0,49	0,09	4,26	22,1	23,6	66,6	5,79	106	279	22,9	154	9,6	16,5
30-40cm	17,8	2,93	10,3	0,53	0,10	4,97	29,2	26,1	89,0	5,91	123	306	26,4	157	14,3	17,0
40-50cm	24,2	3,29	11,3	0,59	0,11	6,00	33,9	32,2	110	5,66	140	346	28,5	153	13,4	18,2
50-60cm	19,0	2,93	10,3	0,52	0,11	5,19	37,0	35,3	92,1	5,45	124	300	25,6	148	13,2	17,5
60-70cm	23,0	3,07	11,0	0,59	0,12	5,71	34,1	32,1	98,0	4,47	135	319	27,3	153	12,3	20,9
70-80cm	12,3	2,43	8,43	0,48	0,08	4,00	24,7	28,5	66,5	<IDL	104	240	23,7	166	10,4	18,7
80-90cm	12,0	2,29	8,19	0,50	0,06	3,66	<IDL	20,9	58,3	<IDL	94,9	223	24,6	237	15,8	13,8
90-100cm	10,5	2,25	8,04	0,44	0,06	3,17	<IDL	14,5	51,7	<IDL	93,1	224	21,5	236	10,3	15,3
Field 2, soil pit B																
0-1cm	17,7	2,73	9,69	0,50	0,09	4,53	31,2	26,1	76,6	6,34	110	318	24,6	149	12,1	20,3
1-2cm	13,7	2,51	8,86	0,46	0,08	4,08	22,2	25,4	68,9	5,41	104	286	22,4	140	10,4	15,1
2-5cm	18,0	2,58	9,21	0,47	0,09	4,25	35,9	25,8	81,5	6,22	106	299	22,6	147	11,2	19,9
5-10cm	17,3	2,49	9,16	0,47	0,09	4,24	24,0	25,7	80,8	6,98	104	303	23,0	145	10,4	22,1
10-20cm	17,0	2,61	9,51	0,49	0,09	4,42	27,2	26,3	80,3	6,73	109	306	23,0	142	10,4	18,2
20-30cm	16,5	2,79	9,50	0,49	0,10	4,67	31,0	25,2	79,6	5,96	115	285	23,0	144	10,5	17,2
30-40cm	22,4	3,25	11,0	0,56	0,10	5,90	39,7	26,9	107	4,31	138	320	26,7	147	11,8	26,1
40-50cm	16,7	2,85	9,89	0,55	0,09	4,98	<IDL	32,0	95,4	5,43	120	283	26,2	156	13,2	19,1
50-60cm	14,6	2,47	8,39	0,44	0,07	3,77	21,6	24,4	62,6	2,98	99,1	228	20,8	199	9,3	12,2
60-70cm	10,8	2,11	8,31	0,51	0,06	3,42	25,4	22,6	56,0	<IDL	85,8	218	27,6	378	11,7	12,6
70-80cm	12,8	2,22	7,99	0,45	0,08	3,63	25,2	24,9	61,3	<IDL	94,5	220	22,5	159	12,9	12,8
80-90cm	14,9	2,39	8,44	0,49	0,07	3,97	24,1	25,4	69,8	4,02	100	234	23,0	169	12,3	14,2
90-100cm	13,3	2,30	8,37	0,47	0,06	3,49	<IDL	14,9	56,8	<IDL	94,6	253	22,5	219	9,7	14,4

Field 2, soil pit A	AS	K_2O	CaO	TIO_2	MNO	FE_2O_3	NI	CU	ZN	BR	RB	SR	Y	ZR	NB	PB
	[PPM]	[%]	[%]	[%]	[%]	[%]	[PPM]	[PPM]	[PPM]	[PPM]	[PPM]	[PPM]	[PPM]	[PPM]	[PPM]	[PPM]
Horizon 1 , 0-10,5cm	18,8	2,62	9,36	0,48	0,08	4,54	31,5	30,3	80,3	5,19	114	328	24,9	155	12,8	25,2
Horizon 2 , 10,5-35c	14,4	2,60	9,06	0,46	0,07	4,12	31,6	21,8	70,5	4,67	103	279	20,7	152	11,3	18,1
Horizon 3 , 35-65cm	18,1	2,72	9,43	0,50	0,11	4,96	34,2	33,4	90,4	4,59	120	298	25,8	139	12,8	20,3
Horizon 4 , 65-84cm	12,0	2,42	8,71	0,53	0,08	3,99	27,5	14,3	67,1	<IDL	101	232	25,0	196	13,3	20,3
Horizon 5 , 84-100cr	9,56	2,04	7,69	0,43	0,05	3,01	<IDL	19,1	47,7	<IDL	84,1	212	20,1	209	10,2	12,5

Table 46: Horizontal elemental distribution on F1, 0-1cm

Field 1 grid samples, 0-1cm	AS [PPM]	K_2O [%]	CaO [%]	TiO_2 [%]	MNO [%]	FE_2O_3 [%]	NI [PPM]	CU [PPM]	ZN [PPM]	BR [PPM]	RB [PPM]	SR [PPM]	Y [PPM]	ZR [PPM]	NB [PPM]	PB [PPM]
F1 R 0-1cm; 1-1	14	2,49	8,56	0,44	0,07	3,61	<IDL	31	66	<3	99	278	21	160	11	16
F1 R 0-1cm; 1-2	15	2,33	8,25	0,43	0,07	3,45	26	17	61	3	91	273	21	165	10	16
F1 R 0-1cm; 1-3	13	2,28	8,21	0,42	0,06	3,38	27	20	60	<3	89	286	21	160	11	10
F1 R 0-1cm; 1-4	15	2,43	8,71	0,45	0,07	3,73	30	20	66	5	99	298	23	194	11	16
F1 R 0-1cm; 1-5	16	2,71	9,53	0,49	0,07	4,05	28	25	69	4	103	304	22	186	12	13
F1 R 0-1cm; 1-6	12	2,45	8,76	0,45	0,08	3,74	<IDL	28	72	5	99	288	22	165	12	19
F1 R 0-1cm; 1-7	14	2,41	8,60	0,43	0,08	3,59	32	26	65	6	94	289	22	171	12	13
F1 R 0-1cm; 1-8	15	2,53	8,84	0,45	0,07	3,73	27	22	69	4	96	301	23	194	10	13
F1 R 0-1cm; 1-9	13	2,39	8,07	0,42	0,07	3,42	29	23	62	3	91	301	22	171	9	12
F1 R 0-1cm; 1-10	14	2,39	8,27	0,43	0,07	3,54	30	19	65	3	92	302	21	165	11	12
F1 R 0-1cm; 1-11	14	2,33	8,14	0,42	0,06	3,47	30	25	64	4	92	294	22	182	12	14
F1 R 0-1cm; 1-12	16	2,45	8,70	0,45	0,07	3,67	<IDL	20	67	5	95	293	22	187	13	13
F1 R 0-1cm; 2-1	14	2,34	8,11	0,45	0,06	3,34	26	27	62	<IDL	90	265	20	191	12	12
F1 R 0-1cm; 2-2	12	2,25	8,14	0,43	0,06	3,36	22	25	60	<IDL	91	268	21	162	11	12
F1 R 0-1cm; 2-3	11	2,46	8,46	0,44	0,06	3,52	25	23	67	5	95	283	22	188	11	17
F1 R 0-1cm; 2-4	19	2,51	8,98	0,48	0,08	3,78	24	16	62	<IDL	97	298	22	172	9	12
F1 R 0-1cm; 2-5	16	2,38	8,92	0,47	0,07	3,73	<IDL	27	62	4	95	294	23	188	11	14
F1 R 0-1cm; 2-6	14	2,51	9,16	0,48	0,08	3,85	22	27	78	5	101	310	25	194	10	16
F1 R 0-1cm; 2-7	15	2,53	9,23	0,48	0,07	3,90	<IDL	20	68	5	101	316	23	195	12	16
F1 R 0-1cm; 2-8	13	2,40	8,87	0,46	0,08	3,73	23	19	65	4	97	304	22	195	11	22
F1 R 0-1cm; 2-9	17	2,47	9,16	0,47	0,07	3,78	<IDL	30	69	4	99	315	24	194	11	13
F1 R 0-1cm; 2-10	15	2,48	9,09	0,46	0,08	3,83	25	24	63	4	99	317	23	196	8	14
F1 R 0-1cm; 2-11	16	2,51	9,21	0,47	0,08	3,88	30	26	67	3	101	315	23	192	12	19
F1 R 0-1cm; 2-12	15	2,58	9,14	0,48	0,08	3,87	29	23	73	<IDL	101	322	24	183	14	14
F1 R 0-1cm; 3-1	14	2,41	8,96	0,45	0,06	3,58	22	23	61	<IDL	97	287	22	171	10	14
F1 R 0-1cm; 3-2	15	2,14	8,53	0,45	0,06	3,51	<IDL	24	60	4	93	284	22	181	13	14
F1 R 0-1cm; 3-3	14	2,37	8,58	0,47	0,07	3,60	<IDL	20	68	4	93	288	23	187	11	10
F1 R 0-1cm; 3-4	13	2,40	8,87	0,47	0,06	3,60	27	20	65	4	98	297	22	210	11	14
F1 R 0-1cm; 3-5	17	2,50	9,01	0,47	0,08	3,80	<IDL	26	71	4	100	308	24	202	11	14
F1 R 0-1cm; 3-6	16	2,49	9,11	0,49	0,08	3,84	<IDL	25	64	6	100	308	23	186	12	14
F1 R 0-1cm; 3-7	14	2,32	8,65	0,46	0,07	3,53	23	21	61	4	95	298	23	182	10	11
F1 R 0-1cm; 3-8	17	2,61	9,78	0,52	0,07	4,19	23	25	79	4	109	338	25	223	12	14
F1 R 0-1cm; 3-9	15	2,57	9,59	0,50	0,09	4,12	30	28	83	4	106	322	25	192	11	16
F1 R 0-1cm; 3-10	15	2,35	8,77	0,45	0,07	3,68	<IDL	21	65	3	96	292	21	166	11	11
F1 R 0-1cm; 3-11	19	2,59	9,72	0,50	0,07	4,15	<IDL	26	80	3	107	334	26	199	10	11
F1 R 0-1cm; 3-12	17	2,57	9,16	0,49	0,08	3,94	23	27	70	4	102	324	23	190	11	11

Table 47: Horizontal elemental distribution on F1, 0-1cm

Field 1 grid samples, 0-1cm	AS [PPM]	K_2O [%]	CaO [%]	TIO_2 [%]	MNO [%]	FE_2O_3 [%]	NI [PPM]	CU [PPM]	ZN [PPM]	BR [PPM]	RB [PPM]	SR [PPM]	Y [PPM]	ZR [PPM]	NB [PPM]	PB [PPM]
F1 R 0-1cm; 4-1	15	2,42	8,85	0,45	0,06	3,66	=	24	66	3	98	292	21	168	11	13
F1 R 0-1cm; 4-2	14	2,48	9,05	0,48	0,07	3,88	22	28	74	4	101	304	23	192	11	18
F1 R 0-1cm; 4-3	17	2,30	8,78	0,47	0,07	3,77	32	20	66	3	96	296	22	189	11	13
F1 R 0-1cm; 4-4	15	2,47	9,20	0,48	0,07	3,96	25	21	71	4	103	305	24	199	13	16
F1 R 0-1cm; 4-5	18	2,58	9,48	0,49	0,09	4,12	27	27	69	5	104	322	24	204	13	11
F1 R 0-1cm; 4-6	14	2,49	9,15	0,47	0,07	3,90	22	23	71	4	101	312	24	194	11	15
F1 R 0-1cm; 4-7	14	2,30	8,35	0,43	0,06	3,53	26	21	58	4	94	284	21	187	11	13
F1 R 0-1cm; 4-8	15	2,51	9,01	0,48	0,07	4,00	<IDL	23	68	3	103	314	24	196	11	16
F1 R 0-1cm; 4-9	14	2,41	8,81	0,47	0,08	3,77	26	17	58	4	99	295	22	182	11	16
F1 R 0-1cm; 4-10	16	2,34	8,83	0,48	0,07	3,81	23	30	68	5	99	296	22	168	10	15
F1 R 0-1cm; 4-11	14	2,52	9,27	0,49	0,07	4,03	22	28	74	4	104	319	23	192	13	18
F1 R 0-1cm; 4-12	13	2,49	8,88	0,47	0,08	3,80	26	23	64	4	99	310	22	186	11	17
F1 R 0-1cm; 5-1	17	2,39	8,81	0,49	0,08	3,76	22	26	64	4	98	288	22	195	11	13
F1 R 0-1cm; 5-2	14	2,49	9,10	0,48	0,08	3,96	26	26	71	4	99	302	23	201	11	14
F1 R 0-1cm; 5-3	16	2,50	8,99	0,47	0,07	3,91	29	24	71	<IDL	100	303	23	185	12	17
F1 R 0-1cm; 5-4	18	2,55	9,28	0,50	0,07	4,07	<IDL	26	76	4	106	317	25	200	13	16
F1 R 0-1cm; 5-5	16	2,43	8,81	0,45	0,08	3,80	28	26	68	<IDL	99	304	23	186	12	14
F1 R 0-1cm; 5-6	15	2,57	9,31	0,48	0,07	4,01	26	25	65	<IDL	102	318	24	199	12	13
F1 R 0-1cm; 5-7	22	2,82	10,63	0,53	0,10	4,72	28	28	91	3	118	367	28	211	14	13
F1 R 0-1cm; 5-8	17	2,64	9,63	0,51	0,08	4,25	<IDL	21	73	3	106	330	25	196	12	14
F1 R 0-1cm; 5-9	15	2,53	9,28	0,49	0,09	4,11	26	27	73	4	102	310	23	190	12	15
F1 R 0-1cm; 5-10	15	2,71	10,03	0,51	0,09	4,52	<IDL	26	81	4	112	339	24	194	13	17
F1 R 0-1cm; 5-11	15	2,65	9,68	0,50	0,09	4,21	26	28	81	4	108	326	24	196	13	18
F1 R 0-1cm; 5-12	14	2,50	8,94	0,46	0,08	3,80	36	20	70	4	99	303	24	188	12	15
F1 R 0-1cm; 1-1,5	16	2,53	8,70	0,47	0,08	3,76	<IDL	22	66	<IDL	98	301	21	161	11	15
F1 R 0-1cm; 1,5-1	13	2,23	8,32	0,45	0,06	3,47	<IDL	15	59	<IDL	93	270	22	172	10	10
F1 R 0-1cm; 1,5-2	15	2,56	9,26	0,50	0,08	3,95	<IDL	23	71	<IDL	104	311	24	203	14	14
F1 R 0-1cm; 1,5-1,5	14	2,29	7,94	0,41	0,07	3,21	<IDL	20	59	<IDL	91	258	18	146	9	12
F1 R 0-1cm; 2-1,5	13	2,41	9,22	0,51	0,07	3,84	22	22	72	4	103	305	23	205	11	15
Min:	11	2,14	8,07	0,42	0,06	3,34	22	16	58	3	89	265	20	160	8	10
Max:	22	2,82	10,63	0,53	0,10	4,72	36	31	91	6	118	367	28	223	14	22
Mean:	15	2,47	8,97	0,47	0,07	3,81	26	24	68	4	99	304	23	187	11	14

Table 48: Horizontal elemental distribution on F1, 1-2cm

Field 1 grid samples, 1-2cm	AS [PPM]	K_2O [%]	CaO [%]	TiO_2 [%]	MNO [%]	FE_2O_3 [%]	NI [PPM]	CU [PPM]	ZN [PPM]	BR [PPM]	RB [PPM]	SR [PPM]	Y [PPM]	ZR [PPM]	NB [PPM]	PB [PPM]
F1 R 1-2cm; 1-1	15	2,42	8,70	0,44	0,08	3,73	<IDL	24	66	<IDL	98	277	22	151	11	18
F1 R 1-2cm; 1-2	15	2,35	8,44	0,44	0,06	3,55	24	25	66	<IDL	94	270	22	165	12	11
F1 R 1-2cm; 1-3	13	2,34	8,61	0,45	0,06	3,61	25	26	62	<IDL	98	302	22	171	11	15
F1 R 1-2cm; 1-4	15	2,66	9,63	0,51	0,07	4,18	24	28	79	5	111	330	25	205	12	17
F1 R 1-2cm; 1-5	13	2,31	8,31	0,43	0,07	3,52	27	21	66	3	94	278	21	164	11	14
F1 R 1-2cm; 1-6	16	2,45	8,86	0,47	0,07	3,83	<IDL	23	70	4	99	289	22	185	11	17
F1 R 1-2cm; 1-7	16	2,46	8,83	0,48	0,08	3,82	26	22	65	4	101	303	24	199	11	12
F1 R 1-2cm; 1-8	16	2,38	8,53	0,45	0,08	3,67	22	27	63	3	95	295	20	171	10	13
F1 R 1-2cm; 1-9	14	2,42	8,65	0,44	0,08	3,66	28	26	67	4	96	317	22	185	11	16
F1 R 1-2cm; 1-10	17	2,54	9,00	0,47	0,08	3,85	24	29	73	3	100	319	22	195	11	13
F1 R 1-2cm; 1-11	17	2,51	8,95	0,47	0,08	3,87	27	25	74	5	101	317	23	193	13	16
F1 R 1-2cm; 1-12	15	2,47	8,99	0,46	0,08	3,82	26	21	67	4	100	311	22	187	10	18
F1 R 1-2cm; 2-1	12	2,26	8,67	0,46	0,06	3,61	<IDL	18	68	4	97	283	24	184	13	17
F1 R 1-2cm; 2-2	13	2,22	8,20	0,43	0,07	3,46	24	22	59	4	92	270	21	168	11	16
F1 R 1-2cm; 2-3	13	2,38	8,52	0,44	0,06	3,64	28	23	63	4	95	284	23	170	12	19
F1 R 1-2cm; 2-4	14	2,43	9,03	0,48	0,07	3,90	<IDL	24	73	3	102	308	23	187	12	15
F1 R 1-2cm; 2-5	14	2,39	8,69	0,46	0,07	3,71	23	21	66	4	97	293	22	168	12	15
F1 R 1-2cm; 2-6	13	2,47	9,01	0,47	0,08	3,86	<IDL	20	70	5	101	308	23	183	10	19
F1 R 1-2cm; 2-7	14	2,42	9,06	0,47	0,07	3,85	23	22	69	5	99	308	21	188	10	19
F1 R 1-2cm; 2-8	16	2,50	9,35	0,48	0,07	3,90	28	20	61	5	102	319	23	196	10	13
F1 R 1-2cm; 2-9	13	2,49	9,28	0,49	0,07	3,90	23	23	69	5	103	321	22	194	10	17
F1 R 1-2cm; 2-10	15	2,45	8,91	0,46	0,08	3,78	27	19	61	5	98	309	21	190	13	11
F1 R 1-2cm; 2-11	14	2,37	8,77	0,45	0,08	3,76	<IDL	28	67	4	97	297	23	169	10	13
F1 R 1-2cm; 2-12	16	2,53	9,19	0,47	0,07	3,93	<IDL	29	70	3	102	321	24	184	9	16
F1 R 1-2cm; 3-1	16	2,50	9,29	0,49	0,08	4,03	28	25	71	4	105	317	24	198	13	17
F1 R 1-2cm; 3-2	12	2,38	8,71	0,46	0,07	3,72	28	25	68	4	97	288	22	182	12	19
F1 R 1-2cm; 3-3	14	2,48	9,27	0,50	0,07	4,04	<IDL	27	74	6	104	318	24	196	11	15
F1 R 1-2cm; 3-4	15	2,30	8,36	0,44	0,07	3,61	24	22	67	4	95	290	21	169	12	11
F1 R 1-2cm; 3-5	14	2,35	8,50	0,44	0,07	3,61	28	25	63	5	93	293	21	169	12	13
F1 R 1-2cm; 3-6	14	2,38	8,81	0,45	0,07	3,73	28	19	64	6	99	306	21	187	12	20
F1 R 1-2cm; 3-7	14	2,26	8,29	0,42	0,06	3,51	27	27	69	4	92	294	22	184	10	13
F1 R 1-2cm; 3-8	15	2,46	9,22	0,46	0,07	3,97	30	23	71	5	104	320	23	197	11	17
F1 R 1-2cm; 3-9	16	2,49	9,00	0,46	0,07	3,85	23	22	69	4	101	314	21	196	11	15
F1 R 1-2cm; 3-10	17	2,56	9,41	0,50	0,07	4,11	23	26	83	4	103	325	25	197	12	14
F1 R 1-2cm; 3-11	15	2,32	8,72	0,46	0,07	3,73	31	24	68	4	99	300	23	172	12	15
F1 R 1-2cm; 3-12	16	2,43	8,97	0,46	0,07	3,85	29	27	72	3	102	316	23	185	12	33

Table 49: Horizontal elemental distribution on F1, 1-2cm

Field 1 grid samples, 1-2cm	AS [PPM]	K_2O [%]	CaO [%]	TIO_2 [%]	MNO [%]	FE_2O_3 [%]	NI [PPM]	CU [PPM]	ZN [PPM]	BR [PPM]	RB [PPM]	SR [PPM]	Y [PPM]	ZR [PPM]	NB [PPM]	PB [PPM]
F1 R 1-2cm; 4-1	17	2,41	8,96	0,47	0,07	3,82	23	25	65	<IDL	100	303	24	188	12	14
F1 R 1-2cm; 4-2	18	2,40	8,65	0,44	0,08	3,82	29	21	70	5	98	300	24	197	10	12
F1 R 1-2cm; 4-3	14	2,42	8,94	0,45	0,07	3,92	<IDL	23	72	5	101	308	23	196	13	17
F1 R 1-2cm; 4-4	15	2,47	8,95	0,47	0,07	3,94	22	25	75	5	99	302	22	193	12	16
F1 R 1-2cm; 4-5	16	2,40	8,44	0,44	0,07	3,70	<IDL	20	70	4	95	299	23	171	10	13
F1 R 1-2cm; 4-6	14	2,54	9,19	0,48	0,07	4,04	<IDL	25	72	5	106	327	24	205	11	16
F1 R 1-2cm; 4-7	14	2,41	8,65	0,44	0,07	3,73	<IDL	20	71	6	98	302	22	170	9	17
F1 R 1-2cm; 4-8	16	2,41	8,86	0,45	0,07	3,87	28	23	70	5	99	306	22	175	12	14
F1 R 1-2cm; 4-9	18	2,51	9,11	0,48	0,07	4,02	27	26	72	3	104	323	26	200	12	13
F1 R 1-2cm; 4-10	17	2,48	9,35	0,48	0,09	4,12	29	24	74	6	104	319	24	192	12	13
F1 R 1-2cm; 4-11	17	2,43	8,89	0,46	0,08	3,88	30	29	74	4	99	305	23	171	12	17
F1 R 1-2cm; 4-12	15	2,48	8,78	0,44	0,08	3,64	25	23	66	3	97	294	22	162	11	13
F1 R 1-2cm; 5-1	17	2,46	9,04	0,48	0,08	4,02	<IDL	28	75	<IDL	103	307	24	191	13	14
F1 R 1-2cm; 5-2	16	2,72	9,81	0,53	0,09	4,34	27	29	76	5	106	325	26	209	11	17
F1 R 1-2cm; 5-3	16	2,54	9,19	0,49	0,09	4,09	29	23	64	4	106	315	24	206	10	14
F1 R -2cm1; 5-4	16	2,41	8,84	0,48	0,08	3,89	23	22	70	<IDL	102	305	25	197	13	13
F1 R 1-2cm; 5-5	15	2,45	9,21	0,48	0,07	4,07	31	23	70	<IDL	104	321	25	205	12	15
F1 R 1-2cm; 5-6	15	2,36	8,70	0,45	0,07	3,76	26	18	62	4	97	302	23	185	13	13
F1 R 1-2cm; 5-7	15	2,35	8,70	0,45	0,07	3,78	28	21	65	<IDL	98	294	22	186	11	15
F1 R 1-2cm; 5-8	15	2,38	8,94	0,47	0,08	3,94	25	22	71	4	101	308	23	203	12	14
F1 R 1-2cm; 5-9	14	2,41	8,73	0,45	0,08	3,84	29	26	70	<IDL	98	297	22	185	12	16
F1 R 1-2cm; 5-10	16	2,38	8,80	0,46	0,07	3,86	24	27	72	<IDL	99	299	23	184	10	12
F1 R 1-2cm; 5-11	18	2,49	9,17	0,47	0,07	4,04	29	22	75	5	105	317	24	187	13	14
F1 R 1-2cm; 5-12	14	2,45	8,70	0,45	0,07	3,84	26	26	71	4	99	313	22	171	12	15
F1 R 1-2cm; 1-1,5	14	2,40	8,56	0,47	0,08	3,75	<IDL	27	66	<IDL	97	283	22	159	13	11
F1 R 1-2cm; 1,5-1	14	2,45	8,87	0,48	0,08	3,86	<IDL	24	68	<IDL	102	297	24	188	13	13
F1 R 1-2cm; 1,5-2	14	2,38	8,49	0,46	0,08	3,71	<IDL	25	73	3	100	286	23	172	12	14
F1 R 1-2cm; 1,5-1,5	13	2,39	8,71	0,46	0,08	3,76	<IDL	24	72	4	100	288	23	168	12	14
F1 R 1-2cm; 2-1,5	14	2,24	8,34	0,45	0,08	3,62	<IDL	24	66	<IDL	97	280	22	171	10	11
Min:	12	2,22	8,20	0,42	0,06	3,46	22	18	59	3	92	270	20	151	9	11
Max:	18	2,72	9,81	0,53	0,09	4,34	31	29	83	6	111	330	26	209	13	33
Mean:	15	2,43	8,88	0,46	0,07	3,83	26	24	69	4	100	305	23	185	11	15

Table 50: Horizontal elemental distribution on F2, 0-1cm

Field 2 grid samples, 0-1cm	AS [PPM]	K_2O [%]	CaO [%]	TiO_2 [%]	MNO [%]	FE_2O_3 [%]	NI [PPM]	CU [PPM]	ZN [PPM]	BR [PPM]	RB [PPM]	SR [PPM]	Y [PPM]	ZR [PPM]	NB [PPM]	PB [PPM]
F2 R 0-1cm; 1-2	19	2,52	9,01	0,48	0,09	4,20	26	20	81	6	106	319	24	150	10	13
F2 R 0-1cm; 1-3	19	2,62	9,20	0,48	0,09	4,34	22	28	83	5	106	335	23	155	12	17
F2 R 0-1cm; 1-4	18	2,78	9,77	0,50	0,09	4,42	33	26	84	6	112	332	25	161	10	18
F2 R 0-1cm; 1-5	19	2,75	9,77	0,52	0,08	4,63	26	31	81	5	115	341	24	164	12	20
F2 R 0-1cm; 1-6	20	2,56	9,17	0,47	0,09	4,30	<IDL	25	73	5	106	331	23	156	11	14
F2 R 0-1cm; 2-1	17	2,59	9,23	0,49	0,09	4,32	30	20	91	5	108	341	25	153	12	20
F2 R 0-1cm; 2-2	19	2,74	10,07	0,53	0,10	4,71	31	30	83	6	117	348	23	157	15	19
F2 R 0-1cm; 2-3	18	2,65	9,61	0,50	0,09	4,52	23	25	82	6	114	333	24	161	12	14
F2 R 0-1cm; 2-4	16	2,45	8,68	0,44	0,08	4,03	27	25	71	5	101	304	21	150	12	15
F2 R 0-1cm; 2-5	15	2,54	9,23	0,49	0,09	4,31	27	29	78	5	110	318	24	160	10	19
F2 R 0-1cm; 2-6	17	2,58	9,27	0,48	0,09	4,34	<IDL	25	75	5	111	322	22	154	11	16
F2 R 0-1cm; 3-1	22	2,71	9,85	0,52	0,10	4,72	<IDL	32	84	5	117	340	26	165	12	16
F2 R 0-1cm; 3-2	21	2,69	9,32	0,49	0,09	4,44	31	27	78	7	110	326	24	157	12	14
F2 R 0-1cm; 3-3	17	2,53	9,11	0,48	0,08	4,33	26	35	83	7	109	322	24	160	12	16
F2 R 0-1cm; 3-4	19	2,48	8,87	0,45	0,07	4,15	22	23	76	6	105	313	22	153	11	13
F2 R 0-1cm; 3-5	20	2,62	9,32	0,49	0,08	4,38	34	24	77	5	110	321	23	157	11	14
F2 R 0-1cm; 3-6	17	2,58	9,11	0,48	0,08	4,35	26	25	73	6	108	321	23	156	10	16
F2 R 0-1cm; 4-1	19	2,88	10,00	0,53	0,09	4,80	27	32	96	6	120	345	26	167	13	20
F2 R 0-1cm; 4-2	20	2,58	9,31	0,48	0,08	4,42	29	26	82	4	110	321	26	158	13	14
F2 R 0-1cm; 4-3	18	2,46	8,94	0,47	0,09	4,20	25	23	77	6	105	317	23	147	11	16
F2 R 0-1cm; 4-4	19	2,62	9,29	0,48	0,08	4,47	33	28	82	6	112	330	25	158	13	17
F2 R 0-1cm; 4-5	20	2,59	9,08	0,47	0,08	4,33	36	24	80	6	108	326	24	147	10	12
F2 R 0-1cm; 4-6	18	2,59	8,82	0,45	0,09	4,12	27	26	74	6	103	305	22	143	9	13
F2 R 0-1cm; 5-1	15	2,49	8,76	0,45	0,07	4,06	22	23	68	4	102	310	21	150	10	17
F2 R 0-1cm; 5-2	16	2,57	9,24	0,48	0,08	4,41	26	29	81	5	111	340	25	160	12	20
F2 R 0-1cm; 5-3	18	2,50	9,04	0,45	0,08	4,26	<IDL	27	81	6	106	316	22	154	11	17
F2 R 0-1cm; 5-4	20	2,42	8,61	0,44	0,08	4,12	37	16	65	4	103	300	22	150	12	13
F2 R 0-1cm; 5-5	18	2,45	8,61	0,43	0,07	4,06	34	28	74	4	101	317	21	144	11	15
F2 R 0-1cm; 5-6	21	2,73	9,60	0,49	0,10	4,71	29	33	92	5	117	342	25	162	14	19
F2 R 0-1cm; 6-1	17	2,92	9,80	0,52	0,09	4,68	24	37	97	6	118	352	26	171	12	18
F2 R 0-1cm; 6-2	17	2,46	8,89	0,48	0,08	4,20	27	20	76	7	106	317	23	151	11	19
F2 R 0-1cm; 6-3	18	2,55	9,20	0,48	0,09	4,34	28	21	93	8	111	333	24	167	9	17
F2 R 0-1cm; 6-4	18	2,55	8,82	0,46	0,09	4,21	25	21	79	6	106	311	23	152	13	17
F2 R 0-1cm; 6-5	16	2,47	8,95	0,48	0,08	4,22	36	21	74	7	106	313	22	150	11	17
Min:	15	2,42	8,61	0,43	0,07	4,03	22	16	65	4	101	300	21	143	9	12
Max:	22	2,92	10,07	0,53	0,10	4,80	37	37	97	8	120	352	26	171	15	20
Mean:	18	2,60	9,22	0,48	0,08	4,36	28	26	80	6	109	326	24	156	12	16

Table 51: Horizontal elemental distribution on F2, 1-2cm

Field 2 grid samples, 1-2cm	AS [PPM]	K_2O [%]	CaO [%]	TiO_2 [%]	MNO [%]	FE_2O_3 [%]	NI [PPM]	CU [PPM]	ZN [PPM]	BR [PPM]	RB [PPM]	SR [PPM]	Y [PPM]	ZR [PPM]	NB [PPM]	PB [PPM]
F2 R 1-2cm; 1-2	16	2,61	9,14	0,48	0,09	4,33	25	20	79	7	112	319	23	153	11	17
F2 R 1-2cm; 1-3	16	2,55	8,92	0,47	0,08	4,24	<IDL	24	76	5	108	308	24	154	12	17
F2 R 1-2cm; 1-4	18	2,42	8,65	0,45	0,07	4,05	29	26	75	4	102	299	24	151	12	14
F2 R 1-2cm; 1-5	17	2,59	9,13	0,48	0,09	4,34	25	30	82	6	110	312	23	159	11	18
F2 R 1-2cm; 1-6	21	2,73	9,84	0,52	0,10	4,73	<IDL	30	96	7	120	349	26	167	10	17
F2 R 1-2cm; 2-1	17	2,50	9,01	0,47	0,09	4,16	30	25	80	4	106	316	23	150	10	15
F2 R 1-2cm; 2-2	17	2,53	9,16	0,48	0,08	4,30	23	26	82	6	107	308	23	153	12	17
F2 R 1-2cm; 2-3	17	2,69	9,92	0,52	0,10	4,69	28	25	83	7	118	335	26	169	13	20
F2 R 1-2cm; 2-4	16	2,55	9,17	0,47	0,08	4,27	33	22	80	6	109	324	24	162	11	19
F2 R 1-2cm; 2-5	16	2,52	9,05	0,46	0,09	4,23	31	27	78	4	108	307	22	155	11	15
F2 R 1-2cm; 2-6	15	2,54	8,99	0,46	0,08	4,23	25	27	77	6	106	303	23	151	10	14
F2 R 1-2cm; 3-1	17	2,62	9,11	0,48	0,08	4,30	25	28	82	6	109	312	24	159	14	16
F2 R 1-2cm; 3-2	16	2,50	8,90	0,45	0,09	4,16	29	28	75	7	104	306	23	153	10	18
F2 R 1-2cm; 3-3	15	2,59	9,26	0,48	0,08	4,34	32	26	83	5	108	319	24	156	12	16
F2 R 1-2cm; 3-4	14	2,59	9,14	0,48	0,08	4,30	27	23	73	5	110	319	25	159	9	16
F2 R 1-2cm; 3-5	17	2,65	9,44	0,49	0,08	4,47	36	29	80	6	113	320	25	164	12	19
F2 R 1-2cm; 3-6	15	2,76	9,60	0,50	0,10	4,63	34	35	91	7	117	328	25	182	12	23
F2 R 1-2cm; 4-1	19	2,71	9,81	0,52	0,10	4,70	<IDL	31	82	6	118	331	24	164	13	18
F2 R 1-2cm; 4-2	16	2,57	9,34	0,49	0,08	4,36	25	22	78	7	110	312	24	163	12	16
F2 R 1-2cm; 4-3	18	2,45	8,82	0,46	0,07	4,14	31	24	71	5	105	297	22	151	13	14
F2 R 1-2cm; 4-4	16	2,46	8,79	0,45	0,09	4,11	31	14	75	6	105	308	22	149	12	16
F2 R 1-2cm; 4-5	19	2,64	9,39	0,50	0,08	4,49	29	24	81	7	111	326	25	159	13	16
F2 R 1-2cm; 4-6	16	2,61	9,30	0,48	0,08	4,42	29	31	81	6	112	328	25	160	11	18
F2 R 1-2cm; 5-1	18	2,54	9,10	0,46	0,08	4,27	26	26	74	6	107	315	21	153	11	16
F2 R 1-2cm; 5-2	15	2,59	9,45	0,48	0,09	4,47	24	22	78	6	116	321	25	162	13	19
F2 R 1-2cm; 5-3	18	2,49	8,76	0,46	0,07	4,16	31	24	71	6	104	302	22	152	11	16
F2 R -2cm1; 5-4	17	2,59	9,32	0,49	0,08	4,46	31	25	78	5	112	313	25	158	11	14
F2 R 1-2cm; 5-5	20	2,48	8,90	0,47	0,09	4,24	27	24	81	5	106	319	23	150	12	15
F2 R 1-2cm; 5-6	20	2,73	9,78	0,51	0,09	4,72	24	38	99	6	118	331	25	165	12	21
F2 R 1-2cm; 6-1	16	2,48	8,79	0,45	0,09	4,09	27	29	77	6	104	297	22	144	12	16
F2 R 1-2cm; 6-2	17	2,52	9,27	0,48	0,09	4,36	34	30	84	6	111	328	23	158	10	17
F2 R 1-2cm; 6-3	20	2,64	9,41	0,50	0,08	4,49	32	31	81	6	114	318	25	161	11	14
F2 R 1-2cm; 6-4	17	2,69	9,33	0,49	0,08	4,51	31	26	81	5	115	325	25	160	12	17
F2 R 1-2cm; 6-5	18	2,63	9,45	0,49	0,08	4,52	30	33	77	7	114	339	25	156	11	16
Min:	14	2,42	8,65	0,45	0,07	4,05	23	14	71	4	102	297	21	144	9	14
Max:	21	2,76	9,92	0,52	0,10	4,73	36	38	99	7	120	349	26	182	14	23
Mean:	17	2,58	9,22	0,48	0,08	4,36	29	27	80	6	110	317	24	158	12	17

Table 52: Elemental composition of root soil

Root soil samples grid samples, 0-1cm	AS [PPM]	K_2O [%]	CaO [%]	TiO_2 [%]	MNO [%]	FE_2O_3 [%]	NI [PPM]	CU [PPM]	ZN [PPM]	BR [PPM]	RB [PPM]	SR [PPM]	Y [PPM]	ZR [PPM]	NB [PPM]	PB [PPM]
F1 A	13	2,22	8,04	0,43	0,06	3,49	22	25	65	3	93	272	21	153	9	14
F1 B	15	2,49	8,86	0,47	0,07	3,92	34	29	71	5	102	316	23	192	11	15
F1 Middle	20	2,57	9,77	0,52	0,08	4,33	<20	26	89	6	111	350	26	207	12	12
F2 A	17	2,50	9,15	0,47	0,08	4,35	37	25	83	6	112	316	24	162	12	19
F2 B	18	2,72	9,83	0,51	0,10	4,74	34	27	94	8	118	336	24	161	13	17
F2 Middle	16	2,45	8,79	0,46	0,09	4,21	30	34	82	7	106	297	22	154	12	16

Table 53: CSA results

Sample:	C [%]	S [%]
F1 canal sediment 5m	1,76	0,02
F2 canal sediment 17m	1,24	0,02
F1 A Horizon 1 , 0-7,5	1,93	0,02
F1 A Horizon 2 , 7,5-37	1,72	0,02
F1 A Horizon 3 , 37-48	2,15	0,02
F1 A Horizon 4 , 48-82	1,36	0,01
F1 A Horizon 5 , 82-100	1,83	0,02
F2 A Horizon 1 , 0-10,5	2,68	0,04
F2 A Horizon 2, 10,5-35	2,23	0,03
F2 A Horizon 3 , 35-65	2,29	0,03
F2 A Horizon 4 , 65-84	1,71	0,02
F2 A Horizon 5 , 84-100	1,40	0,01
F1 A, 0-1cm	2,48	0,03
F1 A, 1-2cm	2,49	0,03
F2 A, 0-1cm	2,80	0,04
F2 A, 1-2cm	2,79	0,04
F1 A root soil	2,17	0,03
F1 B root soil	2,86	0,03
F1 middle root soil	2,15	0,03
F2 A root soil	2,36	0,03
F2 B root soil	2,42	0,03
F2 middle root soil	2,36	0,03

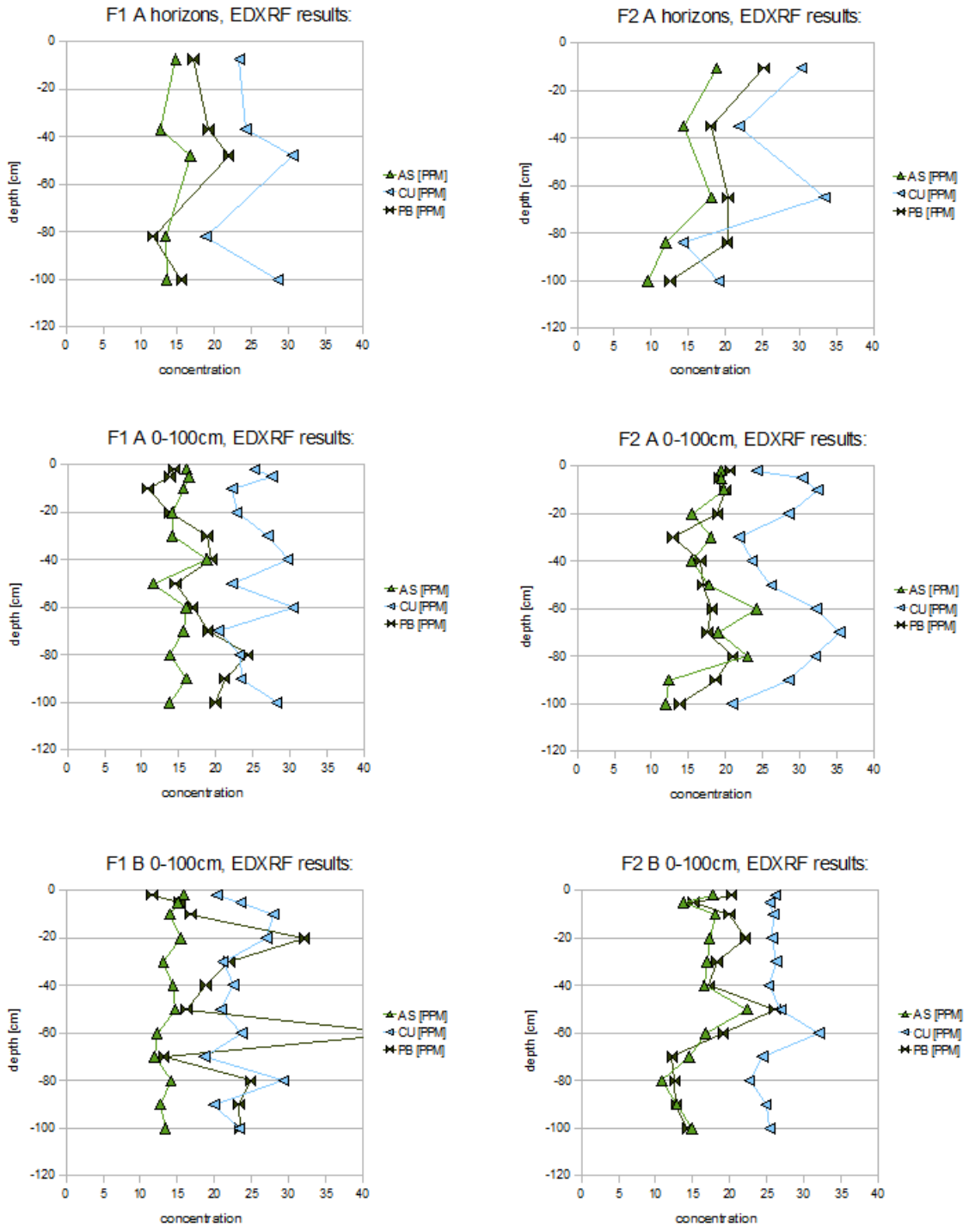

Figure 30: Vertical distribution of As in relation to other heavy metal trace elements

Table 54: ED-RFA results for used standards

	K2O [%]	CaO [%]	TIO2 [%]	MNO [%]	FE2O3[%]	NI [PPM]	CU [PPM]	ZN [PPM]	AS [PPM]	BR [PPM]	RB [PPM]	SR [PPM]	Y [PPM]	ZR [PPM]	NB [PPM]	PB [PPM]
Standard:																
Soil5, n=33																
Standard deviation	0,04	0,09	0,02	0,01	0,18	-	4,32	11,67	3,07	0,67	3,69	9,80	0,88	6,32	0,72	4,07
Average	1,20	2,56	0,60	0,10	6,46	<20	74,25	355,56	84,32	4,56	127,19	363,63	19,58	210,47	6,10	137,36
Reference value	2,24	3,10	0,78	0,11	6,36	13,00	77,00	370,00	94,00	5,00	140,00	330,00	21,00	220,00	9,00	130,00
Average/Reference value	0,54	0,83	0,76	0,95	1,02	-	0,96	0,96	0,90	0,91	0,91	1,10	0,93	0,96	0,68	1,06
Soil7, n=6																
Standard deviation	0,02	0,37	0,01	0,00	0,10	3,18	3,11	4,68	1,37	0,38	1,72	3,80	1,19	5,96	0,47	0,99
Average	0,88	18,62	0,35	0,07	3,50	27,44	15,31	95,60	13,25	7,52	47,29	103,70	19,56	166,11	6,24	50,31
Reference value	-	-	-	0,08	-	-	11,00	104,00	13,40	-	51,00	108,00	21,00	185,00	-	60,00
Average/Reference value	-	-	-	0,84	-	-	1,39	0,92	0,99	-	0,93	0,96	0,93	0,90	-	0,84
GXR 5, n=5																
Standard deviation	-	0,02	0,01	0,00	0,10	3,24	9,38	2,80	0,41	0,25	0,90	2,67	0,78	4,27		0,82
Average	<0.5	0,77	0,34	0,02	4,70	66,24	305,60	26,53	12,06	8,82	35,69	112,31	12,30	167,26	3,61	10,39
Reference value	1,06	1,17	0,37	0,04	4,84	75,00	354,00	49,00	11,20	7,80	41,00	110,00	16,00	140,00	6,70	21,00
Average/Reference value	-	0,66	0,91	0,56	0,97	0,88	0,86	0,54	1,08	1,13	0,87	1,02	0,77	1,19	0,54	0,49
GXR 2, n=2																
Standard deviation	0,01	0,00	0,00	0,00	0,00	-	2,15	1,56	0,81	-	0,04	0,37	0,38	0,19	0,49	2,96
Average	0,69	0,82	0,38	0,11	2,67	20,41	71,77	505,91	18,10	<3	77,44	149,77	15,27	279,38	8,49	677,70
Reference value	1,65	1,30	0,50	0,13	2,66	21,00	76,00	530,00	25,00	3,20	78,00	160,00	17,00	269,00	11,00	690,00
Average/Reference value	0,42	0,63	0,76	0,84	1,00	0,97	0,94	0,95	0,72	-	0,99	0,94	0,90	1,04	0,77	0,98

default values

Average deviations to reference values:

	0,48	0,71	0,81	0,80	1,00	0,93	1,04	0,84	0,92	1,02	0,92	1,00	0,88	1,02	0,66	0,84

Table 55: FIAS and HR-ICP-MS results for plant samples

Sample:	HR-ICP-MS As [ug/kg]	FIAS As [ug/kg]	FIAS / HR-ICP-MS
Maize:			
A leave 125cm	<MDL	141	
A leave 151cm	173	99,9	0,58
A leave 180cm	189	103	0,55
middle leave 44cm	489	387	0,79
middle leave 100cm	212	160	0,75
middle leave 133cm	196	117	0,6
B leave 45cm	457	244	0,53
B leave 150cm	173	58,35	0,34
A stem 120-130cm	<MDL	<MDL	-
A stem 145-155cm	53,4	<MDL	-
A stem 175-185cm	53,0	<MDL	-
middle stem 38-48cm	81,3	<MDL	-
middle stem 95-105cm	48,0	<MDL	-
middle stem 125-135cm	<MDL	<MDL	-
B stem 40-50cm	100	47,49	0,47
B stem 107-117cm	66,9	<MDL	-
B stem 145-155cm	78,6	<MDL	-
A grains	<MDL	<MDL	-
middle grains	<MDL	<MDL	-
B grains	117	46,4	0,4
A root	1260	297	0,24
B root	1220	310	0,25
middle root	2290	545	0,24
Sunflower:			
A leave, 28cm, 1.IN	1020	818	0,8
A leave, 110cm, 8.-9.IN, tip	774	195	0,25
A leave, 110cm, 8.-9.IN, middle	547	-	-
A leave, 110cm, 8.-9.IN, beginning	209	60,4	0,29
A leave, 110cm, 8.-9.IN, basement	178	<MDL	-
A leave, 180cm, 13.IN	188	43,8	0,23
middle leave, 10cm, 1.IN	1210	947	0,78
middle leave 110cm, 8.-9.IN	322	245	0,76
middle leave 190cm, 12.-13.IN	146	<MDL	-
B leave 22cm, 1.-2.IN	-	451	-
B leave 78-90cm, IN 2	609	472	0,78
B leave 182-196cm, 12.-13.IN	637	601	0,94
A stem 105-125cm	66,0	39,0	0,59
A stem 170-190cm	65,1	<MDL	-
A stem 25-35cm	146	31,2	0,21
middle stem 0-20cm	508	414	0,81
middle stem 105-125cm	<MDL	<MDL	-
middle stem 170-200cm	121	65,0	0,54
B stem 100-120cm	52,1	<MDL	
B stem 180-200cm	241	259	1,08
B stem 10-20cm	657	416,1	0,63
A grains	<MDL	<MDL	-
middle grains	<MDL	<MDL	--
B grains	74,2	63,2	0,85
A root	777	265	0,34
B root	2520	1030	0,41
middle root	3210	669	0,21
Vegetable:			
Chili 1	121	44,8	0,37
Chili 2	96,6	<MDL	-
Tomato 1	<MDL	<MDL	-
Tomato 2	<MDL	<MDL	-
Tomato 3	60,9	<MDL	-
Tomato 4	68,4	<MDL	-
Sweet pepper 1	<MDL	<MDL	-
Sweet pepper 2	63,5	<MDL	-
Egg plant 1	183	127	0,69
Potato 1	<MDL	<MDL	-
Potato 2	<MDL	<MDL	-
Eggs:			
Egg 1, yolk	195	<MDL	-
Egg 1, egg white	108	38,5	0,36
Egg 2, yolk	214	<MDL	-
Egg 2, egg white	85,5	<MDL	-
			Average: 0.54

$MDL_{HR\text{-}ICP\text{-}MS}$=*51,78 [ug/kg]* for 250mg DW dissolved in 25ml
MDL_{FIAS}=*33 [ug/kg]* for 250mg DW dissolved in 25ml